HIGHWAY RESEARCH BOARD

Bulletin 332

# *Rigid Pavement Design Studies*

1962





National Academy of Sciences—
National Research Council

publication 1014

# HIGHWAY RESEARCH BOARD

## Officers and Members of the Executive Committee

### 1962

### OFFICERS

R. R. BARTELSMEYER, *Chairman* C. D. CURTISS, *First Vice Chairman*

WILBUR S. SMITH, *Second Vice Chairman*

FRED BURGGRAF, *Director* WILLIAM N. CAREY, JR., *Assistant Director*

### Executive Committee

REX M. WHITTON, *Federal Highway Administrator, Bureau of Public Roads* (ex officio)

A. E. JOHNSON, *Executive Secretary, American Association of State Highway Officials* (ex officio)

LOUIS JORDAN, *Executive Secretary, Division of Engineering and Industrial Research, National Research Council* (ex officio)

PYKE JOHNSON, *Retired* (ex officio, Past Chairman 1960)

W. A. BUGGE, *Director of Highways, Washington Department of Highways* (ex officio, Past Chairman 1961)

R. R. BARTELSMEYER, *Chief Highway Engineer, Illinois Division of Highways*

E. W. BAUMAN, *Director, National Slag Association, Washington, D. C.*

DONALD S. BERRY, *Professor of Civil Engineering, Northwestern University*

MASON A. BUTCHER, *County Manager, Montgomery County, Md.*

J. DOUGLAS CARROLL, JR., *Director, Chicago Area Transportation Study*

C. D. CURTISS, *Special Assistant to the Executive Vice President, American Road Builders' Association*

HARMER E. DAVIS, *Director, Institute of Transportation and Traffic Engineering, University of California*

DUKE W. DUNBAR, *Attorney General of Colorado*

MICHAEL FERENCE, JR., *Executive Director, Scientific Laboratory, Ford Motor Company*

D. C. GREER, *State Highway Engineer, Texas State Highway Department*

JOHN T. HOWARD, *Head, Department of City and Regional Planning, Massachusetts Institute of Technology*

BURTON W. MARSH, *Director, Traffic Engineering and Safety Department, American Automobile Association*

OSCAR T. MARZKE, *Vice President, Fundamental Research, U. S. Steel Corporation*

J. B. MCMORRAN, *Superintendent of Public Works, New York State Department of Public Works*

CLIFFORD F. RASSWEILER, *Vice President for Research and Development, Johns-Manville Corporation*

GLENN C. RICHARDS, *Commissioner, Detroit Department of Public Works*

C. H. SCHOLER, *Applied Mechanics Department, Kansas State University*

WILBUR S. SMITH, *Wilbur Smith and Associates, New Haven, Conn.*

K. B. WOODS, *Head, School of Civil Engineering, and Director, Joint Highway Research Project, Purdue University*

### Editorial Staff

FRED BURGGRAF
2101 Constitution Avenue

HERBERT P. ORLAND
Washington 25, D. C.

N.R.C. HIGHWAY RESEARCH BOARD

Bulletin 332

# Rigid Pavement Design Studies

1962

Presented at the
41st ANNUAL MEETING
January 8-12, 1962

National Academy of Sciences—
National Research Council
Washington, D. C.
1962

$2.00

## *Department of Design*

T. E. Shelburne, Chairman
Director of Research, Virginia Department of Highways
University of Virginia, Charlottesville

### COMMITTEE ON RIGID PAVEMENT DESIGN

William Van Breemen, Chairman
Research Engineer, Engineering Research
New Jersey State Highway Department, Trenton

Harry D. Cashell, Secretary
Chief, Concrete and Concrete Pavement Branch, Physical Research Division
Bureau of Public Roads, U. S. Department of Commerce, Washington, D. C.

Henry Aaron, Chief Engineer, Reinforced Concrete Pavement Division, Wire Reinforcement Institute, Washington, D. C.

Robert F. Baker, Director, Transportation Engineering Center, Ohio State University, Columbus

Phillip P. Brown, Consultant, Soils Mechanics and Paving, Bureau of Yards and Docks, Department of the Navy, Washington, D. C.

Paul F. Carlton, Chief, Research Branch, Ohio River Division Laboratories, Cincinnati

W. E. Chastian, Sr., Engineer of Physical Research, Illinois Division of Highways, Springfield

E. A. Finney, Director, Research Laboratory Division, Michigan State Highway Department, Michigan State University, East Lansing

W. S. Housel, University of Michigan, Ann Arbor

F. N. Hveem, Materials and Research Engineer, California Division of Highways, Sacramento

W. H. Jacobs, Executive Secretary, Rail Steel Bar Association, Chicago, Illinois

C. D. Jensen, Director, Bureau of Materials, Pennsylvania Department of Highways, Harrisburg

Wallace J. Liddle, Chief (Secretary AASHO Committee on Design), Pavement and Base Design Branch, Highway Standards Division, Bureau of Public Roads, U. S. Department of Commerce, Washington, D. C.

John D. McNeal, Research Engineer, State Highway Commission of Kansas, Topeka

Ernest T. Perkins, Director, East Hudson Parkway Authority, White Plains, N. Y.

Thomas B. Pringle, Chief, Civil Engineering Branch, Engineering Division Military Construction, Office of Chief of Engineers, Department of the Army, Washington, D. C.

Gordon K. Ray, Manager, Paving Bureau, Portland Cement Association, Chicago, Illinois

James P. Sale, Assistant Chief, Special Engineering Branch, Research and Development, Military Science Division, Department of the Army, Office, Chief of Engineers, Washington, D. C.

F. H. Scrivner, Pavement Research Engineer, Texas Transportation Institute, A & M College of Texas, College Station

M. D. Shelby, Research Engineer, Texas Highway Department, Austin

W. T. Spencer, Soils Engineer, Materials and Tests, Indiana State Highway Commission, Indianapolis

Otto A. Strassenmeyer, Associate Highway Engineer—Research and Development, Connecticut State Highway Department, Hartford

K. B. Woods, Head, School of Civil Engineering and Director, Joint Highway Research Project, Purdue University, Lafayette, Indiana

# Contents

# Laboratory Studies of Progressive Bond Failure In Continuously-Reinforced Concrete Slabs

JOSEPH H. MOORE and ALBERT D. M. LEWIS, Respectively, Associate Professor of Civil Engineering, Pennsylvania State University and Associate Professor of Structural Engineering, Purdue University

This paper reports the results of research initiated to determine a method of measuring bond failure, to evaluate the effect of repetitive vertical loads in producing progressive bond failure from crack to crack in continuously-reinforced concrete pavements, and to determine the magnitude and distribution of bond stresses in the vicinity of cracks.

To evaluate bond stresses near cracks and to study their change under repetitive loads, a plastic gage was developed to determine minute movements of the steel bar with respect to the concrete. These movements change the rate of compressed air flow through the gage, and linear movements are determined by measuring the rate of air flow. An attempt was made to relate these differential movements to bond stress by assuming that these differential movements, divided by the distance between plastic gages, were strains in the steel.

Pull-out tests on 9-in. concrete cubes were used in arriving at a satisfactory size and configuration for the plastic gage.

Conclusions reached are as follows:

1. The plastic gage used in conjunction with an air flow meter provides a simple and practical means of determining the differential movement of steel bars with respect to concrete without destroying any of the deformation on the bars.
2. Bond stress at points within a region of slip may greatly exceed the average bond stress over this region.
3. Heavy repetitive vertical loads increased the magnitude of slip in regions adjacent to cracks, but bond stresses were not increased in the same proportion.
4. Seven million repetitions of heavy wheel loads resulted in slip of less than 0.002 in. at a distance of 6 in. from a crack; 12 in. from a crack the slip was zero.
5. When cracks are spaced more than 2 ft apart, the possibility of 9,000-lb truck wheel loads producing progressive bond failue in continuously-reinforced pavements on medium plastic subgrades is practically nonexistent.

• SINCE 1955 Purdue University has been engaged in laboratory research on continuously-reinforced concrete slabs. Nineteen concrete slabs 7 or 8 in. thick have been poured in forms in the laboratory and then placed onto special rubber mat subgrades. Longitudinal tensile forces were applied to the slabs to simulate temperature decreases. Vertical static loads were then applied by jacks to simulate vehicle wheel loads. The results of these experiments have been reported by Gutzwiller and Waling (1, 2).

With financial support by the National Science Foundation, this laboratory research has been extended to include studies of progressive bond failure in concrete slabs under dynamic loads. This paper is a report of the first work completed in this phase of the research.

## PURPOSE AND SCOPE OF RESEARCH

The possibility of a bond failure progressing from crack to crack has occurred to many who are interested in the field of continuously reinforced pavements. A report of the American Concrete Institute in 1959 stressed the need for research on bond behavior at cracks (3). The problems involved in such research include the detection of bond failure without removing an appreciable portion of the bonding surface of the steel from contact with the concrete, and the isolation of the many variables affecting stresses in the slab so that their effects might be evaluated separately.

This phase of the research project had a two-fold purpose:

1. To develop a method of detecting bond failure without destroying the deformations on the bars.
2. To apply such a method to laboratory models of continuously reinforced concrete slabs to determine if repetitive vertical loads cause bond failure to progress along the reinforcing bars.

The controlled variables included in the experiments were percentage of longitudinal reinforcement, position of reinforcement, subgrade modulus, longitudinal load on the slab, and magnitude and position of a simulated wheel load. The principal dependent variable measures was the longitudinal movement of the reinforcement relative to the concrete adjacent to the bars. Concrete surface crack widths were also obtained for most specimens. A limited number of measurements of steel strains and vertical deflections of the slab were recorded.

## DEVELOPMENT OF GAGE TO MEASURE SLIP

To implement this research, it was necessary first to seek a means of detecting breakage of bond between reinforcing bars and the concrete without appreciably reducing the bonding area of the bars. After several attempts to create devices for detecting

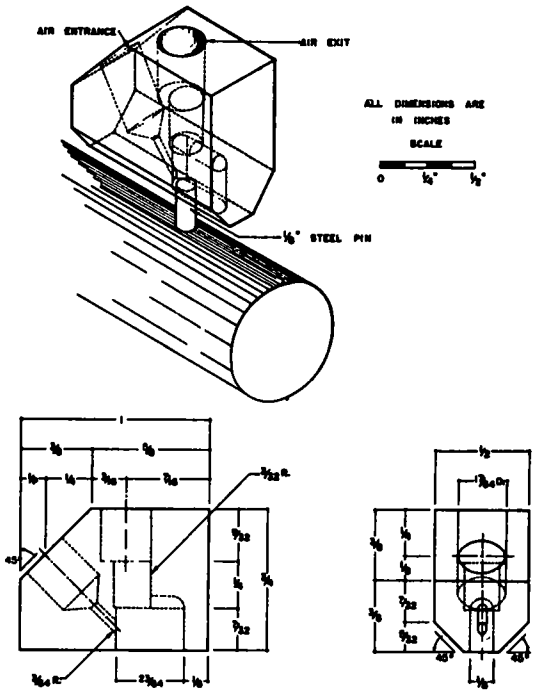


Figure 1. Plastic gage.

such breakage, a plastic gage was developed, which when coupled with an air flow meter provides an accurate measure of the longitudinal movement of the bar with respect to the concrete. In this paper this type of movement is referred to as "slip." Although no attempt is made to define the amount of slip required for bond failure, the plastic gages were used to measure slip along a bar in the vicinity of a transverse crack. The point at which the slip became zero was determined from a plot of the slip values recorded at the gages located along a bar.

The size and positioning of the plastic gage is shown in Figure 1. The gage was 1 in. long and made of $\frac{1}{2}$-in. plexiglass. A $\frac{1}{4}$-in. O. D. polyethylene tubing was cemented into the "air entrance" and "air exit" chambers, and the far end of the "air entrance" tubing was connected to Column Type Precisionaire instruments (manufactured by the Sheffield Corporation of Dayton, Ohio). The Column Type Precisionaire instruments, hereafter referred to as the "column gages," are a type of air flow meter and were used to measure the amount of air flowing through the plastic gages.

The plastic gage was positioned along the longitudinal ridge, two of which are present on any reinforcing bar, so that the air entrance hole was plugged by a $\frac{1}{8}$-in. stainless steel pin that had previously been set into a $\frac{1}{8}$-in. hole drilled into the longitudinal ridge of the bar. The groove in the bottom of the plastic gage into which the stainless steel pin fitted was machined with a $\frac{1}{8}$-in. end mill to obtain a snug yet workable fit. The tubing from the air exit hole of the gage extended to the exterior of the concrete to provide a path for the flow of air as the pin was moved with respect to the plastic gage.

When installed on the bars and cast in concrete, the plastic gage was held in a fixed position by the concrete; therefore, the column gages registered the movement of the steel with respect to the concrete as the steel strained on being stressed. At a crack the steel is strained and this strain gradually decreases as the force in the steel is transferred to the concrete by bond.

In calibration a metal guide was used to prevent lateral movement of the plastic gage. Longitudinal movement of the gage relative to the steel pin was produced through a pusher block machined to slide in the same groove of the metal guide as that used by the plastic gage. The pusher block was activated by pressure from a screw that itself was fitted in a second housing that could be fastened to the reinforcing bar, as shown in Figure 2. Longitudinal movement was measured with a dial gage with 0.0001-in. graduations. A typical calibration curve indicating the spread of points obtained in the calibration process is shown in Figure 3.

The plastic gage was used only to detect movement of the pin in one direction from its "home" position, the "home" position being defined as that at which the steel pin plugged the air entrance hole. Movement of the steel pin away from the air entrance

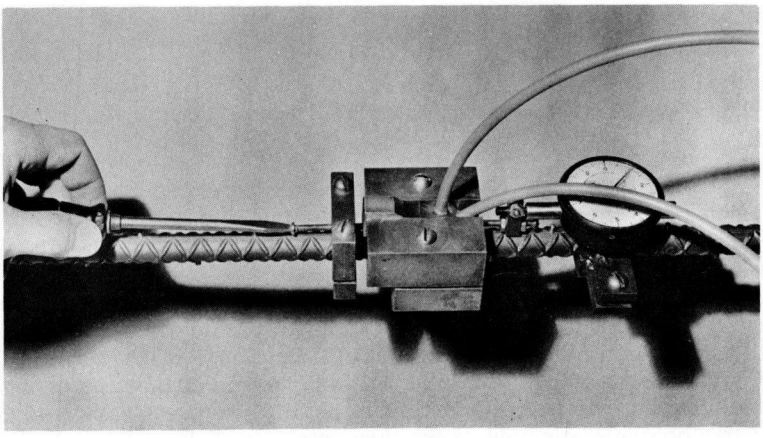

Figure 2. Calibration of plastic gage.

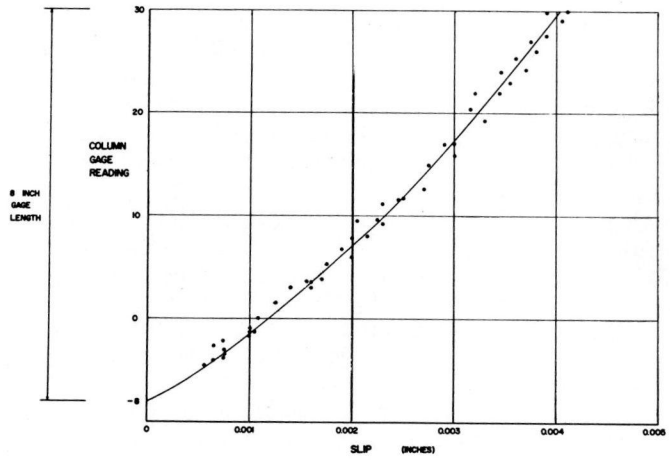


Figure 3. Calibration curve for gage 28, slab 7.

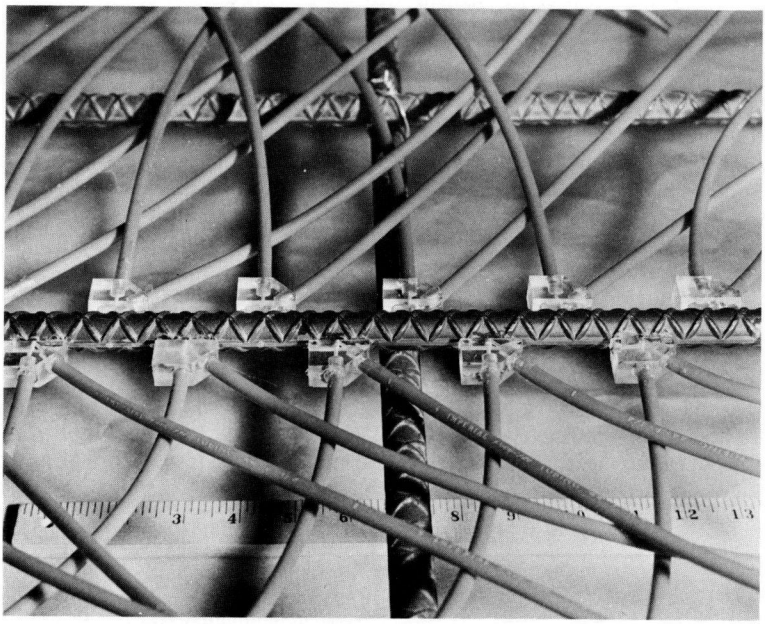

Figure 4. Plastic gages glued in position on reinforcing bars.

hole to allow air to flow through the gage is hereafter referred to as movement in the positive direction, with movement in the opposite direction being referred to as that in the negative direction. It is therefore apparent that the gage must be installed with consideration to the direction of positive movement.

After calibration, the plastic gages were cemented to the reinforcing bars with Duco cement. Long steel guide plates and tape were used to hold the gages in alignment and in their "home" position for 24 hr. Additional thin coatings of Duco cement were then added to seal any small openings along the milled groove between the under side of the gage and the reinforcing bar to exclude cement paste. Figure 4 shows several gages cemented to a bar before placement of the concrete.

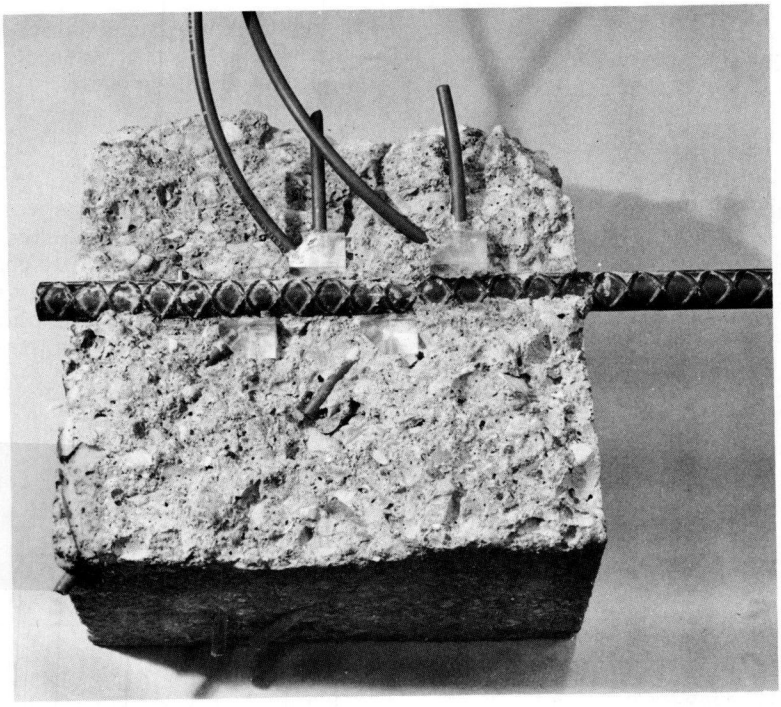

Figure 5. Plastic gages in pull-out specimen after a test.

In the development of the plastic gage numerous simple pull-out experiments were conducted on reinforcing bars fitted with plastic gages and cast in 9-in. concrete cubes. The gages, which were in contact with the bar only along its longitudinal ridge, did not appear to produce planes of weakness in the concrete. In fact it was very difficult to split a specimen along a satisfactory plane to obtain the picture for Figure 5.

The column gages used in this research had pressure regulators and 8-in. graduated vertical columns in which the rate of air flow was indicated by the position of a float. By experience it was found that with the pressure regulators set to 20 psi, movement of the plastic gage along the reinforcing bar from 0.003 to 0.004 in. from its "home" position caused the float to travel the 8-in. calibrated length of the column. Sensitivity decreased as the air pressure was lowered.

## DESCRIPTION OF EXPERIMENTAL SLABS

### Size and Number

Experiments were performed on eight slabs in this phase of the research. Due to limitations in space beneath the loading frame, the slabs were limited to 3 ft by 12 ft by 8 in.

### Materials

Steel. — As shown in Figure 6, each slab was reinforced longitudinally with 0.54 percent steel, provided by five equally spaced No. 5 deformed billet steel reinforcing bars conforming to ASTM A 15-58T and having diamond pattern deformations conforming to ASTM A 305-56T. Properties of this steel are given in Table 1. The longitudinal steel was placed at mid-depth of all slabs except slabs 5 and 7, in which cases it was placed $\frac{3}{4}$ in. below mid-depth.

Concrete. — The concrete was obtained from a local ready-mix company and was to meet the following requirements:

TABLE 1

PROPERTIES OF REINFORCING STEEL

| Property | Steel |
|---|---|
| Yield strength (psi) | 73,000 |
| Ultimate strength (psi) | 120,200 |
| Modulus of Elasticity (psi) | $29 \times 10^6$ |
| Percent elongation over 8-in. gage length | 12.0 |
| Percent reduction of area | 48.7 |

| | |
|---|---|
| 28-day ultimate compressive strength | 4,000 psi |
| Maximum size aggregate | 1½ in. |
| Slump | 2-4 in. |
| Entrained air | 3-6 percent |

Three 6- by 6- by 16-in. beams and six 6- by 12-in. cylinders were cast for flexural and compressive strength tests. Slabs 1 and 2 were initially considered as pilot experiments, and it was decided to use concrete with a higher slump in these tests. Results of tests on the concrete are shown in Table 2.

TABLE 2

PROPERTIES OF CONCRETE FOR SLABS[a]

| Slab No. | Date of Pour | Slump (in.) | Avg. Cylinder Strength (psi) | Avg. Modulus of Rupture (psi) | $E \times 10^{-6}$ (psi) |
|---|---|---|---|---|---|
| 1 | 9/23/60 | 7 | 3,060 | 400 | 3.30 |
| 2 | 11/15/60 | 8 | 3,320 | 423 | 3.50 |
| 3 | 12/23/60 | 4½ | 2,830 | 433 | 2.76 |
| 4 | 1/27/61 | 1½ | 4,285 | 527 | 4.00 |
| 5 | 2/27/61 | 4½ | 3,490 | 394 | 3.40 |
| 6 | 3/24/61 | 4 | 4,000 | 576 | 3.78 |
| 7 | 4/21/61 | 2 | 4,490 | 494 | 4.00 |
| 8 | 5/12/61 | 4½ | 4,710 | 669 | 4.54 |

[a]All cylinder and beam tests made 28 days after pour.

## Forms for Experimental Slabs

The forms consisted of two plywood carts, each 6 ft long, resting on truck casters. The two carts were assembled end-to-end with side and end boards in place to provide a clear space of 3 ft by 12 ft by 8 in. Holes were drilled in the side and end boards of the form to receive the tranverse and longitudinal bars.

Because the object of these experiments was to determine the slip pattern in the vicinity of a crack, a weakened plane was created at midlength of the slab to cause the slab to crack initially at that position. This was done by threading four rows of 12-gage wire through vertically aligned holes in the side boards of the form and tightening them to produce five approximately equal spaces between the longitudinal steel and the bottom of the form. Another four rows of the wire were similarly placed between the steel and the top of the form.

## Other Preparations for Casting

Short lengths of deformed bars were installed at each end of the slab, as shown in Figure 6, to provide adequate strength in fittings for applying longitudinal forces. Threaded adapters were welded to the ends of all bars. Similar adapters had been used in static tests previously reported (2).

The transverse steel bars indicated in Figure 6 were of the same size and grade as the longitudinal steel. These bars not only supported the longitudinal steel, but were used also to tide together the side boards of the forms. Later, hanger bars were attached to these bars to support the slab while it was lowered to the subgrade.

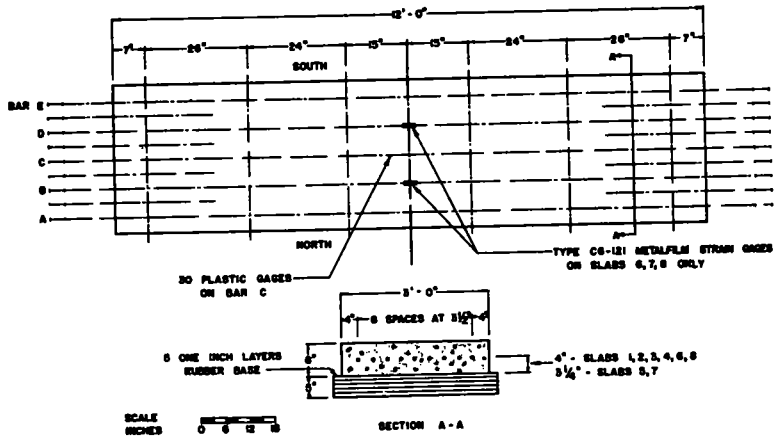


Figure 6. General plan for slabs.

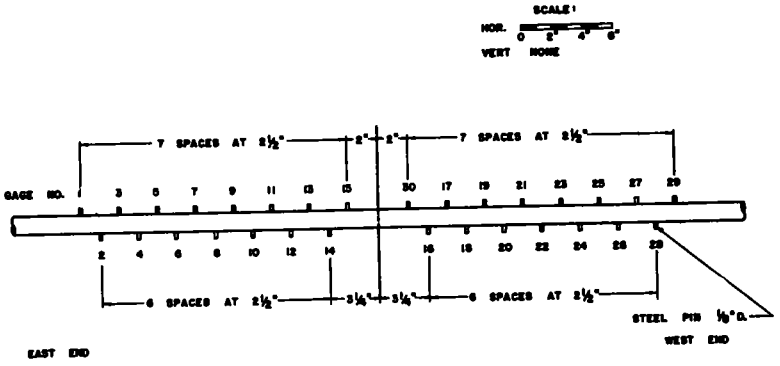


Figure 7. Bar C.

Plastic gages were arranged in a staggered pattern on two sides of bar C (see Figs. 6 and 7). The midpoint of the bar was placed at the location of the prepared weakened plane in the slab. Steel plugs were also embedded in the surface of the wet concrete at 10-in. intervals on lines 7 in. from the longitudinal edges of the slab. Other gage plugs were cemented to the side of the slab at the elevation of the longitudinal steel after the slab was poured. A 10-in. Whittemore strain gage was used to make surface strain and crack width measurements on all slabs except slab 1.

Deflections of the last four slabs were recorded by means of eight dial indicators with 0.001-in. graduations suspended from a framework. The stem of each gage rested against a piece of sheet metal that had been cemented to the surface of the concrete 1 in. from the edge of the slab.

As shown in Figure 6, electric resistance strain gages were bonded to bars B and D at midlength of the last three slabs tested. These gages were waterproofed with an asphalt coating.

## Placing and Curing the Concrete

All slabs were cast inside the laboratory. The truck-mounted concrete mixer was driven inside the building in cold or inclement weather. The date of pour of the slabs is given in Table 2.

To avoid the possibility of disturbing the arrangement of the plastic gages, bar C was removed from the form while concrete was placed up to the level of the other longitudinal bars. Then bar C was lowered into the form with the rows of plastic gages in a horizontal plane. The air exit tubes were then passed through holes that had been drilled in the sides of the form, and the four rows of wire were placed above the steel at midlength point to complete the provision for the initial crack.

After bar C was in position, the pouring of the slab was completed using an internal vibrator to insure filling all spaces around the reinforcement, the gages, and next to the form. After striking off and before initial set had taken place, plugs for the Whittemore strain gage were embedded in the top surface of the slab.

Approximately 2 to 3 hr later a coating of Kurez curing compound was poured on the surface of the slab and left to dry. Within 24 hr, the slab surface was given a second coating of the compound, followed by a third coating approximately 24 hr later. Cylinders and beams from the same pour were also cured by painting with three coats of curing compound, and were tested 28 days after casting.

### Elastic Subgrade

To reduce the variables in the experiments with the slabs, a rubber mat subgrade capable of providing an average subgrade modulus, or load to deflection ratio, of 140 to 145 psi per in. of deflection was used. This mat consisted of a number of 41- by 33- by 1-in. pads of rubber specially prepared by the Firestone Industrial Products Company, Noblesville, Ind., to simulate a soil having medium plasticity. This material had the same composition as that used in the static load tests previously conducted (2). Five layers of mats stacked in brick fashion were used under all slabs. The subgrade modulus was obtained by plate-bearing tests. A plate of 30-in. diameter was used for these tests.

### Positioning Slabs for Loading

After the side and end pieces of the forms were removed, it was possible to roll each slab in turn into position beneath the loading frame. The slab was then transferred from the base of the form to the rubber mat subgrade. Eyebolt hangers were hooked onto the projecting ends of the transverse bars in the slab, and the threaded upper ends of the hangers were engaged by nuts and washers to a longitudinal timber beam supported by blocks on each side of the slab. The nuts at the upper end of the hangers were tightened a uniform number of revolutions to raise the slab free of the form and keep it suspended while the form was removed. The rubber mat subgrade was then laid in brick fashion on the concrete floor beneath the slab, and the slab was lowered onto the subgrade by loosening all of the nuts evenly. A single piece of wrapping paper was placed between the slab and the top of the subgrade to reduce the friction between the rubber and slab.

## LOADING OF SLABS

### Longitudinal Loading

Tensile stresses, simulating a temperature drop, were induced into the slab by applying longitudinal loads to the reinforcing bars projecting from the ends of the slab. The four additional lengths of reinforcing bars spaced between the five longitudinal steel bars at the ends of the slab aided in distributing the force to the concrete as well as in reducing the possibility of fatigue failures in the connections at the ends of the bars. The threaded adapters, which were made from $1\frac{3}{8}$-in. steel rods, were threaded on one end for a nut and were drilled at the other end so that the reinforcing rods might be inserted and welded to them.

A set of two I-beams was then placed transverse to the slab at each end with the projecting reinforcing bars passing between them. Plates and then nuts with washers were fitted onto the adapters with the plates flush against the flanges of the I-beams. Hydraulic jacks were then aligned with pipe columns on each side of the slab, with one end of the pipe column pressing against the set of I-beams at the west end of the slab while the

hydraulic jack piston pressed against a small bearing beam that transferred the jack load to the set of I-beams at the east end of the slab. When compressive loads were applied to the columns through the hydraulic jacks, this same force was transferred through the I-beams to the reinforcing rods protruding from the ends of the slab.

The hydraulic jacks were calibrated before each experiment in a compression testing machine. Each day during loading of a slab the jacks were observed to determine if there had been any loss in load. When such losses reached 2 kips, the jack loads were adjusted back to the original settings. Such adjustments were generally necessary only four or five times during the three-week duration of each experiment.

## Repetitive Vertical Loading Arrangements

Amsler hydraulic jacks were used with a hydraulic pulsator to produce sine-wave loadings at two load points on the slab. The two sine-wave loadings were 180° out of phase and thus simulated the transfer of the wheel load from one load point to the other, as would occur as a truck wheel passed over the crack at midlength of the slab.

For all slabs, except Nos. 7 and 8, the center of load point E (east) was 9 in. to the east of the midlength of the slab; while the center of load point W (west) was 9 in. to the west of the midlength line. These load points were centered transversely on the slab. Figure 8 shows jacks at these two load points. In this figure the west load point is to the right of the crack ①, which is at midlength. For slabs 7 and 8 the east load point was centered over the midlength line and this load location is hereafter referred to as EE; in a similar manner the west load point was centered $4\frac{1}{2}$ ft to the west of the midlength line as shown in Figure 9, and this load position is referred to as WW. As would be expected, there was an increase in deflection at midlength of the slab during a loading cycle when the loads were shifted from E and W to EE and WW.

The vertical loads from the jacks were transferred to the slabs through a tier of circular steel plates of increasing size, the largest of which was 18 in. in diameter. A 1-in. circular rubber mat 18 in. in diameter was placed between the plates and the surface of the slab.

Three Amsler jacks were used to obtain the out-of-phase sine-wave loadings at the two load points. The larger jack, shown over the east or left load point in Figure 10,

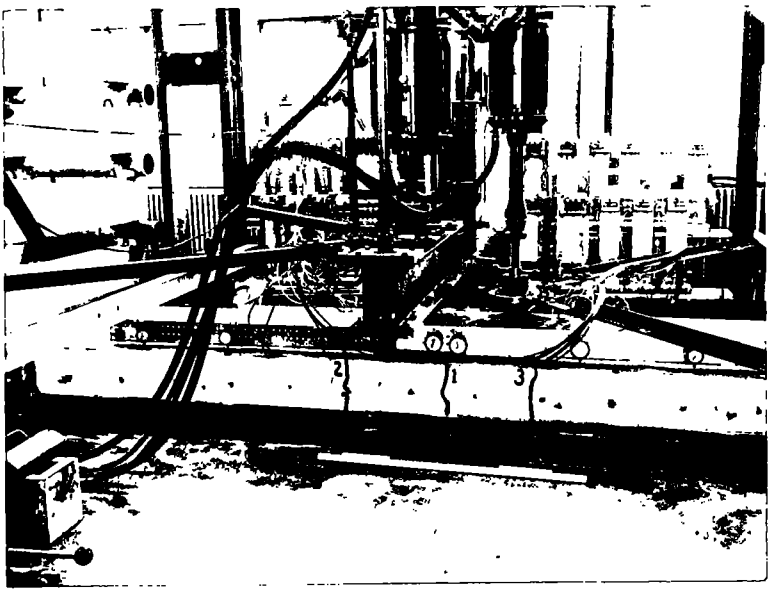


Figure 8. Crack pattern for slab 5.

was connected to the dynamometer shown by the window at the right. The dynamometer supplied a constant force to this jack. The reaction for this jack, as well as for the other two, was provided by a heavy steel beam supported by girders connected to columns. The jack over the west load point (see Fig. 10) was connected to the Amsler pulsator shown at the left. The pulsator was operated at 250 cycles per min to produce a sine-wave loading between some minimum and some maximum value. In general this minimum was 1 kip and the maximum was 9 kips. This type of loading is referred to as 9K-1K. Some slabs were loaded with a vertical loading of 17K-1K. The dynamometer

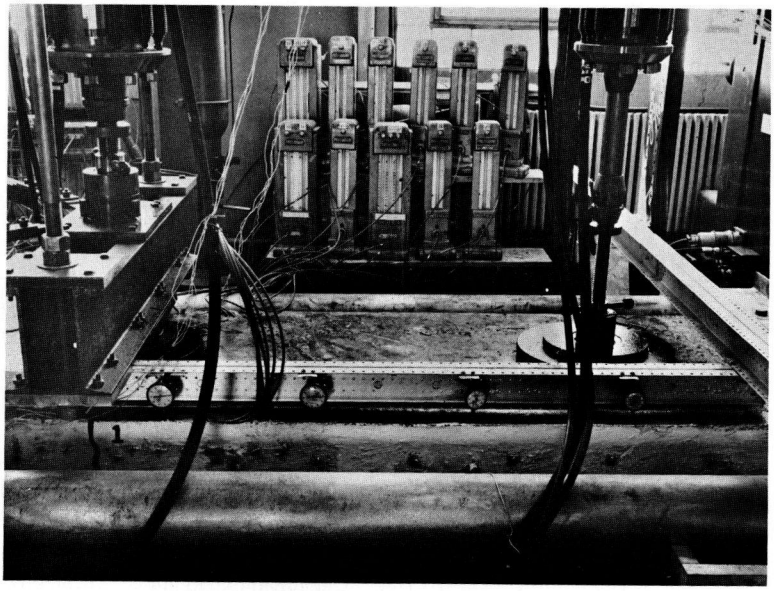

Figure 9. Crack pattern for slab 8.

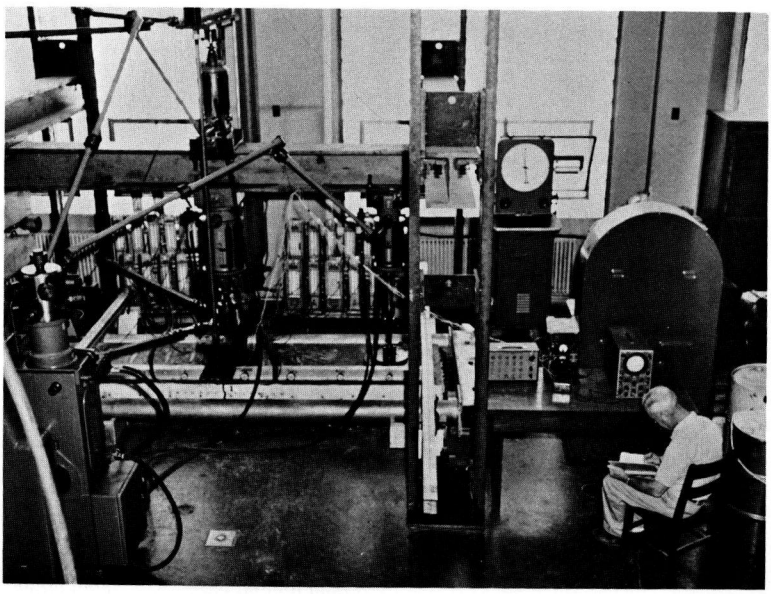

Figure 10. General view of longitudinal and vertical loading arrangement, slab 8.

loading for the large jack was 10 kips for the 9K-1K type of loading, and 18 kips for the 17K-1K loading.

The third jack, also connected to the pulsator, was placed directly over the larger jack which was connected to the dynamometer and was coupled to the larger jack by a loading bracket. Therefore, when the pulsator was on a pressure stroke, the constant force in the larger jack was in part nullified by the force in the third jack; so the load delivered to the slab at the east load point was the dynamometer load minus the pulsator force at this instant. At this same instant, the jack over the west load point was applying a load equal to the pulsator force to the pavement at the west load point. The sum of the loads applied to the pavement at the two load points always remained a constant, but during each cycle the loading arrangement allowed the load at the east load point to become a minimum whereas that at the west load point was a maximum, and vice versa. The loading therefore simulated the passage of a wheel load across the crack from one load point to the other.

## TEST PROCEDURE AND RESULTS

The eight slabs differed somewhat in the quality of the concrete, as can be seen in Table 2. The only difference in the steel arrangement was that in slabs 5 and 7 the longitudinal steel was lowered so that it was $\frac{3}{4}$ in. below mid-depth. The subgrade modulus was maintained constant at 140 to 145 lb per cu in. for all experiments.

The longitudinal load was varied for the first slab to observe its effect on slip. For the second slab this load was maintained at 70 kips. For all other slabs it was maintained at 50 kips.

In general, all slabs received approximately 7,000,000 repetitions of vertical load. This number of loads was considered to be at least equal to the number of truck wheel loads greater than 8 kips which may be expected over a 3-ft longitudinal strip of a heavily travelled highway lane in 24 yr.

The repetitive vertical load was varied from 9K-1K to 17K-1K for the first slab, and then was maintained at 17K-1K for the second and third slabs. The fourth slab was loaded the first 3,500,000 cycles with a 9K-1K loading, and thereafter with a 17K-1K loading. Slabs 5, 6, 7, and 8 were loaded with a 9K-1K loading. This loading was placed at load points E and W for all slabs except slabs 7 and 8 for which it was placed at points EE and WW.

### Loading Procedure

In the loading of slabs, the longitudinal force was applied first. This force generally produced a small crack across the weakened plane at midlength of the slab. After approximately one hour the static load was applied at the E or EE load point through the jack attached to the dynamometer. As shown in Table 3, this load often produced other cracks in the specimen. Within 15 to 30 min the pulsator was turned on and adjusted to deliver a load to the two jacks attached to it, such load varying sinusoidally from a maximum of 9 kips to a minimum of 1 kip for a 9K-1K loading, or from a maximum of 17 kips to a minimum of 1 kip for a 17K-1K loading. the minimum load of 1 kip was maintained to keep positive pressure on the jacks at all times, and therefore prevent their lifting off the slab and shifting position between load cycles. All repetitive loads were applied at the rate of 250 times a min.

Slip readings were made on the column gages at intervals that made for satisfactory plotting of the slip against the logarithm of the number of loading cycles. Generally about twenty sets of slip measurements were taken during the 7,000,000 cycles of vertical loading. The crack width, vertical deflection, and steel strain measurements were taken at less frequent intervals.

### Progressive Slip

Although each slab cracked in a somewhat different pattern from the others, the data obtained from the plastic gages mounted on bar C had common characteristics for all slabs. Figure 11 shows the small amount of additional slip which might be attributed

to numerous repetitions of vertical loading. Data for the slip for all gages in the eight slabs are omitted from this paper but are available elsewhere (4).

TABLE 3

CRACK WIDTH AND SLIP DATA FOR SLABS

| Slab | Loading Conditions | | | No of Cracks | Mid-Length Crack Width (in ) | | Distance to Zero Slip (in ) | |
|---|---|---|---|---|---|---|---|---|
| | Long | Vert | Cycles of Vert Load | | Sides | Top | E | W |
| 1 | 50K | 0 | 0 | 1 | No data | | 9 | 7 |
| | 50K | 10K | 0 | 1 | | | 10 | 10 |
| | 70K | 9K-1K | 6,184,000 | 6 | | | 7 | 7 |
| | 70K | 0 | | 6 | | | 7 | 7 |
| 2 | 70K | 0 | 0 | 2 | 0 0142 | No data | 7 | 14 |
| | 70K | 18K | 0 | 4 | 0 0261 | | 7 | 14 |
| | 70K | 17K-1K | 6,729,000 | 8 | 0 0275 | | 9 | 11 |
| | 70K | 0 | | 8 | 0 0274 | | 9 | 11 |
| 3 | 50K | 0 | 0 | 3 | 0 0097 | -0 0006[a] | 11 | 9 |
| | 50K | 18K | 0 | 5 | 0 0156 | -0 0027 | 9 | 9 |
| | 50K | 17K-1K | 7,290,000 | 5 | 0 0148/0 0150 | -0 0035/-0 0040[b] | 9 | 9 |
| | 50K | 0 | | 5 | ------ | -0 0021 | 9 | 9 |
| 4 | 50K | 0 | 0 | 1 | 0 0077 | -0 0009 | 8 | 5 |
| | 50K | 10K | 0 | 2 | 0 0109 | -0 0023 | 9 | 7 |
| | 50K | 9K-1K | 7,925,000 | 2 | 0 0160 | -0 0032/-0 0040 | 11 | 10 |
| | 50K | 0 | | 2 | 0 0142 | -0 0014 | 11 | 10 |
| 5 | 50K | 0 | 0 | None | 0 | 0 | 0 | 0 |
| | 50K | 10K | 0 | 2 | 0 0112 | +0 0002 | 10 | 12 |
| | 50K | 9K-1K | 7,206,600 | 3 | 0 0136 | -0 0015 | 10 | 9 |
| | 50K | 0 | | 3[c] | 0 0138 | +0 0012 | 10 | 9 |
| 6 | 50K | 0 | 0 | 1[c] | 0 | 0 | 0 | 0 |
| | 50K | 10K | 0 | 2 | 0 0101 | -0 0004 | 7 | 12 |
| | 50K | 9K-1K | 7,072,000 | 3 | 0 0103/0 0109 | -0 0019/-0 0024 | 6 | 12 |
| | 50K | 0 | | 3 | 0 0150 | -0 0016 | 6 | 12 |
| 7 | 50K | 0 | 0 | 1 | 0 0084 | 0 0007 | 10 | 9 |
| | 50K | 10K | 0 | 2 | 0 0135 | 0 0006 | 12 | 9 |
| | 50K | 9K-1K | 7,504,600 | 4 | 0 0154/0 0159 | 0 0148/0 0155 | 10 | 9 |
| | 50K | 0 | | 4 | 0 0154 | 0 0105 | 10 | 9 |
| 8 | 50K | 0 | 0 | 1 | 0 0144 | -0 0019 | 7 | 11 |
| | 50K | 10K | 0 | 1 | 0 0163 | -0 0038 | 7 | 11 |
| | 50K | 9K-1K | 7,573,800 | 1 | 0 0168 | -0 0001/+0 0006 | 7 | 11 |
| | 50K | 0 | | 1 | 0 0122 | -0 0006 | 7 | 11 |

[a] Negative crack width refers to decrease from initial (no loads) reading between gage plugs set on 10-in centers
[b] Observed minimum/maximum readings
[c] This crack not at midlength

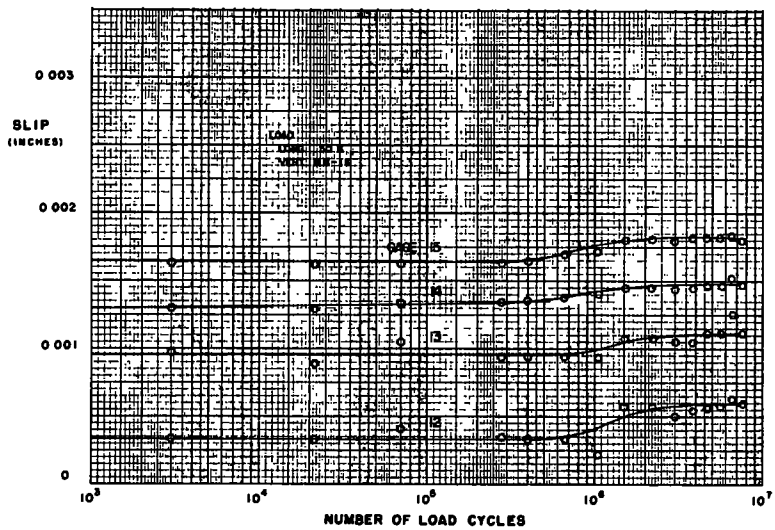


Figure 11. Slip vs number of load cycles, slab 8.

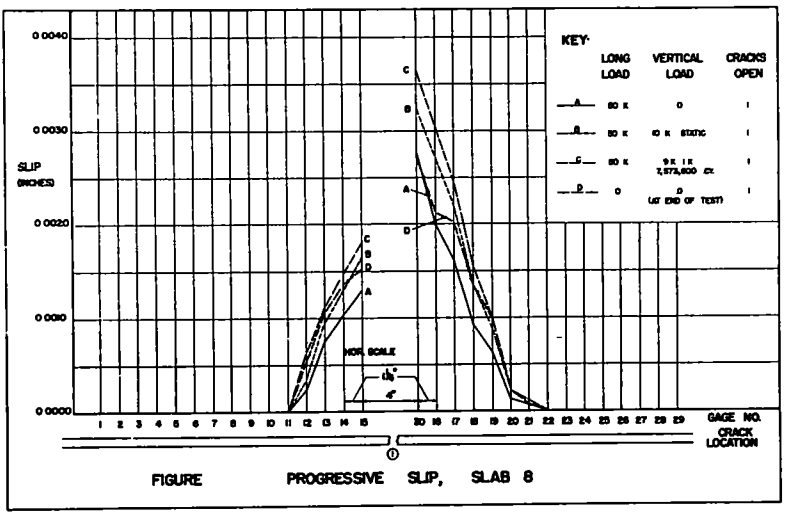


FIGURE PROGRESSIVE SLIP, SLAB 8

Figure 12. Progressive slip, slab 8.

A comparison of curves A and C in Figure 12 reveals more clearly the progressive movement of the steel with respect to the concrete. The crack ① occurred at the weakened plane in this slab and was therefore approximate 2 in. from gages 15 and 30. From the nature of the curves it is apparent that the crack was nearer gage 30 than gage 15. It is also apparent that with only the longitudinal force the maximum observed slip was the nature of about 0.0027 in. (at gage 30), and that gages beyond Nos. 11 and 22 recorded 0 slip. After 7,573,800 cycles of 9K-1K loading the maximum slip had increased to about 0.0037 in. at gage 30, and the values for slip were still recorded as 0 at gages 11 and 22.

Figure 12 is typical of the information obtained from experiments with the other slabs. Because the plastic gage functions only in a positive direction, any crack occuring between gages 1 to 15 or between gages 30 to 29 causes some slip in the negative direction for certain gages and therefore they become useless.

TABLE 4

MAXIMUM EXTENSION OF SLIP AWAY FROM CRACKS

| Slab | Max. Distance from Crack (in.) | | |
|---|---|---|---|
| | 0.002-in. Slip | 0.001-in. Slip. | 0 Slip |
| 1 | 5 | 7½ | 9½ |
| 2 | 6½ | 10 | 14 |
| 3 | 5½ | 7 | 11 |
| 4 | 4 | 6½ | 11 |
| 5 | 4½ | 6 | 12 |
| 6 | 5 | 8½ | 12 |
| 7 | 5½ | 8½ | 12 |
| 8 | 5½ | 7 | 11 |

Tables 3 and 4 reveal some points of interest in regard to the point of zero slip. Table 3 clearly shows that the point of zero slip remained practically constant once the midlength crack occurred. In Table 3 the decreases in this initially recorded distance to zero slip are attributed to later cracks which caused some plastic gages to function in a negative direction and therefore subsequently provide useless data. However, many of the cracks given in Table 3 were outside the middle 5 ft of slab and had no effect on the gage readings. Throughout the experiments it was the desire that the slabs crack only at the midlength weakened plane but this was only obtained in the case of slab 8. Table 4 was compiled using only data from gages unaffected by negative slip. Slab 2, which was loaded longitudinally with 70 kips, exhibited some slip along bar C as far away as 14 in. from a crack. For all the other slabs that were loaded with a 50-kip longitudinal force the point of zero slip was within 12 in. of the crack; i.e., with a

50-kip longitudinal force on an 8- by 36-in. cross-section of slab, 7,000,000 repetitions of vertical loads as large as 17 kips did not produce any slip at points over 1 ft from the cracks.

The point of zero slip did not change when the repetitive vertical loading was increased from 9K-1K to 17K-1K. Also, the slabs with the longitudinal steel $\frac{3}{4}$ in. below mid-depth gave results very similar to those obtained from slabs with this same amount of steel at mid-depth.

## Deflections and Crack Widths

The deflection data observed in these experiments were solely for the purpose of evaluating the severity of the vertical loading system. These data led to a decision to load slabs 7 and 8 at points EE and WW rather than at points E and W as used in the previous slabs. This change was made to be certain of some upward and downward movement of the slab at the midlength point. Deflection as well as crack width data observed for slab 8 are shown in Figure 13.

Although information on crack widths was obtained for all cracks in all slabs with the exception of slab 1, these data are not presented in this paper but are available elsewhere (4). The crack width data for the crack at midlength, called crack ① in all slabs, are given in Table 3. Some crack-width values for top surface cracks recorded in this table are shown as negative and therefore need explaining. Crack-width values recorded in this table are the difference in readings observed on Whittemore gages set on plugs placed at 10-in. intervals on the slab. The base for these readings was the initial no-load condition of the slab. Once a crack occurred, some spalling and change in slab configuration took place; hence the data reflect that the plugs were closer together (horizontally) than they were before the experiment began. The crack widths measured at the elevation of the steel on the side of the slabs are therefore considered more meaningful.

## Steel Stresses

The electric resistance strain gages placed on bars B and D of slabs 6, 7, and 8 were a supplementary part of the instrumentation, and data from these gages were

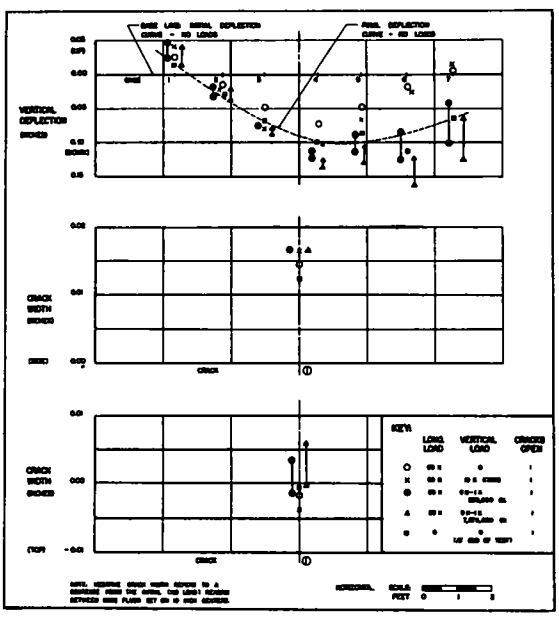

Figure 13. Vertical deflections and crack widths, slab 8.

erratic and therefore of doubtful value. For this reason the data are not reproduced in this paper. The gages did reveal that practically 90 percent of the longitudinal force applied at the ends of the slab was present at the midlength point, and that the steel was stressed to about 50,000 psi under the 9-kip vertical and 50-kip longitudinal loads. The strains caused by the varying vertical loads were not more than a few percent of the strain caused by the longitudinal load.

## SUMMARY OF CONCLUSIONS

As a result of these experiments on short lengths of slabs resting on subgrades with a constant subgrade modulus of 140 to 145 lb per cu in. and subjected to constant longitudinal forces, the following statements can be made:

1. The plastic gage used in conjunction with the Sheffield Column Type Precision-aire instrument provides a simple and practical means of determining the differential movement of steel reinforcing bars with respect to concrete. The plastic gages can be used on alternate sides of the bars and thus provide slip data at intervals as close as $1\frac{1}{4}$ in. without any apparent detrimental effects on the quality of the concrete.
2. These experiments provide evidence that beyond 12 in. from a crack there is no slip between the reinforcing bar and the concrete in slabs subjected to temperature drops which are equivalent to not more than the 50-kip longitudinal force used in these experiments. This length of bar along which some slip occurs remains practically constant from the instant the crack is formed, regardless of the number of repetitions of a heavy vertical load; that is, there is very little, if any, progressive slip due to vertical loads.
3. Once a crack has formed, repetitive vertical loads of as much as 17 kips cause larger slip values throughout the length of bar along which slip first occurs. However, slip values are in general less than 0.002 in. at points 6 in. or more from the crack even after 7,000,000 repetitions of this vertical load.
4. There is practically no possibility of large truck wheel loads causing slip to progress from crack to crack in a continuously reinforced pavement since cracks generally occur in such pavements at intervals much greater than 2 ft. Consequently, the possibility of a progressive bond failure due to such wheel loads is quite remote when about 0.5 percent steel is placed near the middepth of the slab.

## ACKNOWLEDGMENTS

This research was used by the senior author as a thesis project for partial fulfillment of the requirements for the degree of Doctor of Philosophy.

The authors are indebted to G. R. Frederick and H. J. McConkey, Graduate Assistants, who aided in the experiment program and in the preparation of the data and drawings.

## REFERENCES

1. Gutzwiller, M. J., and Waling, J. L., "Stresses and Deflections in Concrete Pavements Continuously Reinforced with Welded Wire Fabric." HRB Bull 238, 48-63 (1960).
2. Gutzwiller, M. J., and Waling, J. L., "Laboratory Study of Pavements Continuously Reinforced with Deformed Bars." Jour. Amer. Concrete Inst., 51: No. 3 (Sept. 1959).
3. Subcommittee VII, ACI Committee 325, "Continuous Reinforcement in Highway Pavements." Jour. Amer. Concrete Inst. 30: No. 6 (Dec. 1958).
4. Moore, J. H., "Dynamic Response of Reinforced Concrete Slabs." Ph. D. thesis, Purdue University (Aug. 1961).

# Concrete Pavement Designs in Five Countries of Western Europe

GORDON K. RAY, Manager, Paving Bureau, Portland Cement Association, Chicago, Ill.

Highway building agencies in Great Britain and the countries of western Europe use a wide variety of concrete pavement designs as do the engineers from various highway departments in the United States. Concrete pavement thicknesses observed on a recent visit to five different countries ranged from 5 to 11 in. on a wide variety of subbase types and thicknesses. Jointing arrangements also varied from plain pavements with a short joint spacing of 15 ft to pavements containing distributed steel and expansion joints at approximately 120 ft.

Joints were formed by sawing premolded fiber inserts and by hand-forming the plastic concrete. In addition, some agencies use a parting strip that is placed on the subgrade below the dummy groove. Practices with regard to distributed steel, load transfer devices, and tie bars are quite similar to those followed in this country.

All countries visited have experimented much more extensively with prestressed pavement than the United States. Both highway and airfield pavements have been built under a wide variety of service conditions. These include post-tensioned slabs that are prestressed in both directions and also in the longitudinal direction only. There are also a number of prestressed pavements in which longitudinal prestressing is accomplished by the use of flat jacks and end abutments, either fixed or elastic, with or without transverse steel. A review of the prestressed projects in Europe indicates a need for additional research on this type of construction in the United States.

• TOO OFTEN there is a tendency to think that the United States leads the world in highway development and, of course, highway research and pavement engineering. Perhaps it does lead in total pavement mileage, dollars expended, rates of construction, and vehicle-miles driven on highways; however, a recent visit to England and several countries of Western Europe has convinced the author that the United States is not necessarily leading the world in amount of highway research, quality of construction, or ingenuity, or economy of construction.

Although the Atlantic Ocean, the language barrier, and travel limitations imposed by many highway building agencies make a free interchange of highway research information difficult, the United States would profit by a closer knowledge of designs, research, and experience in other countries. This does not imply that the various countries in Europe have complete interchange of information on pavement research or that they have unanimity of opinion with regard to pavement design methods or details either. Rigid pavement design details in Europe vary almost as much from country to country as they do here from state to state. Pavement thicknesses, subbase design, joint spacing, and use of steel have changed over the years to give the best service for their individual conditions of climate, soil, traffic, and engineers' personal preferences much as they have in the United States.

This paper covers some of the aspects of rigid pavement design. More details of the prestressed pavement projects will be included in the report of the subcommittee on prestressed pavement of the Rigid Pavement Design Committee. All countries

visited in Europe have shown much more interest in prestressed pavement than this country and all those visited have built experimental projects.

## UNITED KINGDOM

In the United Kingdom, highway research is carried on by the Road Research Laboratory of the National Government at Harmondsworth and additional research on concrete and soil-cement by the laboratory of the Cement and Concrete Association at Wexham Springs. Many of the large contractors in England have their own laboratories with well-equipped, well-staffed research organizations. One organization, the Pavings Development Group, made up of engineers, contractors, equipment, and material people, has the specific function of studying design and construction techniques of other countries. This they accomplish through papers by engineers from other countries at their annual meeting and by sponsoring trips to other countries to inspect highway and airport facilities.

The most common design in England is similar to that used in New Jersey. Transverse expansion joints are usually spaced at 80-ft intervals with 1¼-in. diameter dowels at 12-in. centers. The grooves above the expansion joint fillers are sawed in the hardened concrete. Distributed steel for this design is welded wire fabric weighing 111 lb per 100 sq ft. On the M-1, the London-to-Birmingham motorway (England's first real expressway) the concrete portion was 11 in. thick on a 7-in. subbase of gravel, cement-treated gravel, or crushed concrete choked with sand. On the M-1 slabs were 80 ft long with expansion joints and contraction joints alternated at every other joint or 120 ft with expansion joints only.

The concrete, which was not air-entrained, had a compressive strength of over 4,000 psi at 28 days. Water-cement ratios are usually less than 0.5 by weight and slumps are very low, requiring heavy vibration or tamping to insure consolidation and permit finishing.

In England the legal wheel load is 11¼ tons. Total gross loads of 250 tons may be carried on selected routes controlled by the Ministry of Transport. The design life used on bridges is 100 years.

To improve surface riding qualities construction specifications now require the use of "articulated" finishers. These are much the same as the long wheel-base, float-type finishing machines now used on many of U. S. projects.

One full-scale test road, 2¼ mi long, has been built at Alconbury Hill by the Road Research Laboratory to compare concrete of various designs and thicknesses with several different types and thicknesses of flexible base. This project, built in 1957, is subjected to normal traffic consisting of over 4,000 commercial vehicles per day.

Several short sections (about 500 ft long) of prestressed pavements were built as experiments on various industrial driveways and access roads, but most did not carry heavy volumes of truck traffic. They all contain internal prestressing tendons in either both directions or diagonally. All have performed satisfactorily.

At the Gatwick Airport near London, there are two prestressed concrete aprons and three prestressed taxiway slabs, two of them 970 ft long. They are 5 and 6 in. thick, carry heavy airline traffic, and are performing well with no signs of distress. Both transverse and longitudinal prestressing tendons are employed with the amount of prestress varying from 100 to 300 psi. All were post-tensioned. It is doubtful whether this design was more economical than the conventional concrete design used elsewhere at the airport.

## FRANCE

In France, highway research is carried on by the Central Laboratory of Bridges and Highways of the French Government Department of Public Transportation (Laboratoire Central de Ponts et Chaussees, Ministere des Travaux Publics et des Transports). Additional research on cement and concrete is carried on in the laboratory of the cement industry in Paris (Centre d'Etudes et de Recherches de L'Industrie des Liants Hydrauliques). M. A. Mayer, President of the latter institution, prepared a paper on prestressed pavement for the Highway Research Board in 1960.

Most concrete highways in France are plain concrete also without air-entrainment, The Paris Southern Motorway (L'Autoroute de Sud), a six-lane expressway, leading into Paris from the South for 26 mi, was built between 1956 and 1960. It is 10 in. thick on $5\frac{1}{2}$ in. of sand base stabilized with cement on a 4-in. subbase of fine sand in some sections and on a $5\frac{1}{2}$-in. gravel subbase in others. Expansion joints were used at approximately 195 ft and sawed contraction joints at 15-ft intervals. Dowels were used in expansion joints but not in contraction joints.

Concrete in this project had about $5\frac{1}{2}$ sacks per cu yd and a 28-day flexural strength of 640 psi. A low-slump concrete was used and riding qualities are poor. In an effort to improve ridability the French have modified their specifications on one or two new experimental projects to permit a higher slump and the use of American-type equipment with some type of longitudinal float.

The legal axle load in France is a 15,000-lb single axle. Most trucks have two single axles and pull a full trailer with two single axles.

France has built several prestressed projects, first on the Orly Airport (Fig. 1) and an airfield near Algiers (Fig. 2) and later in 1960 on a highway near Paris. The highway project is an experimental road $1\frac{1}{2}$ mi long consisting of 38 demonstration or test sections. Five different contractors built prestressed pavements of their own design to provide a specified amount of prestress in the longitudinal direction. Slabs were built with both longitudinal and transverse prestress and with only longitudinal prestress. Prestressing was accomplished by various combinations of longitudinal, transverse, diagonal, and peripheral tendons and by longitudinal post-stressing obtained by applying external longitudinal compression against either fixed or elastic abutments without the use of internal longitudinal tendons. (Post-stressing is a term

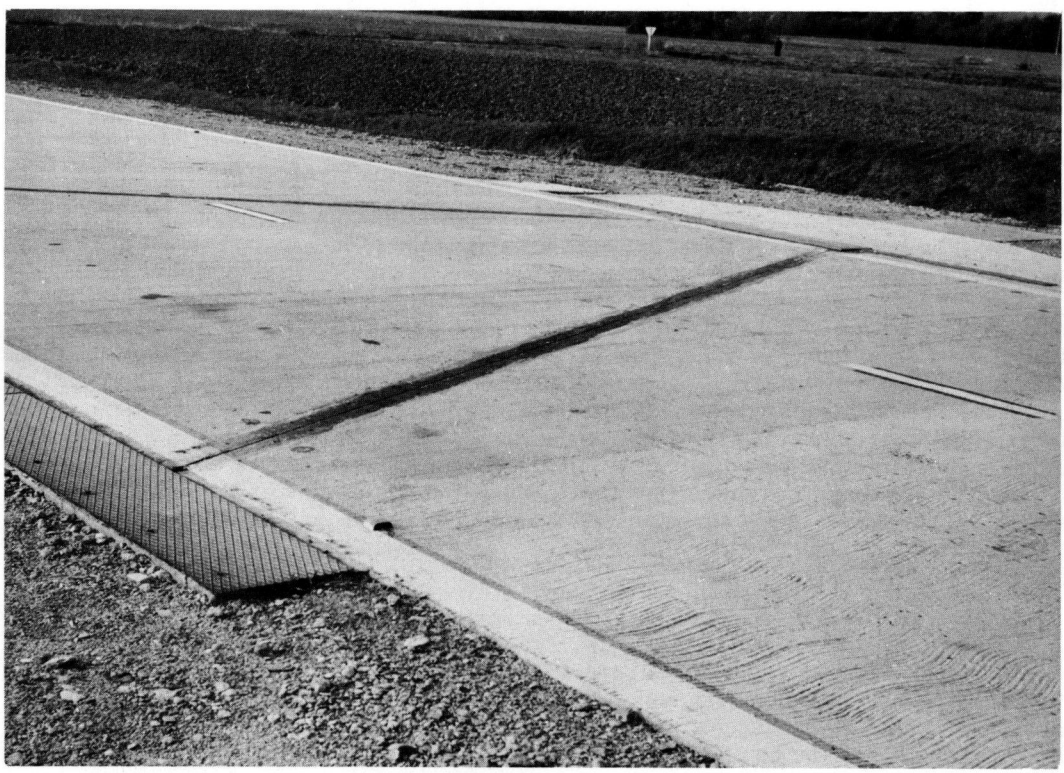

Figure 1. Transverse wedge section for applying longitudinal prestress to section of experimental highway pavement near Fontenay-Tresigny, France.

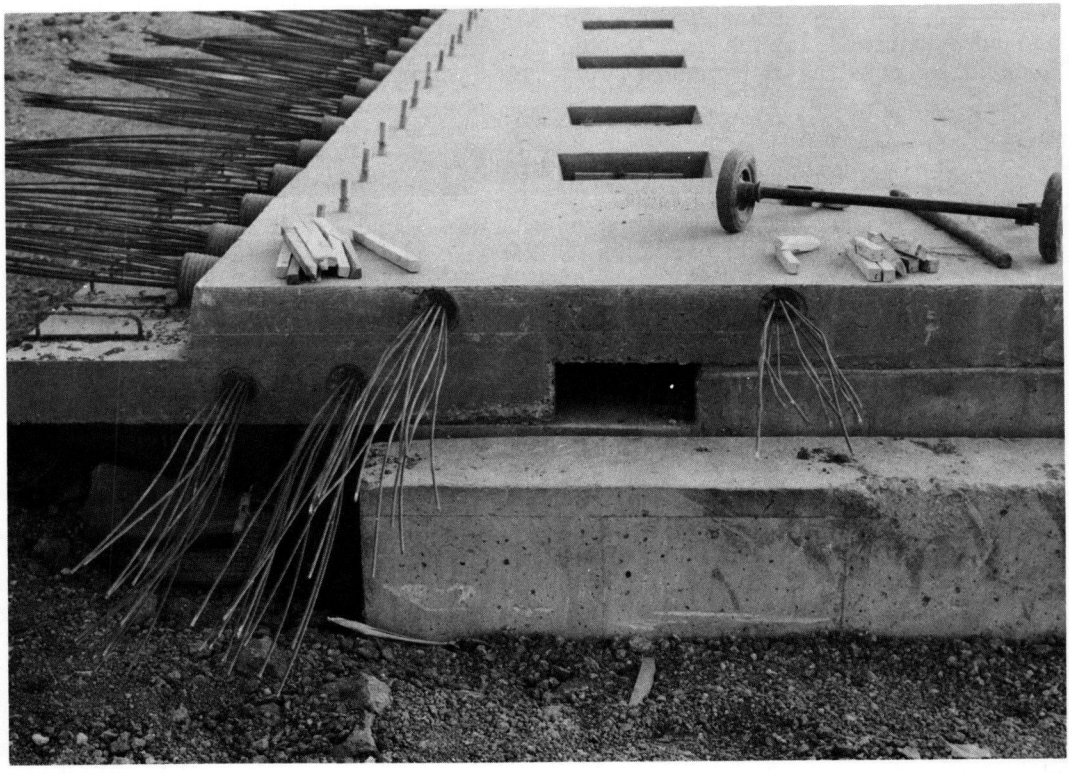

Figure 2. Details of anchorages for prestressed runway under construction at Maison Blanche Airport near Algiers during 1960. Longitudinal wires at left are part of elastic underground abutment which is post-tensioned. The wires in foreground are transverse prestressing for elastic abutment.

developed by subcommittee on Prestressed Pavement in its report to describe prestressing accomplished without longitudinal steel by using flat jacks, wedges, or other means for placing pavement in compression against fixed or elastic abutments.)

This is a daring research project employing many different ideas in a thin (4.7-in.) slab on a regular highway carrying rather large volumes of heavy commercial traffic. Much should be learned from the careful observation being carried out by the Central Laboratory of Bridges and Highways.

At Orly Field near Paris there is a 1,400- by 82-ft., 7-in. thick prestressed taxiway built in 1953 by the post-stressing method. This project with transverse prestressing tendons for post-tensioning and with elastic abutments and flat jacks for post-stressing in the longitudinal direction was the pioneer in this type of prestressing without internal longitudinal steel tendons. It is performing well under heavy aircraft loads with no serious distress although some transverse cracks are apparent. These cracks reportedly developed during a cold spell the first winter after construction, before the slab was subjected to loading. There was an earlier prestressed runway at Orly built in 1947 of precast slabs with diagonal joints and rollers. It was overlayed some years ago. It was reported to be quite rough.

Using the Orly taxiway as a model, the French later built a taxiway and two runways at Algiers on a large civil airport. These were an 8,000- by 197-ft runway and 6,700- by 82-ft taxiway in 1954, both 7.1 in. thick in 1960 and 1961. All three were placed on a 12-in. gravel subbase and had an initial longitudinal prestress of about 240 psi. Transverse prestressing was obtained by post-tensioning internal steel tendons. Longitudinal prestressing was by flat jacks in transverse joints jacking against elastic-type abutments consisting of underground prestressed slabs anchored beneath the main slab. Engineers claim this method of construction in Algiers was cheaper than the conventional

concrete design at the same airport. For aprons, 12 in. of plain concrete was used, and curved taxiways for the same traffic. There was no evidence of distress or failure in any of the prestressed pavement built in 1954. The 1960 runway was not yet complete.

## SWITZERLAND

Switzerland has a rather unique organization, Betonstrassen, Wildegg (Concrete Roads Association), which is unlike anything in the United States. This organization, supported by cement manufacturers in Switzerland, is responsible for the many miles of smooth-riding, durable, quality concrete roads. Betonstrassen designs all concrete for the various state (canton) construction agencies determining thickness, jointing arrangement, steel quantities, and mix design. It also writes the specifications and supervises all construction, providing engineers and inspectors. After the pavements are completed Betonstrassen maintains nearly all concrete on a service contract basis ($0.01 per sq yd per yr for roads that are 10 to 30 years old, $0.005 for new roads) with small teams of experienced, qualified maintenance personnel. It also maintains a research laboratory.

Concrete pavements are used extensively in Switzerland on their two-lane primary highways, rural farm highways, village streets, and mountain and forest roads. Current as well as all planned projects for "Autobahnen" (Switzerland's express highway or motorways system) will also be largely concrete. In all cases the pavement is designed for the anticipated conditions of soil and traffic. Farm roads may be only 8 ft wide and 5 in. thick, Autobahns are about 8 in. thick, and other classes of pavements fall somewhat in between.

Expansion joints are usually omitted and contraction joint spacings vary from 15 to about 35 ft. All the concrete roads in Switzerland are doweled. Mesh is used on most pavements (4 to 5 lb per sq yd) except on some farm or forest roads where edge or corner bars are used. On some recent projects doweled contraction joints are used at every third joint interval and intermediate joints are simply warping joints tied with deformed hook bars. Most joints are machine vibrated with inserts or sawed, except on farm or forest roads where they are hand formed.

Concrete pavement is air entrained and all no-slump central mix concrete placed with tampers and heavy vibrating beams. It is finished with longitudinal floats imported from the United States and riding qualities are the best in Europe. Incidentally, the surface left by the longitudinal float is the final surface finish. No handwork or burlap drag is necessary except on steep grades where the surface is scored transversely at close intervals. Recently on such grades they have accomplished a special surface by using an upper layer of concrete without sand to form a rough texture.

On all roads a granular subbase sometimes stabilized with cement is used. On peat deposits, and there are many in Switzerland, concrete is used frequently. Here granular subbases and concrete pavement thickness are reduced to eliminate unnecessary weight. Joint spacings are shortened to about 15 ft and all joints are doweled and all slabs contain distributed steel. This design has worked excellently. Although the pavements may settle over a period of time, there is no cracking, and riding qualities are maintained except for the gradual depression. On one 23-year-old project, total settlement has been approximately 2 ft without pavement failure.

On main roads red, white, and black concrete are used to designate acceleration and deceleration lanes, road edges, and foot paths or cycle lanes which are frequently placed immediately adjacent to roadway slabs.

Switzerland has also built several prestressed pavements. Two of these are post-stressed without longitudinal steel tendons. The first, built in 1956, is 1¼ mi long and includes a horizontal curve. Prestressing was obtained by means of large transverse wedges that were jacked horizontally to impart the longitudinal prestress against fixed end abutments. Transversely the slab is reinforced with deformed bars. Another pavement, built in 1960, is 0.8 mi long, 5.9 in. thick, and 34 ft wide. To insure adequate longitudinal prestress during cold winter weather on this project, and to prevent loss of prestress due to creep and to prevent buckling due to high temperature expansion,

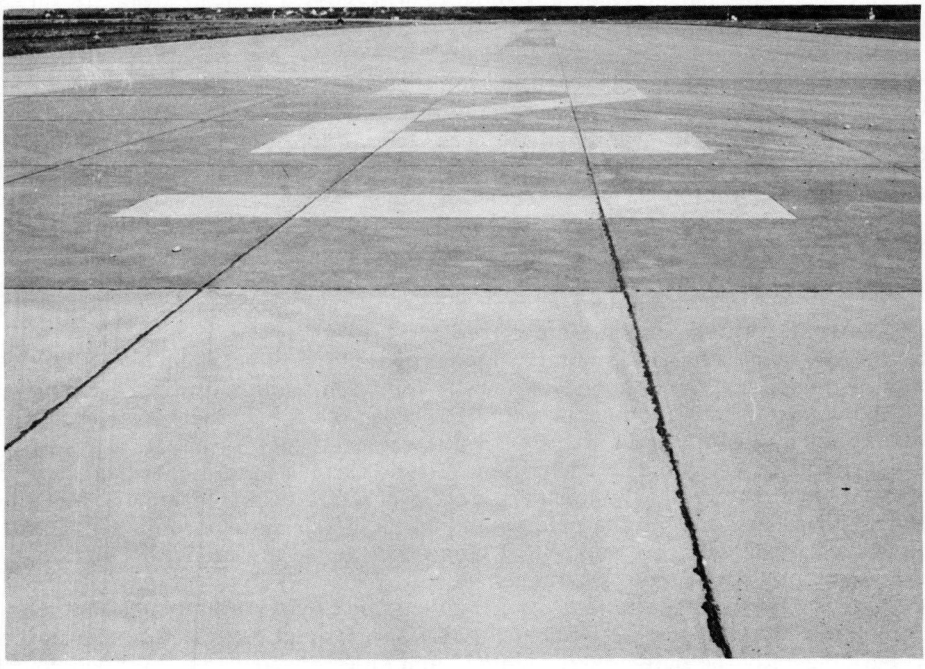

Figure 3. Concrete runway, Zurich Airport, Switzerland, illustrating use of colored concrete to form runway numbers. This eliminates need for special traffic paint.

the flat jacks were left in the joints and connected with automatic hydraulic pumps in a roadside building to insure a uniform amount of prestress over a period of about two years, when jacks will be removed and joints filled with concrete and immobilized. Both of these prestressed projects are serving normal mixed traffic and both are in excellent condition with no defects or failures.

The concrete pavement in Switzerland is excellent in all details, justifying its use on all classes of Swiss roads (Figs. 3 and 4).

## FEDERAL REPUBLIC OF GERMANY

In Germany there are several organizations interested in research on concrete pavement. The Forschungsgesellschaft für das Strassenwesen E. V. Koeln (a highway research corporation similar to the Highway Research Board), the Forschungsinstitut der Zement Industrie (the technical research organization of the cement industry in Germany) and the Deutsche Beton-Verein E. V. (The German Concrete Contractors Association).

Concrete is used in Germany primarily on the autobahn system. All of the original

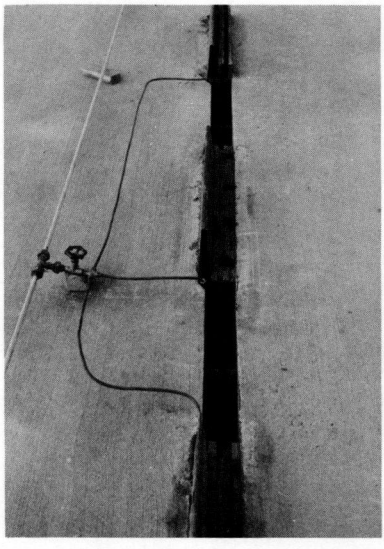

Figure 4. Flat jacks used for post-stressing runway pavement at Maison Blanche. Jacks activated by hydraulic fluid through tubing system from large hydraulic pumps are used in combination with flat steel plates to obtain desired amount of joint opening and slab compression. Round dowels between jacks are used to prevent buckling at joints.

system was concrete, but inasmuch as most of it was built without granular subbase and without air entrainment, much of the 20-27-year-old pavement is showing distress from scaling or pumping.

New autobahn concrete is 8.5 to 10 in. thick but it is all air entrained and all placed on substantial subbase, usually a $2\frac{3}{4}$-in. bituminous stabilized base on a sand gravel subbase about 12 in. thick. On most projects contraction joints are spaced at 40 to 60 ft with expansion joints at 180 ft, all doweled. The recent trends seem to be toward shorter contraction joint and longer expansion joint spacings. All slabs contain mesh weighing about 62 lb per 100 sq ft. The longitudinal wires are spaced more closely together along slab edges. On one experimental project near Baden-Baden they used a 30-ft contraction joint spacing and built sections with expansion joints at 300, 600, and 900 ft (Fig. 5). On this same project they also built test sections with three types of subbase, cement-treated, asphalt-stabilized and tar-stabilized.

Joints in Germany are sawed and final surface texture is obtained by brooming. Germany also uses no-slump concrete usually mixed in traveling mixers riding on the forms. All concrete is placed under roofs riding on the forms which keep the slab protected from sun and rain for 24 hr.

Germany has not yet adopted a longitudinal-type float but the riding qualities of recent projects are excellent. On all autobahns a strip of white concrete is built along both edges about 18 in. wide along the median and 24 in. along the outside edge. Shoulders are sometimes black concrete and sometimes the reverse is true with a darkened roadway with normal grey concrete shoulders.

The German highway departments are trying some novel maintenance methods to retain some of the older prewar autobahns. On one project near Bad Nauheim they were rebuilding only the outer 12-ft lane on each side of a four-lane divided roadway. The new lane was 10-in. mesh pavement with contraction joints at 26 ft and expansion joints at 105 ft to match the joints in the original inner lane. Subbase was being used under the new outer lane which is separated from the inner lane by a longitudinal wood board expansion joint. Finally, the inner lane was mudjacked with a sand cement slurry to correct for any settlements and match the elevations of the new outer lane. In other areas where the old original autobahn has only isolated slab failures these are

Figure 5. Concrete Autobahn near Baden-Baden, Germany, showing use of black concrete shoulder, white concrete strip for edge marking, and normal colored concrete roadway.

sometimes replaced with precast, prestressed slabs, 40 ft long, produced in a prestressing plant and placed in one quick operation, reopening to traffic in a short period.

In Germany, too, they are building prestressed pavement, but they no longer consider it experimental on airports (Fig. 6). There are several airfield and highway projects all prestressed in both the longitudinal and transverse directions using internal steel tendons and post-tensioning. So far there are about 1,500,000 sq yd of air-field pavement all built on a competitive basis with conventional concrete. Slabs are usually about 500 ft long and steel bridge type of expansion joints or rubber and steel plate combinations (similar to those used on the Jones and Laughlin experimental project near Pittsburgh) are used at each joint. Near Bingen they built a prestressed highway pavement 2,950 ft long, 25 ft wide, and 6.4 in. thick in 1958, made up of six 492-ft slabs. These were on a 6-in. bituminous stabilized base on 16 to 24 in. of gravel subbase. This project also contains precast concrete curb and gutter, concrete shoulders and precast concrete guard rails (Fig. 7).

## BELGIUM

There was no opportunity to observe normal highway pavements in Belgium, but inspections were made of prestressed highway and airport pavement. The airport at Brussels has two projects. One is a taxiway made up of pretensioned, precast trapezoids only 4 in. thick. Although this is carrying aircraft traffic with no indications of

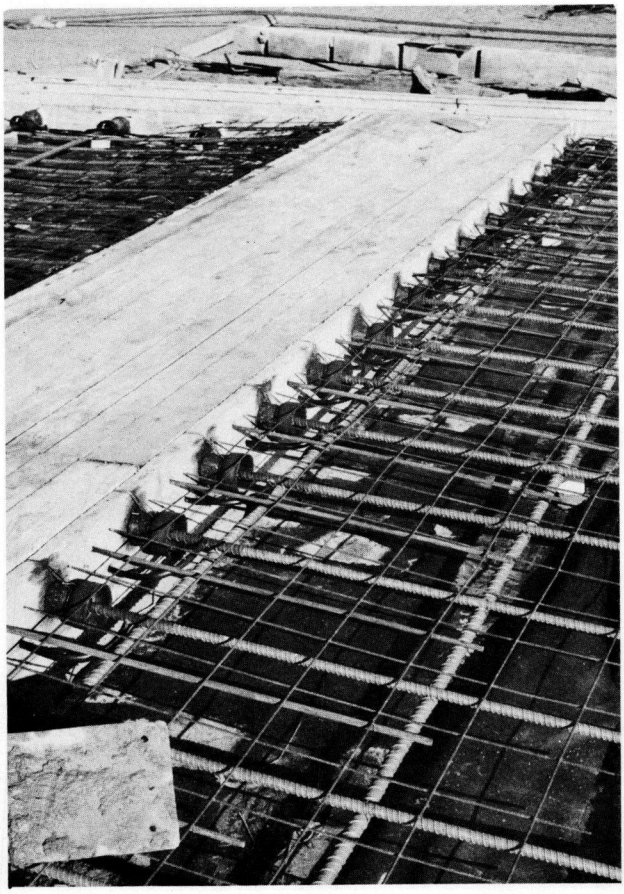

Figure 6. Details of slab end reinforcing and conduit placement for post-tensioning tendons in runway slab under construction at new Wahn Airport serving Cologne and Bonn.

failure, it is quite rough and uneven. The 10,800-ft runway and a 2-mi highway project, both built in 1960, employ the French method of post-stressing using fixed abutments and flat jacks in transverse joints at 350- to 450-ft intervals. Transverse prestressing is provided by post-tensioned wires. On both projects, tunnels are provided under every second or third joint and some of the flat jacks are left in so that additional compression can be applied, after slab creep and contraction due to lower temperatures, without interruptions to traffic. These tunnels also serve as tie downs or anchors to prevent buckling at these joints.

Figure 7. Precast concrete curb and gutter sections and precast concrete guardrails used adjacent to prestressed highway section near Bingen, Germany.

This method of correcting the amount of prestress during the early life of the pavement is considered necessary in slabs without internal longitudinal tendons unless an excessively high amount of prestress is applied initially. The highway project is definitely experimental including 3.2-, 3.9-, and 4.2-in. pavement thicknesses, three different levels of prestress, transverse prestressing in some sections and transverse reinforcing in others, and two horizontal curves with transverse abutments outside the curves.

## SUMMARY

It is apparent from this brief description of projects in these five countries that the United States is not the only country having engineers interested in concrete pavement design.

In spite of the many prestressed projects described, it is not intended to infer that these are standard designs or that they are more economical than conventional pavements for highways. They are really experiments to investigate construction methods and to determine performance characteristics.

It is not claimed that their designs are better than those in the U.S. or that they have necessarily advanced further or faster. However, closer study by American engineers of research and development in all foreign countries is recommended.

# Experience in Texas with Terminal Anchorage of Concrete Pavement

M. D. SHELBY and W. B. LEDBETTER, Respectively, Research Engineer, and Design Engineer, Texas Highway Department

The excessive movement of terminals (or ends) of concrete pavements has long been a source of trouble to the highway engineer. Recently a new concept in the handling of terminal movement of concrete pavements adjacent to structures has been introduced employing terminal anchorages. A system of shallow, inexpensive, reinforced concrete anchor lugs, 2 ft wide and 3 ft deep, is cast monolithically with the concrete pavement near the terminals, acting to restrain a major portion of terminal pavement movement by developing the resistance of the soil. In March 1959 a two-lug anchorage system was placed at the terminals of a jointed, unreinforced concrete pavement. Since that time a number of projects have been built employing lug anchorages, including four- and five-lug anchorage systems on continuously reinforced concrete pavement. Experience to date with these terminal anchorage systems is reported, together with their design basis. At present the lug anchorage systems are performing well in restraining terminal movement and a more widespread use of this design concept is predicted.

•THE TERMINALS (or ends) of a concrete pavement present a unique problem to the highway engineer. Like most materials, concrete changes volume significantly with changes in its temperature and moisture content. This volume change is three dimensional on an unrestrained specimen of concrete, but due to a pavement's long length practically all volume change of interest occurs as a change in pavement length. Furthermore, the significant portion of this length change occurs only within several hundred feet of the terminals, depending on the extent of subbase friction present.

Experience in Texas indicates that unreinforced concrete pavement resting on a granular type of subbase will, as it undergoes volume changes, normally crack transversely about every 10 to 20 ft along the pavement length. Therefore, current practice in Texas in designing this type of pavement is to create transverse planes of weakness (contraction joints) every 15 ft to induce controlled cracking at these locations. In the interior portion of the pavement, each 15 ft slab shrinks and expands slightly due to temperature or moisture content changes in the concrete. This interior portion is effectively restrained and the concrete is not allowed to expand and contract freely. In this portion of the pavement there is no significant problem in the handling of these volume changes. However, in the end portions, where volume changes are relatively unrestrained, problems arise that sometimes create detrimental results.

In this portion, the cracks formed from the planes of weakness often open considerably. Even though these cracks are sealed, deleterious material often finds its way into them while the crack is open. Then when the concrete expands, the cracks cannot close fully, resulting in an internal compressive force buildup with an outward push or growth increasing toward the terminals. As a consequence, after many cycles of pavement expansion and contraction, the pavement, in effect, grows or enlarges in length due to a progressive crack opening. This growth of jointed unreinforced pavement can seriously damage an adjacent structure.

Figure 1 shows an abutment where concrete pavement growth has closed the expansion joint, ruptured the concrete abutment, and pushed the bridge. This may be noted by the position of the rocker arm supporting the steel girder.

On jointed, reinforced concrete pavements current practice in Texas is to place only a nominal amount of steel in the pavement, which will permit contraction joint spacing to be increased from the previously mentioned 15 ft to around 60 ft. Although there are not as many joints with this type of pavement as with jointed unreinforced concrete pavement, these joints open wider, with the result that pavement growth occurs with this type of pavement much the same as with jointed unreinforced concrete pavement.

Figure 1. Bridge abutment showing damage resulting from concrete pavement growth pushing on bridge abutment.

A third type of concrete pavement, which is gaining widespread acceptance in Texas, is continuously reinforced concrete pavement (1). With this type of pavement, enough steel is added to the concrete to eliminate all contraction joints. These contraction joints, in a sense, are replaced with a series of closely spaced, hairline cracks, held tightly closed by the reinforcing steel (2). The cracks are small enought to prevent the intrusion of foreign material, consequently the problem of pavement growth due to progressive crack opening in the end portions appears to have been eliminated. (In Texas, a project containing this type of pavement has been in service for 10 years and no problems of pavement growth have occurred.) However, the foregoing is not to be misconstrued to indicate that terminal movements have not occurred with continuously reinforced concrete pavements. As the name implies, this type of pavement acts structurally as a continuous unit. Experience in Texas indicates that the end 150 to 300 ft moves— depending on the degree of subbase friction present. Due to the reinforcing steel, shortening as well as lengthening of the pavement occurs with changes in concrete temperature and moisture content. Experience in Texas seems to indicate a terminal movement of plus or minus $1\frac{1}{2}$ in. might be expected with continuously reinforced concrete pavements over a granular type of subbase (3).

Various methods have been used to provide for this movement and still maintain a smooth riding surface, prevent intrusion of water into the subbase, and provide the necessary load transfer across the terminal points. One or more expansion joints have been used at terminals, consisting of the relatively inexpensive sealed doweled joint or occasionally the relatively expensive steel finger joint. Figure 2 shows one of the steel finger joints on a continuously reinforced concrete pavement. The joint is designed to allow up to $1\frac{1}{2}$ in. of movement while providing the necessary load transfer, etc.

Recently, an entirely new concept of handling terminal movements has been introduced. Preliminary studies have been initiated on the campus of the University of Virginia. The design employs a series of inexpensive, shallow, rigid lugs, cast monolithically with the pavement slab, that act as a series of restraining members and, by developing passive resistance of the soil, restrain a major portion of terminal pavement movement. To the author's knowledge this concept, being new, has not been fully explored either in the laboratory or in the field, and few published data can be found. In one report, (4) this subject was discussed and a number of model studies were reported which yield some valuable information on predicting the behavior of such an anchorage system under stress conditions that might be imposed through the restraining of pavement volume changes.

In this report, experience in Texas to date with the use of the lug anchorage systems in both jointed and continuously reinforced concrete pavement is discussed, summarizing

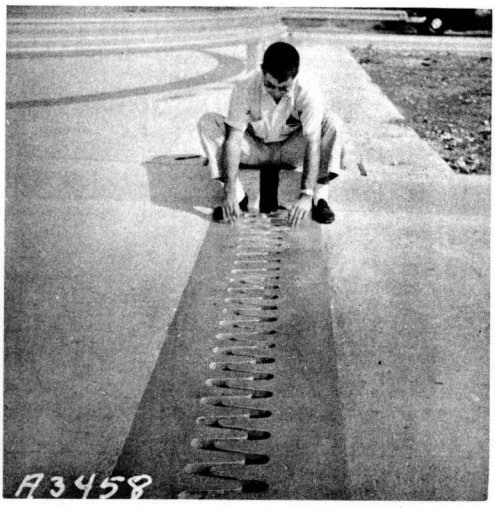


Figure 2. Finger joint at terminal of continuously reinforced concrete pavement.

current design concepts and design details employed as of this writing. Before continuing, it should be emphasized that the problem of terminal treatment of concrete pavements has been receiving increased attention in several sections of the country and the design and use of an anchorage system such as reported herein is rapidly changing as experience is gained and investigations reveal further information on the subject. In all probability, many changes will have been made in terminal anchorages between the writing and the publishing of this report.

## JOINTED PAVEMENT EXPERIENCE

In March 1959, District 12 (Headquarters in Houston) constructed the first terminal anchorage system in Texas. This system was used at the terminals of a jointed, unreinforced concrete pavement adjacent to structures on each of the approaches to three sets of twin structure overpasses on Interstate 45 north of Houston (Project I 45-1(12)67). Two anchor lugs, 3 ft deep and 2 ft thick, were placed monolithically with a 10-in. reinforced anchor slab at each pavement terminal. The pavement, which also was 10 in. thick, contained corrugated metal contraction joints at 15-ft intervals and no expansion joints other than at pavement terminals adjacent to structures. Figure 3 shows the lug anchorage design used on this project. Figure 4 shows the reinforcing steel in the lug trench before the concrete placement.

The design basis for this anchor system was, to a large degree, engineering judgment. It is difficult, if not impossible, to ascertain what forces will develop by preventing pavement growth. By preventing this growth from the beginning of the pavement life, the contraction cracks in the terminal portions of a pavement are prevented from progressive opening, thereby reducing the amount of infiltration of foreign material. Consequently, growth forces in all probability would be much lower than on projects where infiltration of foreign material into the contraction joints occurred. Some pavements in Texas have grown or lengthened several inches as a direct result of progressive crack opening near the terminals, but to assume that an anchorage system must be designed to restrain several inches of movement appears to be unnecessary. Therefore, two lugs were tried by District 12.

This first project has been under observation since its completion and the performance of the lugs to date has been outstanding. Some hairline longitudinal and transverse cracking has occurred directly over one of the lugs in the outside lane at the Rankin Road overpass on this first Harris County project shortly after completion, but these cracks are not detrimental to the pavement in any way and have not increased in size since their formation. In an attempt to ascertain the cause of this cracking, two cores were drilled along one of the longitudinal cracks. The cores, drilled down to the steel reinforcement, verified the assumption that the longitudinal cracks were directly over the longitudinal horizontal portion of the stirrup bars. This steel was found to be embedded to a depth of $3\frac{1}{8}$ in., which appears to rule out the possibility of high stresses causing a bond split-out failure resulting from insufficient cover. The cracks have not changed since they were discovered and the cracking occurs only in the outside lane directly over the lug anchor. Therefore, it is reasonable to assume that in all probability the cracks are due to excessive surface hydration shrinkage in the 3 ft 10 in. thick section of concrete.

As of this writing the expansion joints look as good as the day they were placed, the

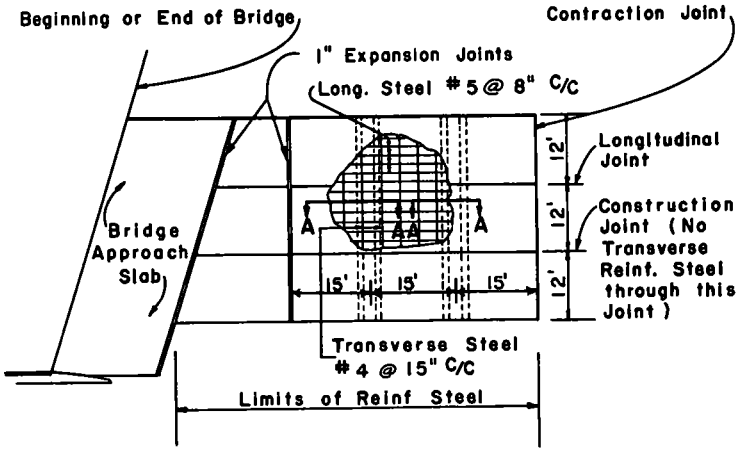


PLAN VIEW

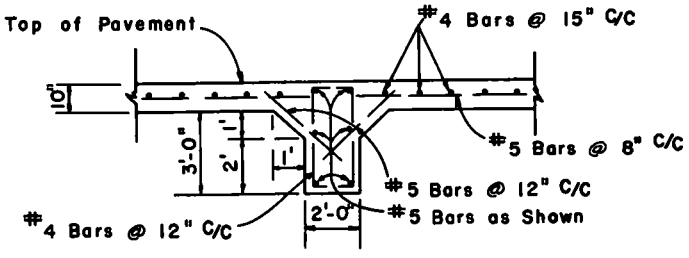


SECTION "A - A"

Figure 3. Typical district 12-lug design-jointed pavement.

contraction joints are all tight and relatively free of foreign material, and the riding surface is very smooth. This can be contrasted to other projects of approximately the same age, in the same area, and of the same or similar design which have grown in excess of 1 in. thus closing the expansion joints provided and creating pressure on the structure abutments.

With the apparent success of this design approach in preventing a major portion of concrete pavement growth, several additional projects have incorporated the design. Table 1 gives all the jointed concrete pavement projects completed or currently under progress as of this writing which require lug-type terminal anchorages. Terminal anchorages are being used on 21 jointed projects in several sections of the State and therefore under different climatic, traffic, and soil conditions.

Three projects (References 1, 2, and 11, Table 1) were selected for close observation and expansion joint measurements. Brass gage plugs were installed on either side of selected expansion joints on each of these three projects. These three projects, all being among the first to employ a terminal anchorage system, were selected for study because they represent the three most commonly used jointed pavement designs in Texas. With these gage plugs, joint movements to the nearest 0.01 in. can be accurately measured. The plugs were installed in July 1960, and measurements made during the next twelve months are reported. Figure 5 shows the results of the measurements

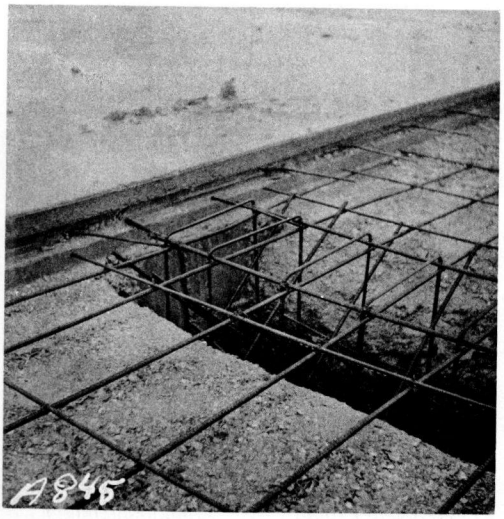


Figure 4. Trench showing lug reinforcement.

taken on each of the projects. It is apparent that any conclusions drawn from the measurements to date would be highly speculative and of doubtful validity. Several more seasons of measurements and observations will be needed before any firm conclusions can be reached. However, it can be said that when compared with projects built in approximately the same location at the same time without lug anchors, the anchors thus far are performing well, restricting a major portion of pavement growth. The small movements measured are expected due to the fact that movement is required to develop full resistance of the soil.

Based on the success thus far with a two-lug anchorage system in preventing pavement growth, a recommended design was prepared for use on all jointed pavement projects in which some type of anchorage of the pavement is desirable and is shown in Figure 6. This recommended design is not considered standard or final but rather as preliminary and subject to change; and, as mentioned previously, the basis of the design has been largely experienced.

TABLE 1

JOINTED CONCRETE PAVEMENT PROJECTS CONTAINING TERMINAL ANCHORAGES

| REF NO. | COUNTY | PROJECT | HIGHWAY AND LIMITS | CONCRETE DESIGN | | LUG DESIGN | | | | DATE CONTRACT LET |
|---|---|---|---|---|---|---|---|---|---|---|
| | | | | THICKNESS (IN.) | TYPE | DISTANCE FROM BRIDGE TO FIRST LUG (FT.) | NUMBER AND SPACING OF LUGS (FT.) | NUMBER AND SIZE OF EXPANSION JOINTS (IN.) | DISTANCE FROM LAST LUG TO FIRST CONTRACTION JOINT (FT.) | |
| 1 | Harris | I 45-1(12)67 | IH 45: Traffic Interchanges, Rankin Rd., FM 1960, and Spring Cypress Road | 10 | CPCD-15 | 55 | 2 @ 15 | 2 ea - 1 | 15 | 5/57 |
| 2 | Harris | I 10-7(11)797 | IH 10; 0.9 Mi. E. of Lynchburg-Crosby Rd. E. to Cedar Bayou | 12 ML[1]<br>9 FR[3] | CPCD-15<br>CPCD-15 | 60 | 2 @ 15 | 2 ea - 1 | 15 | 11/56 |
| 3 | Harris | I 10-7(12)779 | IH 10: SH 73-US 59 Interchange Fr. Jenson Drive to Gregg Street | 10 | CPCD-15 | 45 | 3 @ 45 | 1 ea-3 5/8 | 15 | 7/57 |
| 4 | Harris | U 514(20) | US 59; 0.12 Mi. N. of Langly Rd. N. to 0.21 Mi. N. of Mt. Houston Road | 10 | CPCD-15 | 60 | 2 @ 15 | 2 ea - 1 | 15 | 10/56 |
| 5 | Harris | I 32(23) | IH 45: Fr. SH 225 S. to Sims Bayou | 9 ML(W)<br>8 FR | CPCD-15 | 45 | 2 @ 15 | 2 ea - 1 | 15 | 12/57 |
| 6 | Montgomery | I 370(13) | IH 45: 2.0 Mi. S. of Conroe S. to 2.2 Mi. S. of San Jacinto River | 11 | CPCD-15 | 55 | 2 @ 15 | 2 ea - 1 | 15 | 9/57 |
| 7 | Harris | I 519(19) | IH 45; 0.15 Mi. North of Airline Dr. North to Steubner Road | 11 ML[2]<br>8 FR[3] | CPCD-15 | 50-75 | 2 @ 15 | 2 ea - 1 | 15 | 5/57 |
| 8 | Harris | I 45-1(10)34 | IH 45: From Sims Bayou S. to Almeda-Genoa Road | 10 | CPCD-15 | 35 | 2 @ 15 | 2 ea - 1 | 15 | 11/57 |
| 9 | Harris | U 514(21) & F 514(22) | US 59; 0.21 Mi. N. of Mt. Houston Rd. N. to FM 525 | 10 | CPCD-15 | 60 | 2 @ 15 | 2 ea - 1 | 15 | 12/57 |
| 10 | Montgomery | I 370(14) | IH 45: 2.2 Mi. S. of San Jacinto River South to 0.8 Mi. N. of Spring Creek | 11 | CPCD-15 | 70 | 2 @ 15 | 2 ea - 1 | 15 | 3/58 |
| 11 | Harris | F 514(23) | US 59: From FM 525 N. to Humble | 10 | CPJR-61'-6" | 60 | 2 @ 15 | 2 ea - 1 | 15 | 10/58 |
| 12 | Randall | U 60(17) | US 60 & 87: Fr. S. 45th Ave. to Parker St. (Amarillo) | 10 | CPCD-15 | 41 | 2 @ 20'-6" | 2 ea - 1 | 20'-6" | 10/59 |
| 13 | Harris | I 10-7(13)785 | IH 10: From Oats Rd. to Freeport Street | 12[1] | CPCD-18 | 60 | 2 @ 15 | 2 ea - 1 | 15 | 9/58 |
| 14 | Harris | I 45-1(39)061 | IH 45: From FM 525 to FM 1960 | 10 | CPJR - 61'-6" | 35 | 2 @ 15 | 2 ea - 1 | 15 | 6/59 |
| 15 | Harris | I 10-7(68)788 | IH 10: From Greens Bayou to Haydon Road | 11 ML[1]<br>9 FR[1] | CPJR - 61'-6" | 60 | 2 @ 15 | 2 ea - 1 | 15 | 3/60 |
| 16 | Fort Bend & Harris | F 514(38) etc. | US 59; 2.5 Mi. W. of Stafford to T & NO - Alief Road Overpass Approach | 9 | CPJR - 61'-6" | 55-75 | 2 @ 15 | 2 ea - 1 | 15 | 8/60 |
| 17 | Montgomery & Harris | I 45-1(19)67 | IH 45: 0.2 Mi. N. FM 1960 to Spring Creek (Montgomery County Line) | 10 | CPJR - 61'-6" | Variable | 2 @ 15 | 2 ea - 1 | 15 | 9/60 |
| 18 | Harris | I 610-7(26)801, etc. | IH 610: From Caplin Street to IH 10 | 10 ML<br>8 FR | CPJR - 61'-6" | 40'-6" | 2 @ 20'-6" | 1 ea - 1 1/2 | 20'-6" | 9/60 |
| 19 | Montgomery | I 45-1(52)85 | IH 45: League Line Rd. to 2.0 Mi. S. of Conroe | 10 ML<br>8 FR | CPJR - 61'-6" | 40'-6" | 2 @ 20'-6" | 1 ea - 1 1/2<br>1 ea - 1 | 20'-6" | 1/61 |
| 20 | Angelina | F 271(8) | US 59; Diboll S. to a point 0.5 Mi. N. of the Neches River | 10 | CPCD-15 | 7'-6" from end project | 2 @ 30 | none | 7'-6" | 3/61 |
| 21 | Harris | F 514(42) | US 59: From Humble to 0.62 Mi. N. of the San Jacinto River Bridge | 10 | CPJR - 61'-6" | 80'-6" | 2 @ 20'-6" | 2 ea - 1 | 20'-6" | 5/61 |

Abbreviations: CPCD-15 - Concrete Pavement, Contraction Joint Design. Joints spaced at 15 foot intervals.
CPJR-61'-6" - Concrete Pavement, Jointed, Reinforced. Joints spaced at 61'-6" intervals.
ML - Main Lane
FR - Frontage Road
ML(W) - Main Lane (Widening)

Notes: 1. Shell concrete with 100#/SY Asph. Surf. End 90 ft. Class A Concrete, contains lugs.
2. Shell concrete (including lugs) with 125#/SY Asph. Surf.
3. Gravel Concrete

The thickness of the lug (2 ft), though perhaps excessive from a design standpoint, is felt desirable to facilitate construction. By being 2 ft thick, mechanized trenching equipment can easily be employed to excavate for the lug. The reinforcing steel design is based on the lug acting similarly to a cantilevered beam loaded with a nonuniform distributed load that induces a moment couple in the pavement at either edge of the lug.

With the preceding as a basis for judgment in the design of a lug-type terminal anchorage for jointed concrete pavements, Texas is continuing to build terminal anchorages on jointed pavements, and the design will be closely observed and evaluated for the next several years, and where required, revised as necessary to achieve the most economical and practical terminal anchorage.

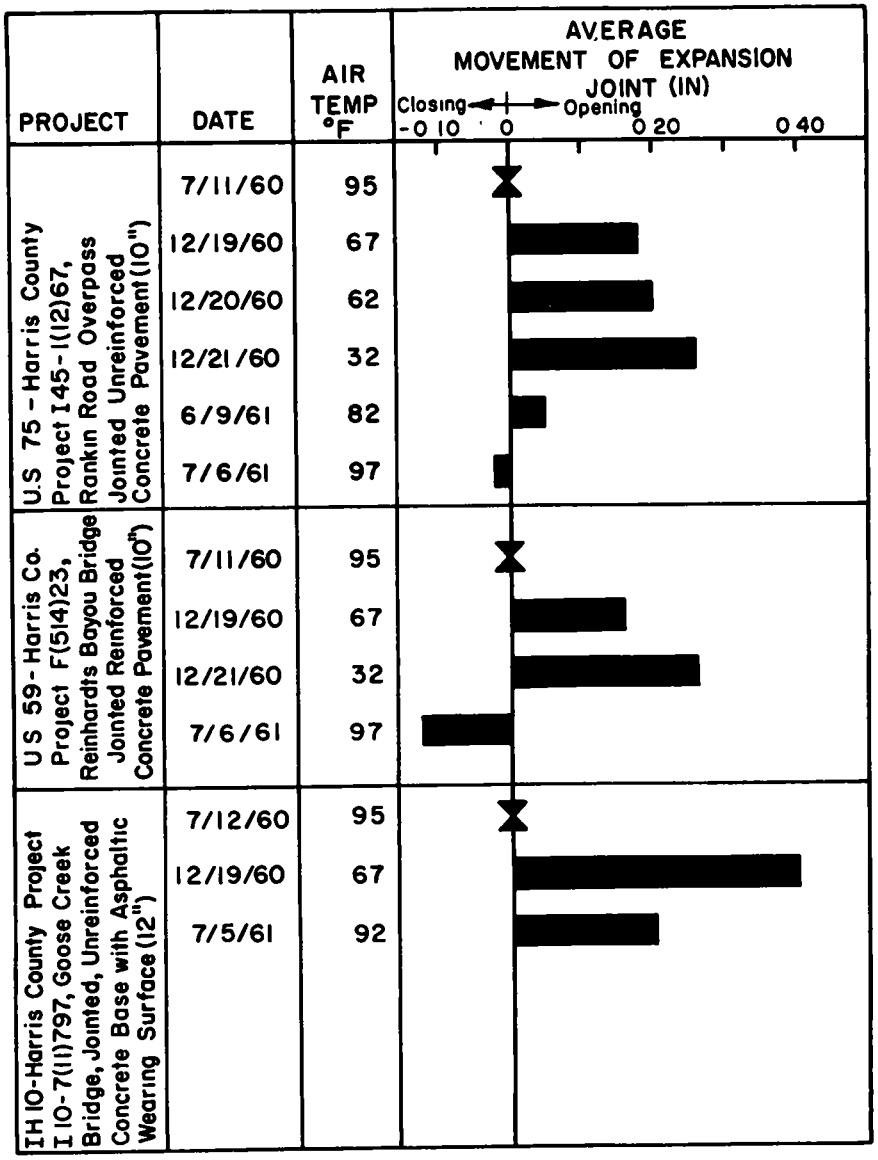


Figure 5. Jointed concrete pavement measured terminal movements.

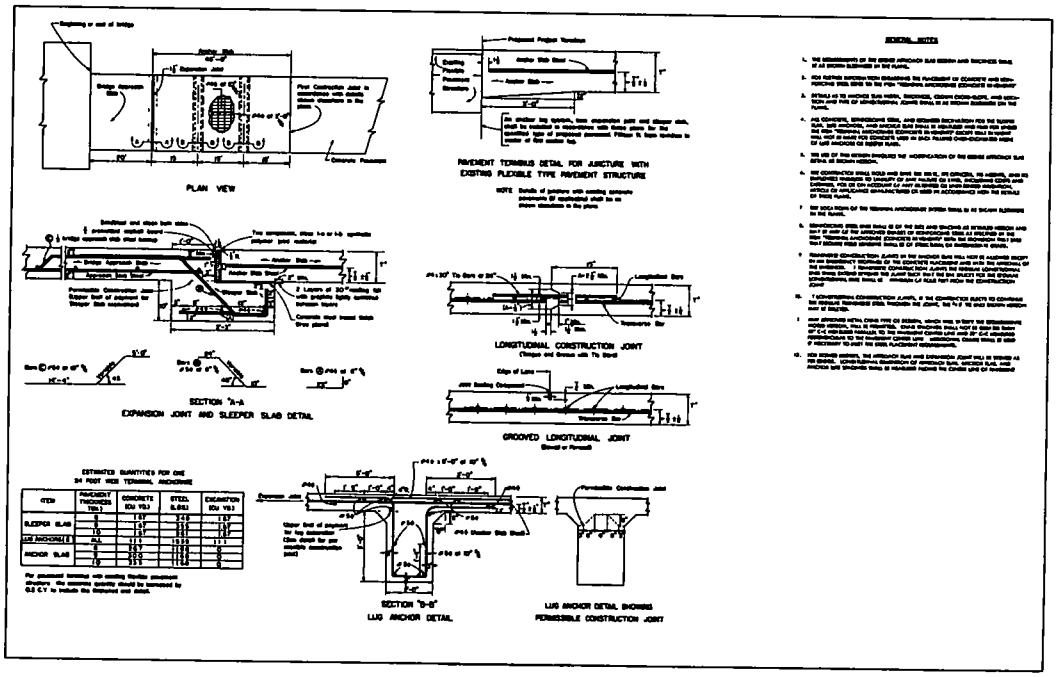

Figure 6. Terminal anchorage for concrete pavement jointed, TA(CPJ)-61, Texas Highway Department.

## CONTINUOUSLY REINFORCED CONCRETE PAVEMENT

In a properly designed and constructed continuously reinforced concrete pavement over granular, high friction subbase, the cracks that occur are held tightly closed by the reinforcing steel, which practically eliminates the factor of pavement growth through infiltration of foreign material into the cracks. This in turn reduces the effects of climatic conditions (rainfall) on the performance of the pavement and its anchorage system. By eliminating the factors of pavement growth and weather conditions and by formulating a few simplifying assumptions, a rational lug anchorage design can be developed based on known factors or variables such as expected end movements, extent of restraint desired, and load-deformation properties of the soil encountered.

### Expected End Movement

As mentioned previously, expected pavement end movement in Texas on a high friction subbase is in the neighborhood of $1\frac{1}{2}$ in. At first glance this may seem to be a rather small movement, expecially when it is compared with the 4-in. movement experienced on an Illinois experimental continuously reinforced concrete pavement (5). However, the majority of the Illinois pavement was placed directly on silty clay types of subgrades which have relatively low friction coefficients, whereas the Texas pavement was placed on a high-friction crushed rock subbase. Also, temperature extremes are greater in Illinois than at the project location in Texas. It is believed that these factors may account, in part at least, for the wide differences in observed end movements between the Texas and Illinois pavements.

### Terminal Restraint

The extent of restraint desired depends on the relative costs involved between restraining all movement and allowing some or all movement to take place by providing suitable expansion joints. Experience in Texas suggests that any joint presently designed to permit all of the expected movement to take place either is prohibitive in cost or does not satisfactorily provide the necessary load transfer and weatherproofing. On

the other hand, from a study of retaining wall design, to fully restrain all movement would also be prohibitive in cost if not impossible to accomplish. Therefore, a combination of terminal anchors and a low cost expansion joint would seem to offer the most logical solution to the problem.

## Soil Properties

Concerning the load-deformation properties of the soil, two properties are of interest in the design of the terminal anchorage system. The anchorage system may overstress the soil in two ways. One way is by forming a shear failure along the weakest plane of the soil. This failure plane may either be a curved plane similar to that experienced in passive soil failures of retaining walls, or a relatively straight horizontal plane, extending from the bottom of the lugs to the header bank beneath the structure. This soil property, which the authors call shear strength, determines the minimum distance between lugs and the total distance from the header bank to the last lug in the anchorage system. The other form of soil stress is through a localized failure in the vicinity of each lug similar to a foundation bearing or "punching" failure— hence the authors name this type of failure a bearing failure. The soil bearing properties determine the number and size of the anchor lugs. The Texas Highway Department uses the triaxial method to measure the shear properties of soils and considerable experience has been obtained in Texas soils (6). The penetrometer test, used in Texas for measuring bearing properties in connection with bridge foundation design, has been correlated with triaxial tests and used throughout the State (7).

## Design Development

In developing a rational design for the anchor lugs, it is assumed that a well-compacted soil will allow the anchor lug to move about ½ in. before the soil's full shear and bearing resistances are developed. Using typical weak subgrades found in many areas of the State, an ultimate shear strength of 8 psi and an ultimate bearing capacity of 8,000 psf might be expected. Climatic records indicate that the average maximum temperature change that can be expected in the concrete pavement in the areas of Texas where concrete is most widely used would not exceed 70 F. From the preceding assumptions and factors, a total restraining force of 107,700 lb per ft of width of pavement would be required in an 8-in. thick slab. This value may be arrived at in two ways: (a) by assuming the 70 F temperature change, then computing the restraining force from Hooke's law and reducing it for a ½-in. movement in 300 ft, or (b) by assuming the 1½-in. observed movement occurs in the 300 ft (determined from observation of continuously reinforced concrete pavement) and computing the force by considering a restraint of 1 in. in 300 ft.

Using the previously mentioned soil properties, a total of five 3-ft deep lugs, or seven 2-ft deep lugs, spaced over a minimum distance of 95 ft from the terminus of the slab are needed to carry the developed restraining force without overstressing the soil in either shear or bearing.

The lug length, or depth selected, is 3 ft rather than 2 ft because the 3-ft lug design is believed more economical. The lug thickness of 2 ft was selected for the same reasons as stated earlier in the jointed concrete pavement lug design discussion.

Based on this criteria, a recommended terminal anchorage design detail has been prepared, as shown in Figure 7. The detail is by no means a standard detail but is subject to revision as experience warrants. A marked similarity can be seen between this detail and the one shown in Figure 6 (lug anchorage for jointed pavement). Slightly more reinforcement has been placed in the lug anchor shown in Figure 7. Whether or not more reinforcement is fully warranted will not be definitely known until the design has been subjected to actual stresses for several years. The detail is designed for use with an 8-, 7-, or 6-in. thick concrete pavement— the number of lugs varying with the thickness of pavement. This is readily understood when considering that the restraining force is directly related to the cross-sectional area of the concrete— the smaller the concrete area, the lower the restraining force and consequently the less the number of lugs required.

TABLE 2

CONTINUOUSLY REINFORCED CONCRETE PAVEMENT PROJECTS
CONTAINING TERMINAL ANCHORAGES

| REF NO | COUNTY | PROJECT | HIGHWAY AND LIMITS | CONCRETE THICKNESS (IN.) | LUG DESIGN | | | DATE CONTRACT LET |
|---|---|---|---|---|---|---|---|---|
| | | | | | DISTANCE FROM BRIDGE TO FIRST LUG (FT) | NUMBER AND SPACING OF LUGS (FT) | NUMBER AND SIZE OF EXPANSION JOINTS (IN.) | |
| 1 | Walker | I 45-2(3)102 | IH 45 From Montgomery County Line N to Huntsville Loop | 8 | 36<br>41<br>46<br>61 | 5 @ 16<br>4 @ 21<br>3 @ 26<br>2 @ 41 | 1 ea - 1 1/2 | 1/60 |
| 2 | Harris | U 514(36), etc | US 59 From Lancashire Lane to Kirby Lane | 8 ML<br>6 FR | 30 | 5 @ 20 | 1 ea - 1 1/2 | 11/60 |
| 3 | Jefferson | US 1281(5) | SH 347 From SH 73 Northwest 2 0 Mi | 7 | 36 | 5 @ 16 | 1 ea - 1 1/2 | 3/61 |
| 4 | Dallas | I 35E-6(41)445 | IH 35E From a point S of Southwell Rd to the North City Limits of Dallas | 8 ML<br>8 FR | 36 | 5 @ 16 | 1 ea - 1 1/2 | 4/61 |
| 5 | Dallas | I 35E-6(89)443 | IH 35E From a point N of SH 114 to a point South of Southwell Road | 8 ML<br>8 FR | 36 | 5 @ 16 | 1 ea - 1 1/2 | 4/61 |
| 6 | El Paso | I 10-1(49)024 | IH 10: Trowbridge St to T & NO Overpass at Ft Bliss Spur | 8 | 30 | 5 @ 15 | 1 ea - 1 1/2 | 4/61 |
| 7 | Harris | I 45-1(65)50 | IH 45 Fr Quitman St to Interchange with North Loop Freeway | 8 | 30 | 5 @ 20 | 1 ea - 1 1/2 | 4/61 |
| 8 | Harris | I 45-1(55)49 | IH 45: Vicinity T & NO RR Bridge to vicinity of Hogan St Bridge | 8 | 30 | 5 @ 20 | 1 ea - 1 1/2 | 4/61 |
| 9 | Jefferson | U 1052(55) | SH 73: From SH 87 to US 69 | 8 ML<br>6 FR | 36 | 5 @ 16 | 1 ea - 1 1/2 | 3/61 |
| 10 | Jefferson | I 10-8(47)846 | IH 10: From Walden Rd in Beaumont to 0 6 Miles Northeast of FM 365 | 8 ML<br>6 R | 36 | 5 @ 16<br>4 @ 16 | 1 ea - 1 1/2 | 6/61 |
| 11 | Smith | I 20-6(24)537 | IH 20: From Van Zandt County Line to 6 6 Mi East | 8 ML<br>7 SCL | 36 | 5 @ 16<br>4 @ 16 | 1 ea - 1 1/2 | 6/61 |
| 12 | Harris | I 610-7(80)814 | IH 610: From Woodway Dr to Hempstead Road | 8 ML<br>6 FR | 30 | 5 @ 20 | 1 ea - 2 | 6/61 |
| 13 | Jefferson | U 1052(56) | SH 73: 0 181 Mi E of US 69 to 0 203 Mi W of US 69 | 8 | 36 | 5 @ 16 | 1 ea - 1 1/2 | 6/61 |
| 14 | Dallas | I 35E-6(54)418 | IH 35E: 1 2 Mi N of Ellis County Line to near South City Limits of Dallas | 8 ML<br>7 SCL | 36 | 5 @ 16<br>4 @ 16 | 1 ea - 1 1/2 | 8/61 |
| 15 | Smith | I 20-6(19)514 | IH 20 6 6 Mi E of Van Zandt County Line to 0 44 Mi E of US 69 | 8 ML<br>7 SCL | 36 | 5 @ 16 | 1 ea - 1 1/2 | 8/61 |

Abbreviations ML = Main Lane, FR = Frontage Road, SCL = Speed Change Lane, R = Ramp

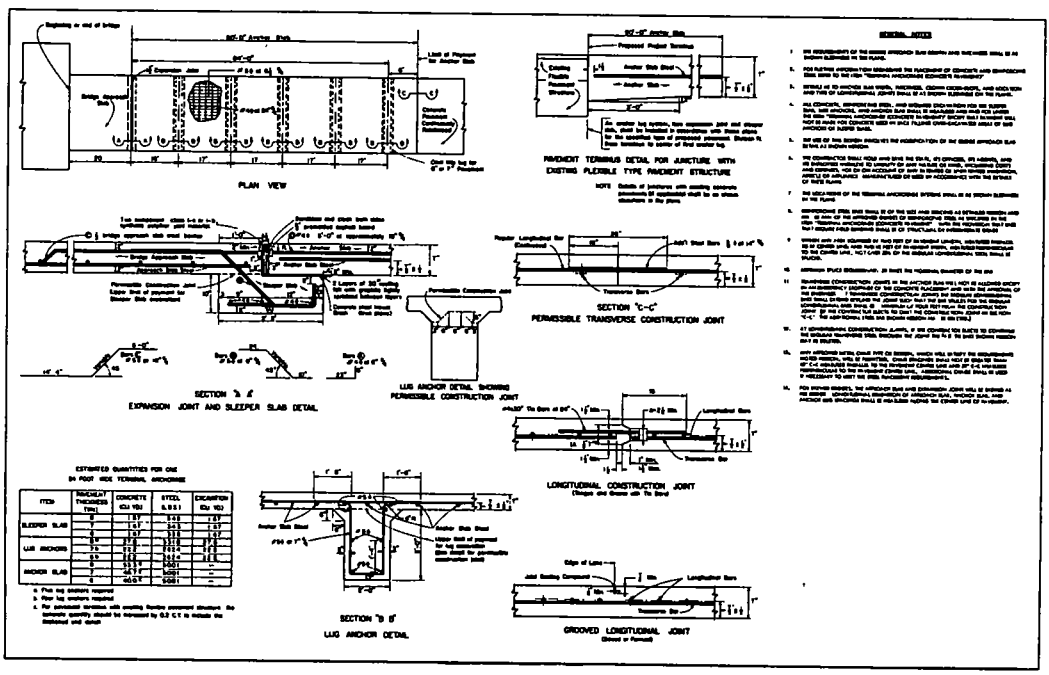


Figure 7. Terminal anchorage for concrete pavement continuously reinforced, TA(CPCR)-61, Texas Highway Department.

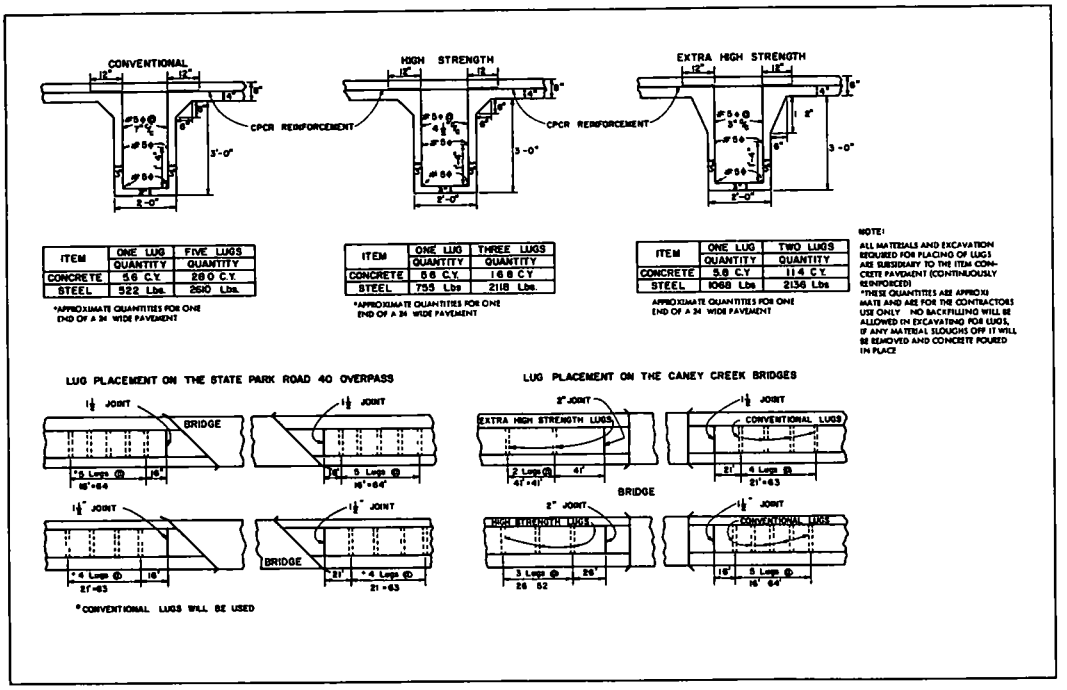


Figure 8. Lug details for Walker Co. CPCR experimental project I45-2(3)-102.

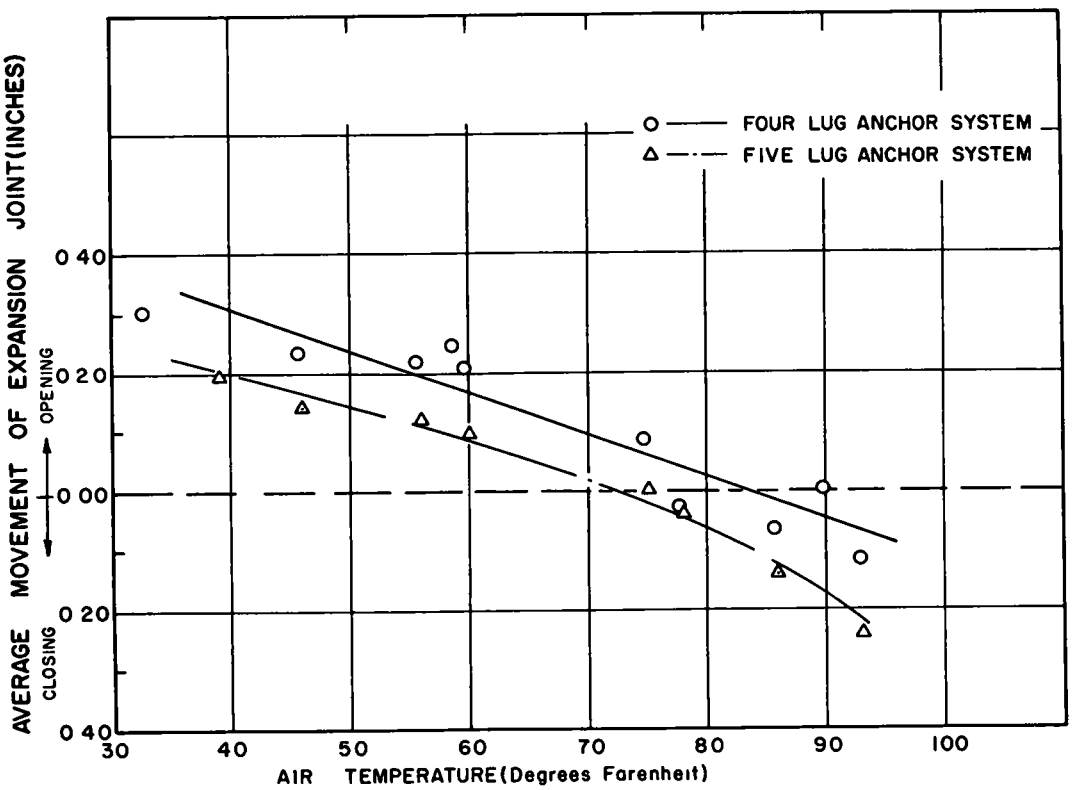


Figure 9. Average terminal joint movements for various air temperatures at the State Park Road overpass (project I45-2(3)102, Walker Co.).

## Terminal Anchorage Projects

As of this writing there are 15 continuously reinforced concrete pavement projects in Texas, completed or under construction, employing lug anchorages at terminals. Table 2 gives all 15 projects. Although the majority of the projects are located in the coastal region of the State, a few are being built in other areas which will afford an excellent means of comparing the effects of different soil, traffic, and climatic conditions.

Inasmuch as this design is highly experimental and as yet largely unverified, an experimental project was constructed varying the terminal anchorage design (Reference 1, Table 2). In addition to the five-lug design, four-, three-, and even two-lug designs were constructed. The designs used and their locations are shown in Figure 8. For this project, it was assumed that the restraining force was correct; therefore, the fewer the number of lugs, the greater the stress on each lug and hence the more reinforcing steel required as shown in the figure.

Brass gage plugs were installed on either side of all the expansion joints on this experimental project. With these gage plugs, joint movement to the nearest 0.01 in. can be accurately measured. The plugs were installed as the concrete was being placed, the earliest set being placed in September 1960. Measurements have been made at selected intervals for approximately one year as of this writing, and the results are shown in Figures 9 and 10. Figure 9 represents the older concrete placed in September 1960. It is apparent that the movements are relatively minor (being less than 0.40 in.

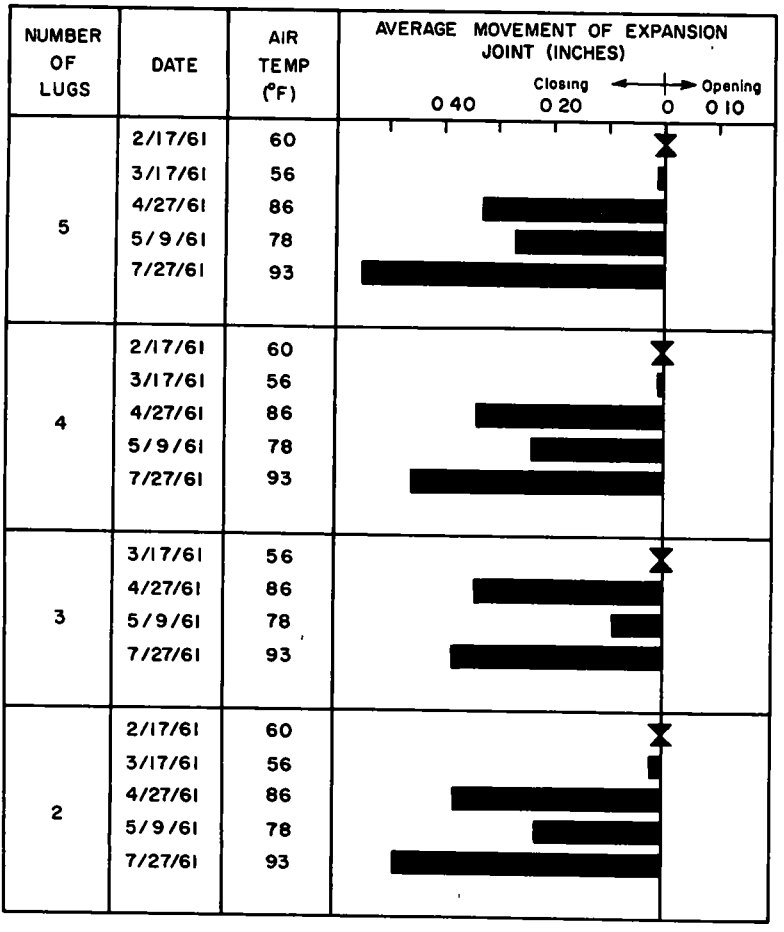


Figure 10. Continuously reinforced concrete pavement measured terminal movement at the Caney Creek Bridge (project I45-2(3)102, Walker Co.).

in either direction). There seems to be a correlation between terminal joint movement and air temperature for small movement, but it would be erroneous to assume that this relationship would necessarily continue for temperatures higher or lower than those shown. The difference in movement between the four-lug system and the five-lug system is negligible as seen from the parallel lines in the figure. The difference in the location of the two lines is due to the different air temperatures at time of concrete placement for each design. Figure 10 shows the result of measurements taken at the Caney Creek Bridge location. Here, no apparent correlation exists between air temperature and terminal movement. All of the observed movement has been in the closing of the joint which is due to the low temperature at which the concrete was placed. All results of measurements shown on Figures 9 and 10 represent only the beginning of the experimental research program. Many more seasons are required before any definite information can be obtained on the suitability of one design over another.

Although it has been mentioned several times in this report, the authors believe it to be important enought to re-emphasize that the information presented herein represents only the beginning of the study that will be made on pavement anchorages. Few data of definite value have been obtained to date. Movement vs short time measurements have been made on the Walker County lug anchorage project and the results are shown in Figure 11. The figure shows that, as the surface temperature of the concrete dropped, the terminal joints opened slightly (pavement contracted) and, as the surface temperature of the concrete raised, the terminal joints closed slightly. The rate of change of joint movement for the two-lug system was almost the same as for the five-lug system. However, this should not be misconstrued to indicate that the two-lug is necessarily satisfactory. The pavement is still too young, and insufficient measurements have been taken to draw such an inference. Also, the amount of movement occuring to date indicates that this movement is insufficient to establish the full passive

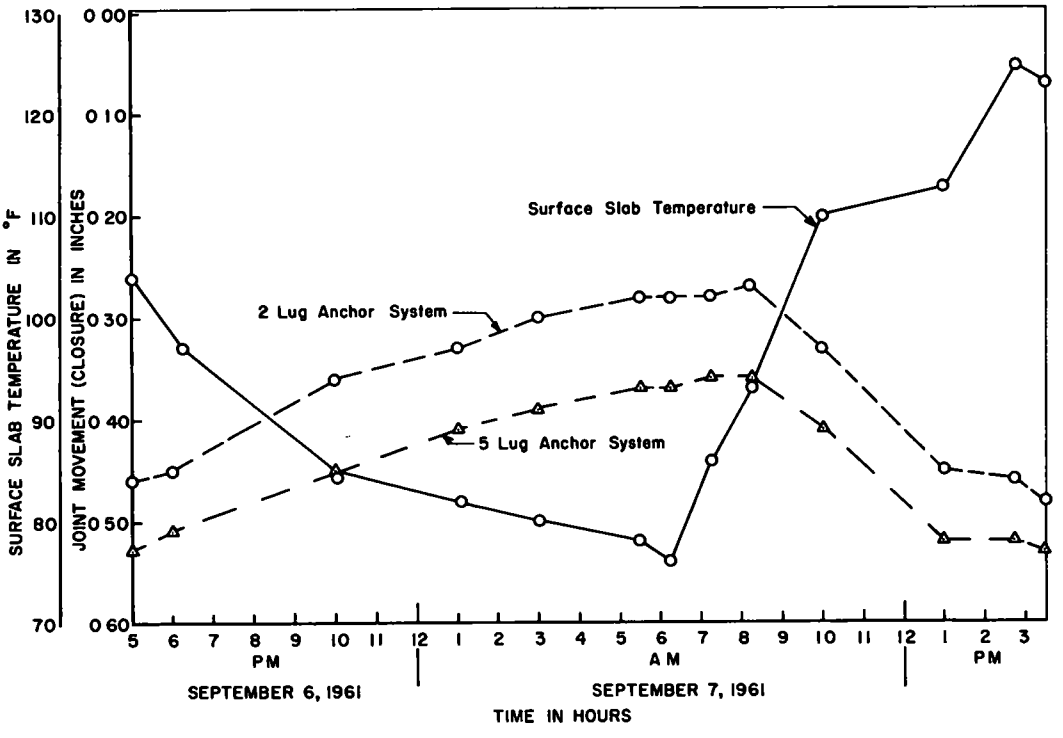


Figure 11. Joint movement vs time for a selected short period at the Caney Creek Bridge (project I45-2(3)102, Walker Co.).

resistance of the soil. Until sufficient movement occurs to develop pressure on all the lugs any results will not be indicative of the number of lugs in the system. Therefore, the figure is presented for information only, and no conclusions are drawn from it at this time.

## CONCLUSION

In this report, the authors have attempted to present the knowledge gained to date in Texas through the use of terminal anchorages for concrete pavements. The problems of terminal pavement movements is a major one presenting unique problems to the highway engineer. Concerning one method of possible solution to this problem, the terminal anchorage system, the following conclusions are offered:

1. Lug-type terminal anchorages are performing in an outstanding manner after two years in service on jointed types of pavements.
2. Insufficient time has elapsed since the construction of the first lug-type terminal anchorage system for continuously reinforced concrete pavement to form any conclusions. However, it is believed that this type of approach to the problem is sound and the major task involves a decision as to which anchorage system will give the best all around solution.
3. This report is considered a progress report, presenting only the magnitude of the problem and the methods now under study in Texas toward solving the problem. As more information is obtained further reports will be written.
4. The authors feel the design details presented herein will help alleviate the detrimental terminal movements of concrete pavement in Texas. However, these designs are not necessarily the final answer.

## REFERENCES

1. Shelby, M. D., and McCullough, B. F., "Experience in Texas with Continuously-Reinforced Concrete Pavement." HRB Bull. 274, 1-29 (1960).
2. McCullough, B. F., and Ledbetter, W. B., "LTS Design of Continuously Reinforced Concrete Pavement." Jour. Highway Division, Proc., ASCE, 86: No. HW4 (Dec. 1960).
3. Beck, A. F., "The Case for Continuously Reinforced Concrete Pavement." Texas Highway Department, unpublished report (1958).
4. Zuk, W., "Analysis of Special Problems in Continuously-Reinforced Concrete." HRB Bull. 214, 1-21 (1959).
5. Lindsay, J. D., "A Ten-Year Report on the Illinois Continuously-Reinforced Pavement." HRB Bull. 214, 22-49 (1959).
6. McDowell, C., "Triaxial Tests in Analysis of Flexible Pavements." HRB Research Report 16-B, 1-28 (1954).
7. "Foundation Exploration and Design Manual." Texas Highway Department, Bridge Division (Aug. 1956).

## *Discussion*

R. A. MITCHELL, Highway Research Engineer, Virginia Council of Highway Investigations and Research, Charlottesville—The authors have made a valuable contribution with this report. The fact that they are continuing to observe and take measurements on such a large number of pavement anchors ensures that their subsequent reports are anxiously awaited.

Under "Design Development" it is suggested that the authors have used the following quantities in determining the force required to control end movement: (a) temperature range, (b) pavement thickness, (c) end movement if anchors are not used, (d) end movement permitted with anchors, and (e) total length of pavement moving. Presumably they also assume a modulus of elasticity and a thermal coefficient for the pavement. Are these quantities, along with the shear and bearing capacities of the soil, the only ones used to determine the size, number, and spacing of the anchor units? The method of analysis used by the authors is not explicitely stated in the paper but presumably

such quantities as subgrade friction, slab and anchor stiffness, and compressive modulus of the subgrade were not used in the analysis.

For several months the writer has been engaged in an extensive theoretical and experimental study of pavement anchors. Tentative results indicate that subgrade friction, subgrade modulus, and anchor and slab stiffness, as well as most of those quantities suggested by the authors, are of first order importance in determining the behavior of an anchored pavement. The quantities suggested by the writer may be difficult to evaluate but to ignore them would seem to be an unwarranted simplification.

In his project, the writer is making a parameter study using a high-speed computer. By studying the degree of importance of the various parameters it is hoped that a practical and accurate design method can be developed. A design procedure presenting precalculated relationships in the form of curves is being developed. A report on this project will be submitted in the future.

# Investigations of Prestressed Concrete for Pavements

BENGT F. FRIBERG, Consulting Engineer, St. Louis, Missouri

This paper is intended to describe, correlate, and apply to design and development of prestressed concrete pavements three exploratory research projects that were included in nine experimental investigations for master's thesis work at University of Missouri, Rolla.

Creep in concrete slabs under compressive stress in outdoor exposure on subgrades was much less than in slabs in the laboratory. Creep was greater near the upper surface than in slab bottom portions; as a result, slab ends warped upward and the prestress redistributed itself toward the bottom away from the slab ends, the most favorable distribution to counteract the high flexural tension stresses under axle loads. Prestress in long pavement slabs could be applied below center depth to obtain favorable distribution and to avoid upward end warping.

At early age, concrete tension strength increased much faster than compressive strength. Modulus of deformation (elasticity) reached mature values early, and critical limits of extensibility were low at early age, especially so in high ambient temperatures. Under burlap curing insulation, the strain variations incident to daily concrete temperature cycles during curing could be accommodated by the concrete without cracking at median, but apparently not at high construction temperatures. Prestressing could be applied at early age, except at low construction temperatures. The best possible curing and insulation should protect the concrete at least up to the time of prestressing.

Consideration must be given to tension stresses in end zones, and at and between prestressing cable anchors. "Bursting" cracks occurred in line with the force, incident to failure, at all single loadings against an edge. Tension cracks perpendicular to the edge between loads occurred at the lowest failure loads applied symmetrically. The tension stresses along the edge, between spaced anchorages, could be expected at least to equal the average prestress in magnitude, and would add to flexural edge stresses caused by wheel loads. Prestressing along anchorage edges would be advisable.

•STRENGTH properties of concrete are not fully utilized in conventional concrete pavements. Stresses are limited to the concrete's relatively low strength in bending; as a result, pavement deflections as limited by strains are generally less than could be accommodated by subgrades. Effective compressive prestress in pavements might make possible thinner pavements, more efficient pavement design, long uncracked slabs, and improved performance. The challenge has motivated these investigations into related unknown concrete behaviors.

The following research program, consisting of three related projects, was selected for exploratory investigations in a cooperative arrangement between the Missouri State Highway Commission, the U.S. Bureau of Public Roads, and the University of Missouri at the School of Mines and Metallurgy at Rolla, Missouri:

1. Part A. – Observations of continuing length changes, and warping and curling

behavior in short slabs simulating prestressed pavements on a typical highway subgrade from construction to two years age.

2. Part B. — Investigation of early-age strengths and associated deformations in compression and tension standard tests at different ambient temperatures applicable to pavement construction, for indication of early pavement stresses and application of prestressing.

3. Part C. — Investigation of stress distributions and concrete failures near concentrated loads applied against an edge of thin concrete slabs, simulating anchorages at ends of pavement slabs.

All projects covered conditions on which few or no experimental data had been published. They were intended as exploratory work, to indicate need for more exhaustive investigations.

Materials and concrete portions were intended to duplicate those in normal Missouri pavement construction, and were the same in all three projects except as specifically indicated.

This paper covers all three projects and includes information of particular interest for research on prestressed pavements, for conventional pavement studies, and for important indications for pavement design. Complete information and data on the research work are available in the reports and theses.

## PART A — LENGTH AND PROFILE CHANGES IN PRESTRESSED SLABS ON SUBGRADE

Substantial creep deformations have been observed in prestressed products and structures; similar deformations in pavements could influence the continuing effectiveness of even relatively low pavement prestress. Pavements might, however, behave quite differently, warranting investigation. Observations of differential length changes, longitudinal contour changes, and flexural restraints in prestressed slabs, including slabs with no prestress, served to indicate mutual effects of prestressing and contour changes. A few indoor slabs of equal cross-section and prestress served to give correlation with conventional creep tests.

### Construction Data

Regular, normal density (called here, dense), and air-entrained concretes were used in duplicate series; each included four slabs 5½ and four 8 in. thick, subjected to 0, 100, 300, and 500 psi longitudinal prestress, a total of 16 slabs. The slab width of 25 in. was chosen to accommodate the nests of railroad springs for maintaining constant prestress. The 222-in. field slab length was the longest obtainable for commercial-alloy threaded prestressing rods, two in each slab. The four 5½-in. correlation laboratory slabs of dense concrete were only 54 in. long, but in material and prestressing details similar to the longer field slabs.

Site Arrangement. — The field slabs were constructed during a three-week period in August 1956 on an experimental site at Rolla, prepared to simulate a highway grade 44 ft wide and extending about 100 ft in east-west direction. The soil was silt loam, group classification A 7-6 (16), with hardpan 2 to 3 ft below the surface. The top 6 in. of the grade was reworked and rolled to 105 percent standard Proctor, 101.5-pcf average field density. A dense-graded stone subbase 7 in. thick was placed on the grade full width in two layers, rolled to 95 percent standard Proctor 125- to 145-pcf field density.

Slab Construction. — The concrete slabs were placed 54 in. c/c with their length axis in north-south direction. The slab sides were coated with heavy asphaltic roofing cement as soon as they were dry, following form removal. The 29-in. spaces between the slabs, and a short distance beyond the end slabs and the south end of the slabs, were filled with well-tamped soil. Slab side forms were wood; the end forms for the prestressed slabs were heavy steel face plates used to distribute the prestressing forces evenly, put in place before concreting and left undisturbed. The holes for the prestressing rods were formed with cold drawn seamless tubing, withdrawn to leave open holes 3/16 in. larger than the prestressing rods. Heavy semifinished nuts and hardened

steel washers transferred the stressing forces from the threaded rods to the slab end plate at the south end, and to spring backup plate, spring nests, and steel end plate at the north end. Figure 1 is a general view from the west.

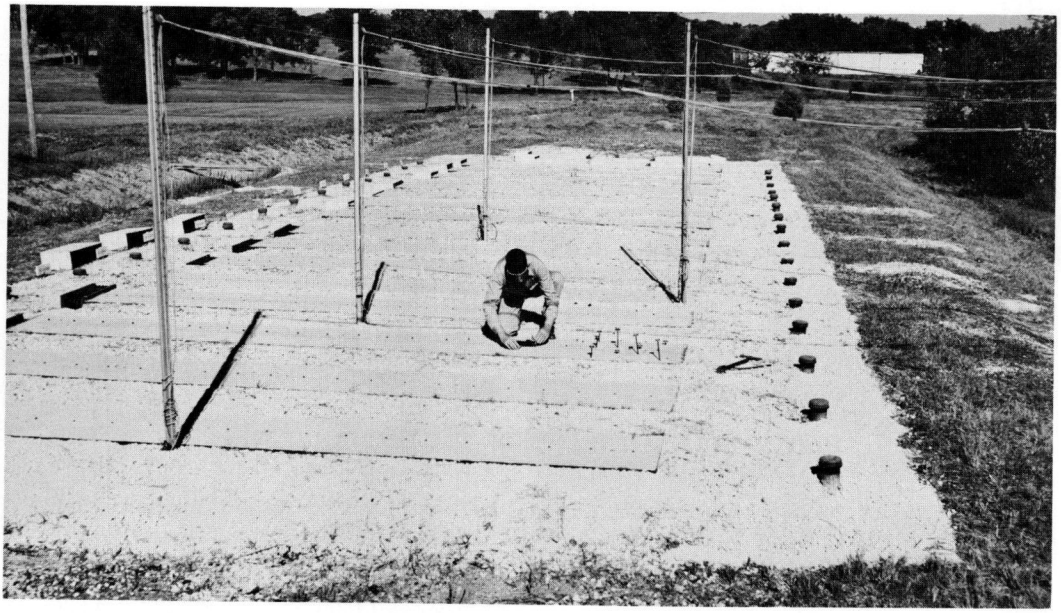

Figure 1. General view of test slabs from west.

Prestressing. — Prestress was applied at 3- to 6-day age by two hydraulic centerhole jacks coupled to the prestressing rods. Prestressing force was checked by jack pressure and by computed working height dimensions of the stress maintaining spring assemblies. Figure 2 shows closeup of slab with steel plates and spring assemblies at the north end. Table 1 gives the slabs in order from west to east, slab identification in this report, construction data, and nominal and probable actual prestress. Weights of the stress transfer steel plates 1 to 1½ in. thick at the south end, and the plates and spring assemblies extending about 10 in. at the north end, are included in Table 1. Change in prestress since construction has been small.

Materials and Concrete. — Concrete was of normal pavement composition, 1: 1.97:, 3.36 for the dense, and 1: 1.72:, 3.34 for the air-entrained concrete (by dry rodded volume), with 5.6 gal of water per sack of cement and 1.51 cement factor, resulting in 75 percent surplus mortar. The cement was type 1. Coarse aggregate was crushed hard limestone 1 in. maximum size. Air content averaged 4.5 percent (pressure method). The slump was 2½ to 3½ in. Compression strengths are given in Table 2. All slabs were cured with wet burlap, removed during the evening of the third day.

## Field Slab Instrumentation

Each slab was instrumented for observation of temperatures, length changes, and longitudinal vertical contour changes. Temperatures were measured in temperature wells at nine points in each slab. Length change measurements employed specially built temperature compensated 50- and 200-in. length-change gages, and five gage points spaced 50 in. and set ½ in. below the slab surface, covering 100 in. on each side of midlength. Length change instruments are shown in Figure 3. The slabs were laid at different temperatures; to permit simple continuing comparisons between slabs, length change zero readings were reduced to 70 F slab temperature.

For contour change observations, specially built 10-in. clinometers were used, measuring successive slopes between pairs of points spaced 10 in., 22 points, numbered

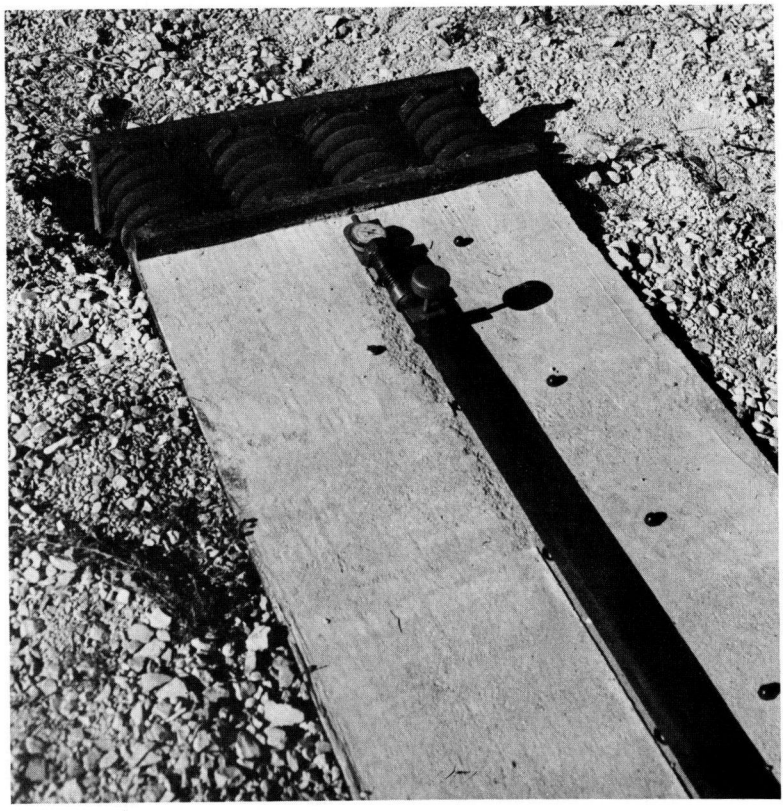

Figure 2. Steelplate and spring assembly at north end of slab prestressed to 500 psi, showing 200-in. gage in place.

1 to 22 inclusive from south to north, covering 210 in. of length, the center gage length straddling midlength, and the end points 6 in. from the slab ends. The special clinometer and slope change gage points are shown in Figure 4. Alternating points were center-drilled and slotted, the clinometer screw was always placed in the center-drilled points. Differential progressive wear of the screw and points introduced errors; however, the reversed direction of the clinometer on gage lengths symmetrical with respect to the midlength paired out instrument errors in the average slopes for one-half slab length from midlength to end.

Temperatures. — Average slab temperatures and temperature gradients were determined from the temperatures in the many wells at different depths. Temperature gradients were determined from the average temperature curves, (positive when bottom temperature higher than top temperature), as the linear average temperature gradient from top to bottom, with deviations from actual temperatures balanced both above and below mid-depth.

Length, Slope, and Contour Changes. — Original gage measurements were made not later than the day following construction, at a time of small temperature gradient. Subsequent length changes, determined at points $\frac{1}{2}$ in. below the concrete surface, were all reduced to mid-depth, by correction for slope observed simultaneously on the gage lengths straddling the length change point.

The initial clinometer readings, taken as soon as possible after construction at zero temperature gradient, are referred to as "level." In drawing contours, by summation of the 10-in. slope increments, clinometer point 12, 5 in. north of midlength, was chosen as common (zero) reference point. Absolute elevation changes were not observed.

TABLE 1

EXPERIMENTAL FIELD SLAB CONSTRUCTION DATA

| Slab Type | Length (in.) | Location[a] | Slab Mark | Slab Depth (in.) | Nominal Prestress (psi) | Date Placed | Date Pre-stressed | Actual Applied Pre-stress[b] (psi) | Steel at Ends (lb/in. of slab width) South | North |
|---|---|---|---|---|---|---|---|---|---|---|
| Dense concrete | 222 | 1 | R80 | 8 | 0 | 8/10 | | | 0 | 0 |
| | | 2 | R81 | 8 | 100 | 8/13 | 8/16 | 100 | 2.4 | 7.0 |
| | | 3 | R83 | 8 | 300 | 8/16 | 8/20 | 290 | 3.0 | 9.7 |
| | | 4 | R85 | 8 | 500 | 8/22 | 8/28 | 460 | 3.6 | 18.5 |
| | | 5 | R550 | 5-1/2 | 0 | 8/8 | | | 0 | 0 |
| | | 6 | R551 | 5-1/2 | 100 | 8/13 | 8/17 | 100 | 1.6 | 5.0 |
| | | 7 | R553 | 5-1/2 | 300 | 8/23 | 8/27 | 310 | 2.0 | 8.5 |
| | | 8 | R555 | 5-1/2 | 500 | 8/28 | 9/3 | 470 | 2.0 | 8.8 |
| Air-entrained concrete | 222 | 9 | A80 | 8 | 0 | 8/18 | | | 0 | 0 |
| | | 10 | A81 | 8 | 100 | 8/20 | 8/24 | 100 | 2.4 | 7.0 |
| | | 11 | A83 | 8 | 300 | 8/28 | 9/3 | 240 | 3.0 | 9.7 |
| | | 12 | A85 | 8 | 500 | 8/24 | 8/29 | 510 | 3.6 | 18.5 |
| | | 13 | A550 | 5-1/2 | 0 | 8/15 | | | 0 | 0 |
| | | 14 | A551 | 5-1/2 | 100 | 8/17 | 8/21 | 100 | 1.6 | 5.0 |
| | | 15 | A553 | 5-1/2 | 300 | 8/18 | 8/22 | 290 | 2.0 | 8.5 |
| | | 16 | A555 | 5-1/2 | 500 | 8/21 | 8/25 | 500 | 2.0 | 8.8 |
| Correlation | 54 | | C0 | 5-1/2 | 0 | 11/30 | 12/3 | 0 | | |
| | | | C1 | 5-1/2 | 100 | 11/30 | 12/3 | 100 | | |
| | | | C3 | 5-1/2 | 300 | 12/15 | 12/18 | 280 | | |
| | | | C5 | 5-1/2 | 500 | 12/15 | 12/18 | 520 | | |

[a]In order from west.
[b]Based on measurements of spring heights in May 1958.

TABLE 2

COMPRESSION STRENGTH

| Cement | Compression Strength[a] (psi) 3 Days | 7 Days | 28 Days | Modulus of Elasticity |
|---|---|---|---|---|
| Dense | 2,490 | 3,195 | 4,500 | 5,200,000[b] |
| Air-entrained | 2,200 | 2,800 | 4,300 | 4,750,000[c] |

[a]Cylinders, job cured. [b]At 28 days. [c]At 14 days.

Three separate changes in contour were observed:

1. Curling. — The daily change in contour, in response to variable expansion and contraction because of varying temperature gradients.
2. Warping. — The change in contour resulting from differential shrinkage or swelling, due to moisture and material variations from top to bottom, and from creep under prestress, with varying effects in top and bottom parts of the slab, and from the subgrades departing from their original contour.
3. Slab Tilt. — A result of variations in soil settlement or swell, causing the slabs to tilt toward the north or south.

Curling observations permit some deduction concerning subgrade support variations near slab ends, because curling curvatures can be computed, knowing temperature gradients, thermal coefficient of the concrete, and the elastic properties of the concrete slab.

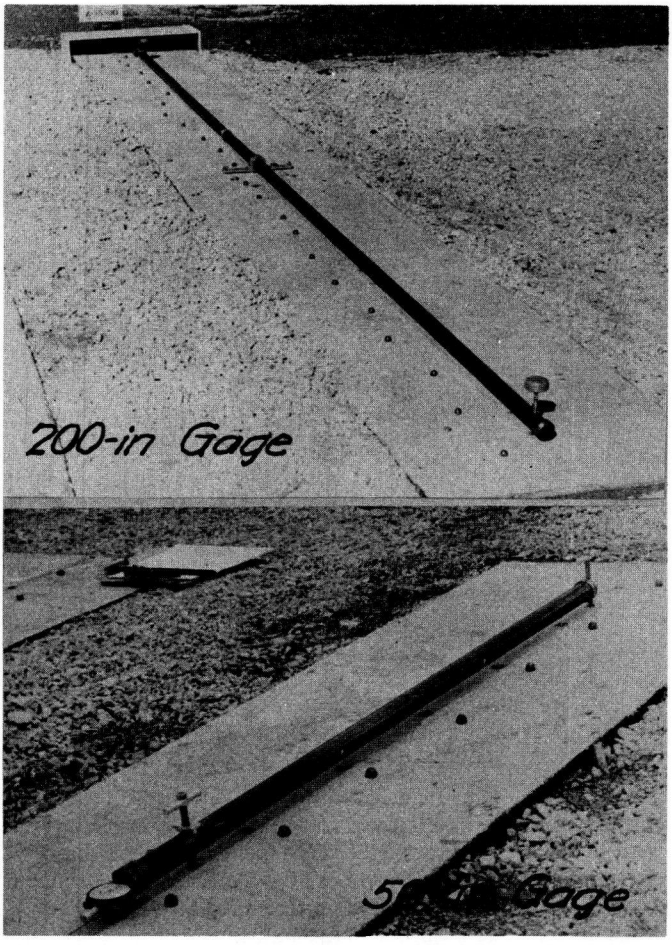


Figure 3. Temperature compensated length-change gages in place on slabs.

The term "warping" is used specifically for the slower and much more uncertain progressive and seasonal contour and slope changes. Warping contours were determined for conditions of zero temperature gradients. They show no appreciable variation on any one day.

The third contour change, "tilt," developed gradually, with adjacent slabs generally codirectional. No systematic relation between tilt and other experimental variables could be discerned; accordingly, it has not been considered in the analysis of research data.

## Record of Observations

The extensive instrumentation made possible an accurate record of length and contour changes of all slabs from the time of construction. Generally three sets of observations were made on any one day: early in the morning, near noon, and late in the evening. The slabs were in observation each day during the curing period, one day a week during the first month, and one day a month thereafter through June 1957. Measurements were made also about June 1 and September 1, 1958. One set of readings included at least 9 thermometer readings, 21 clinometer readings, and 5 length readings on each slab.

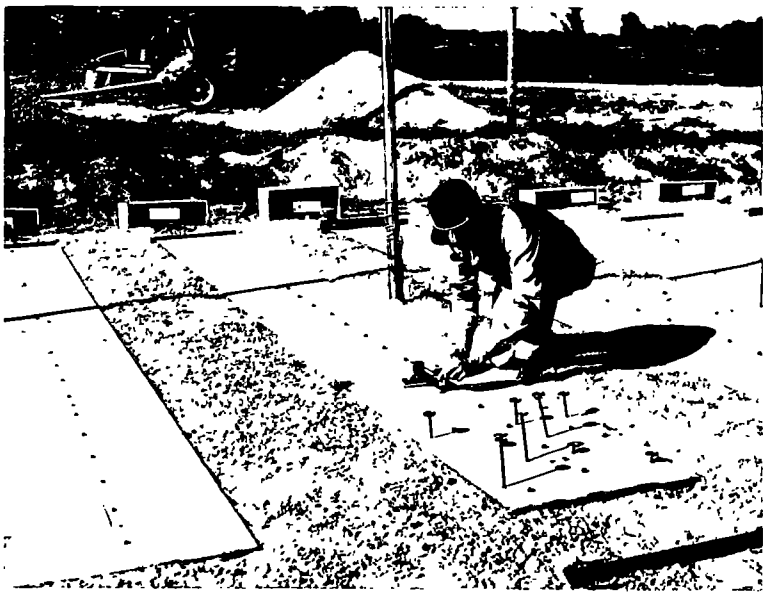

Figure 4. Clinometer measurements—thermometers in temperature wells; acorn nuts protecting clinometer points between measurements.

Typical Slab Data for One Day. — Typical basic information for one individual slab, obtained from the three observations on one day, is shown in Figure 5 for Slab A 553, September 15, 1956; at 4-week age:

Diagram A shows temperature averages and temperature gradients, also observed length changes from the zero readings at 70 F, adjusted to center depth. Length change for the forenoon and afternoon average temperature changes both corresponded to 0.0000050/deg. F coefficient of thermal expansion in this case.

Diagram B shows longitudinal slab contours obtained by summation of slope readings at morning, noon, and evening. Slight tilting toward north is evident. Typical upwardly curved contour existed through the day, the dishing averaged 0.13, 0.06, and 0.115 in. at morning, noon, and evening, respectively. Warping contour would be very near the 6:10 AM contour, the evening contour indicates slightly lower warping slopes, typical of a slow upward adjustment during the night.

Diagram C shows slope changes during the day for consecutive 10-in. clinometer lengths between slab midlength and the two end points, average of values for corresponding north and south gage intervals. If curling were unrestrained, slope changes would show straight line variation from zero at slab midpoint, increasing at a constant rate determined by thermal coefficient and change in temperature gradient. At the ends there is no flexural restraint to curling, but restraint increases inwardly from the ends. The rate of slope change at the end must be that corresponding to unrestrained curling, and is represented by the tangent to the slope change curve. The slope deviations from the tangential rate of unrestrained curling near the end show influence of curling restraint on slope change with increasing distance from the ends. A horizontal tangent to the curling slope change curve, at or near midlength, indicates full restraint to curling.

Diagram D shows slopes of consecutive 10-in. clinometer lengths from midlength, average of the corresponding north and south values, for the morning and noon observations, and the interpolated warping slopes for zero temperature gradient. Restraint to warping increases from the ends where subgrade support is lacking, toward the concentration of subgrade support under central parts. The tangent to the warping slope curve at the end indicates substantially unrestrained change in warping slope; i.e, unrestrained warping curvature. The tangent to the warping slope curve at midlength shows

the warping curvature for the partial or complete restraint of warping. These warping curvature observations could be used to compute warping restraint stresses, inasmuch as the actual stresses near the ends in the prestressed slabs could be estimated accurately.

More than 1,000 sheets of sets of information accumulated during the two years of observation. Diagrams like Figure 5 for one slab on one day were analyzed for all slabs on pertinent days to determine progressive and seasonal slab changes. Only summaries of the data and major indications are given in this paper.

Climate. —The weather during construction was hot and dry to August 18, cool and dry August 19 to 21. Warmer than seasonal temperatures prevailed through September and October. The fall of 1956 was much drier than normal, with less than 2 in. per month average precipitation. The mean monthly temperatures at Rolla vary from 78 F in July to 35 F in January. Normal monthly precipitation is 4 in. per month from March to September, with a normal monthly maximum of 4.8 in. during May; winter precipitation is 2.2 in. per month from December to February. During 1957 the lowest temperatures occurred in January; precipitation during the winter and spring was much higher than normal to June, and substantially lower than normal during the second half of 1957. During 1958 temperatures were lower than normal during February, March, June, and July. Precipitation was below normal during the winter and spring, substantially above normal during July 1958.

## Principal Data

Progressive length changes for different levels of prestress indicate average shrinkage and creep, as shown in Figure 6 for all slabs. Contour change observations show differences in prestress effect near top and bottom of slabs; illustrated as warping slopes near the ends they are shown in Figure 7 for all slabs.

Deviation of actual from nominal values of prestress should be kept in mind when studying the data. The large difference between slab A 83 and other 300-psi slabs is explained by its 20 percent low prestress. Excessive shortening of slab A 555 is believed due to its position at the east end of the site with less adequate side fill on the exposed longitudinal edge.

## Correlation Slabs

The four $5\frac{1}{2}$-in. correlation slabs (Table 1) were built with concrete materials and proportions identical with the dense field slabs. The slabs were cured for three days, the side forms stripped at 48 hr, and the bottom forms at 14 days. The slabs were prestressed at 3-day age, and supported above the floor while in indoor exposure until April 1, 1957. Temperature in the heated room ranged from about 75 to 91 F, with relative humidity from 30 to 40 percent, averaging 33 percent. The correlation slabs were instrumented for observation of temperatures and length change. The slabs were moved out to the field site at 105- and 120-day age, April 1, 1957.

For the correlation slabs, unit length changes are shown in Figure 8. Comparative total length changes from construction to 28 days for the indoor and for the field slabs (which expanded seasonally after the first month) are given in Table 3. Immediately after transfer to the field on April 1, swelling took place in all correlation slabs for a month or two, with seasonal length change at about the same rate as in the longer field slabs thereafter.

TABLE 3

TOTAL LENGTH CHANGES IN SLABS

| Prestress Shortening (psi) | Slab Length Change (%) | |
|---|---|---|
| | Indoor | Field |
| 0 | 0.019 | 0.005 |
| 100 | 0.017 | 0.009 |
| 300 | 0.032 | 0.013 |
| 500 | 0.040 | 0.020 |

## Curing Period Temperatures and Restraint Stresses

Heat release during setting was noticeable in the slabs as a modest temperature rise only on the construction day. The morning and noon temperature

# A.

## TEMPERATURES

Air: 66F 94F 80F.

Concrete:

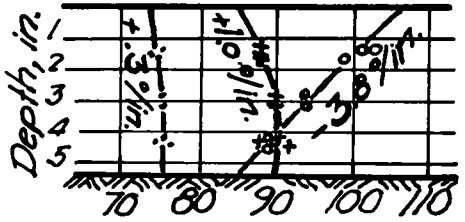


• Ave. 75F (6 10).

○ (11 55) Ave. 96F ○

+ (6 45) Ave 89F +

## LENGTH CHANGE

| Time, central std. | Change from Zero @ 70F: S. slope, rad. | Gage lengths, 100-50 in. | 50-0 in. | 0-50 in. | 50-100 in. | N. slope, rad. | 200 in. change at mid-depth, in. |
|---|---|---|---|---|---|---|---|
| 6 10 | .0033 | -.013 | -.008 | -.008 | -.011 | .0026 | -.027 |
| 11 55 | .0018 | -.005 | -.002 | -.002 | -.004 | .0014 | -.006 |
| 6 45 | .0032 | -.009 | -.005 | -.004 | -.008 | .0024 | -.013 |

A.M.: +2F, +0.021"; P.M.: -7F, -0.007".

Thermal coefficient: 0.0000050.

Length change at 70F: -0.032".

# B.

## CONTOURS

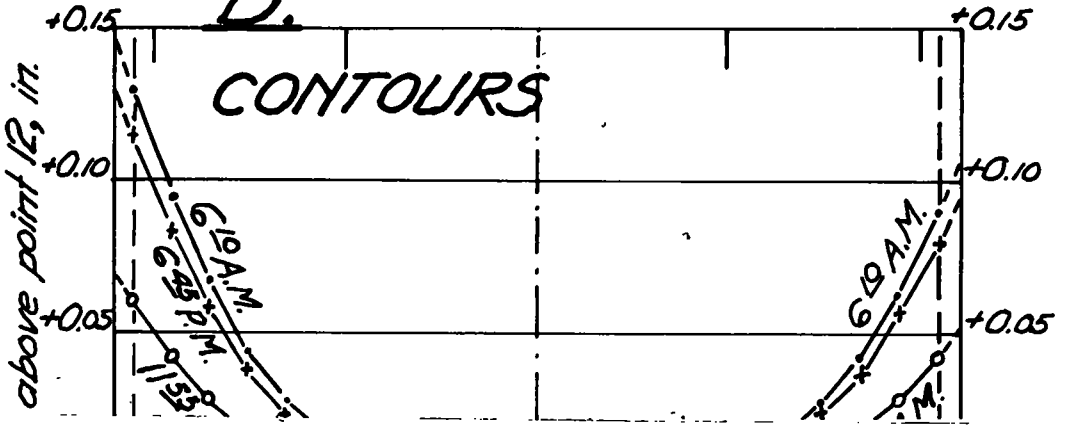

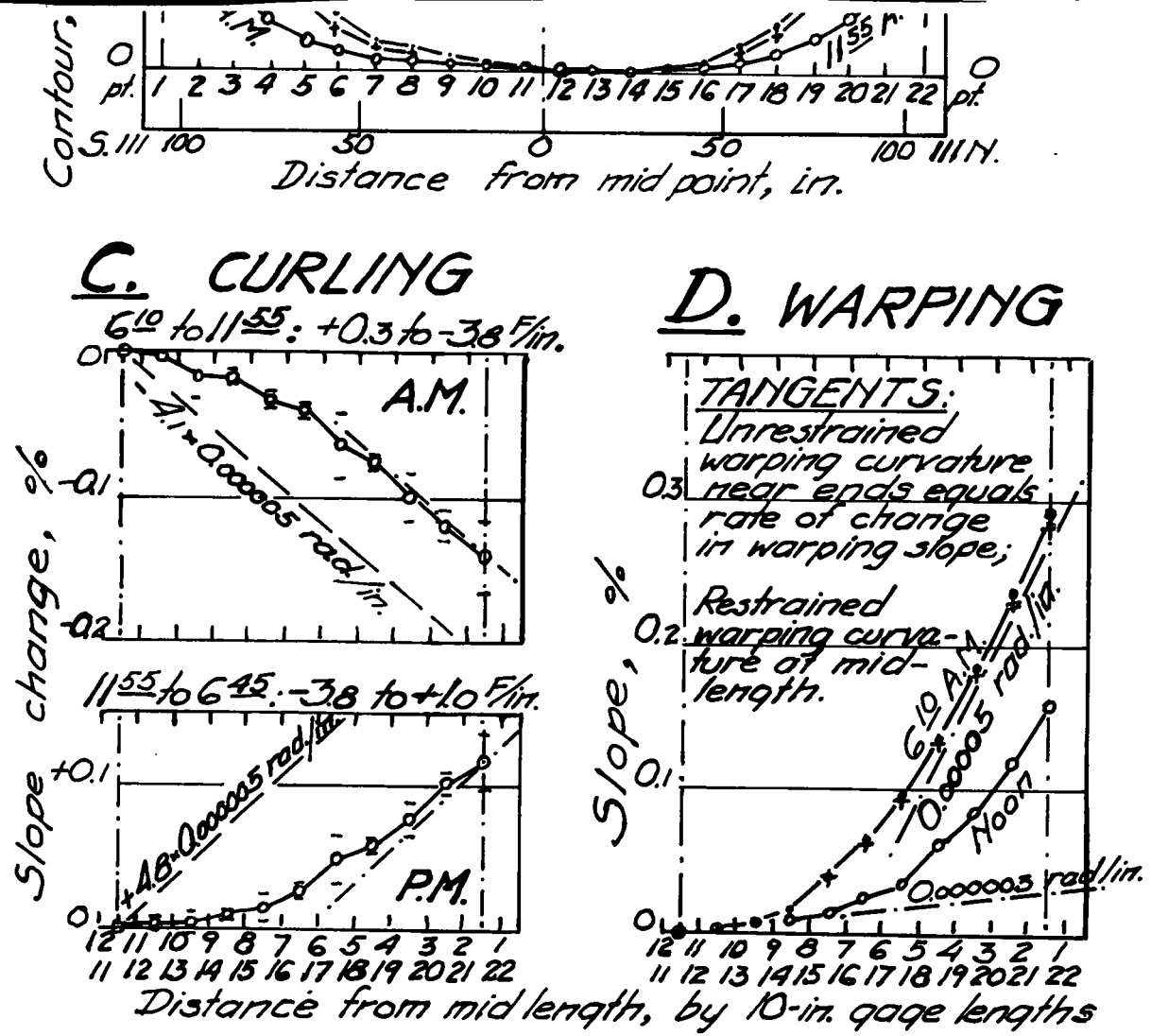


Figure 5. Experimental record for slab A 553 on September 15, 1956: (A) Temperature and length change data; (B) Contours, from clinometer readings; (C) Curling slope changes for morning and afternoon temperature change; (D) Warping slopes, averages for south and north halves.

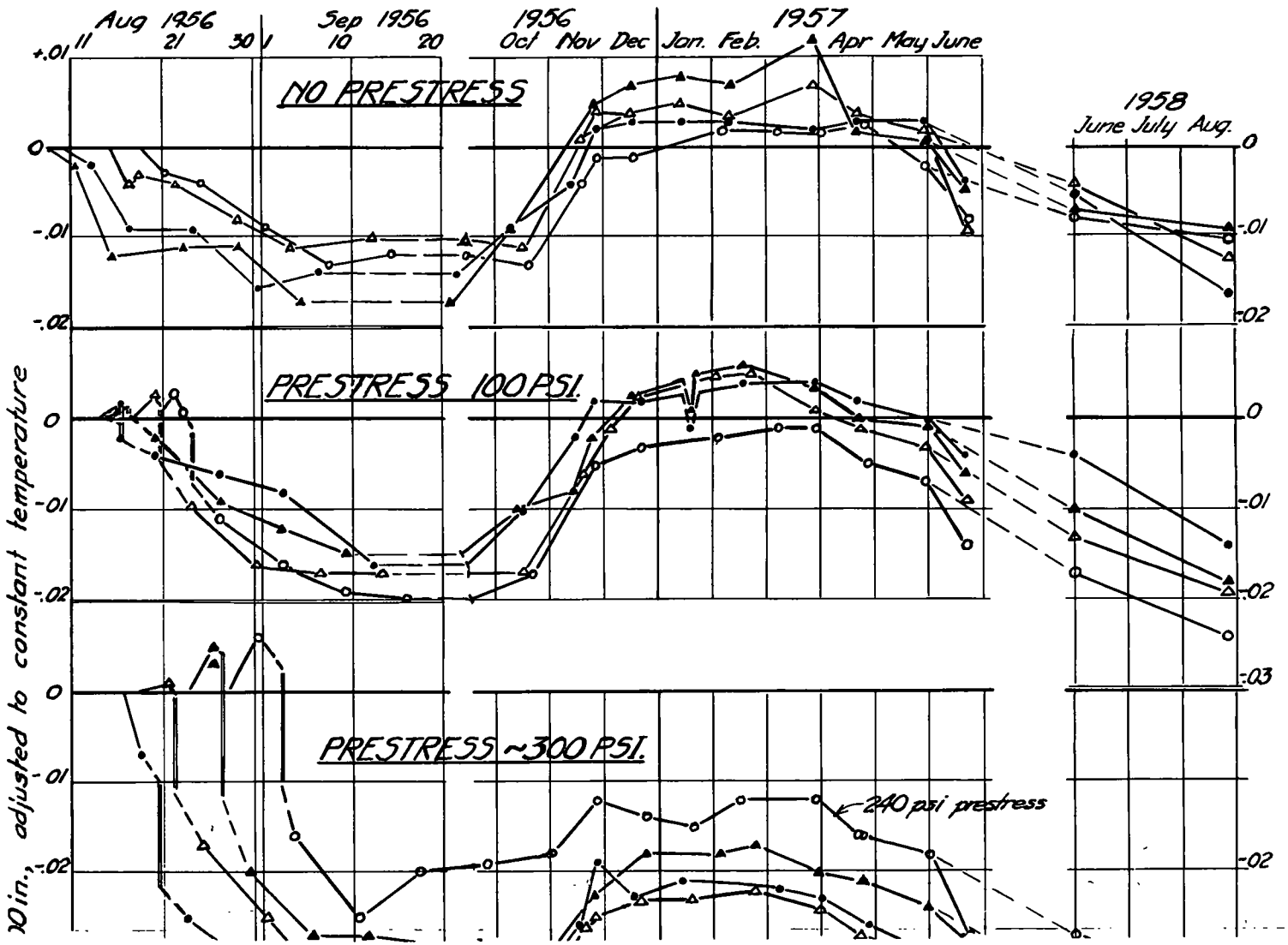
Aug 1956
11
21
30
Sep 1956
10
20
1956
Oct Nov Dec
1957
Jan. Feb.
Apr May June
1958
June July Aug.
NO PRESTRESS
PRESTRESS 100 PSI.
PRESTRESS ~300 PSI.
+.01
0
-.01
-.02
-.03
240 psi prestress
10 in., adjusted to constant temperature

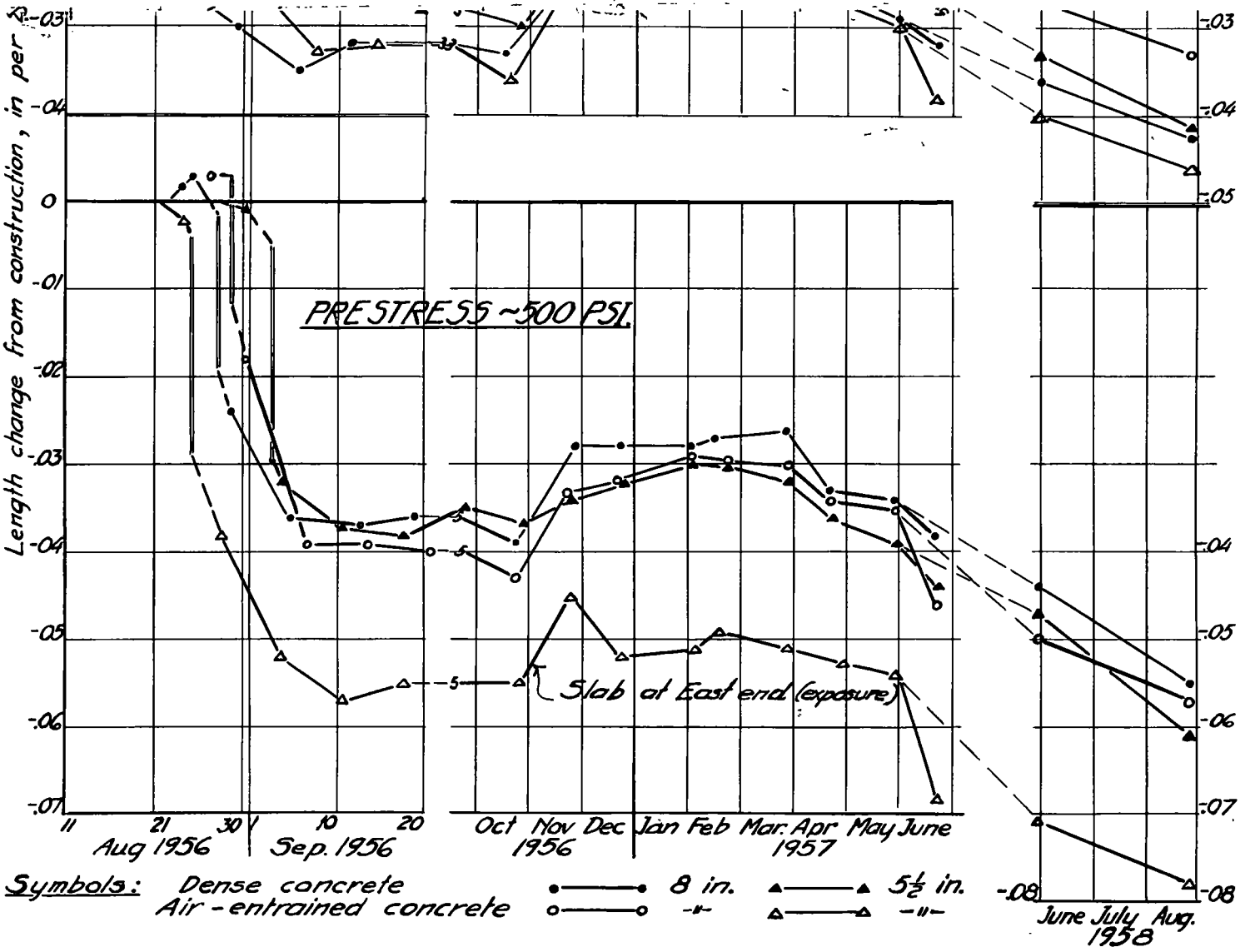


Figure 6. Progressive length changes of all field slabs to two years, adjusted to mid-depth and to 70 F temperature.

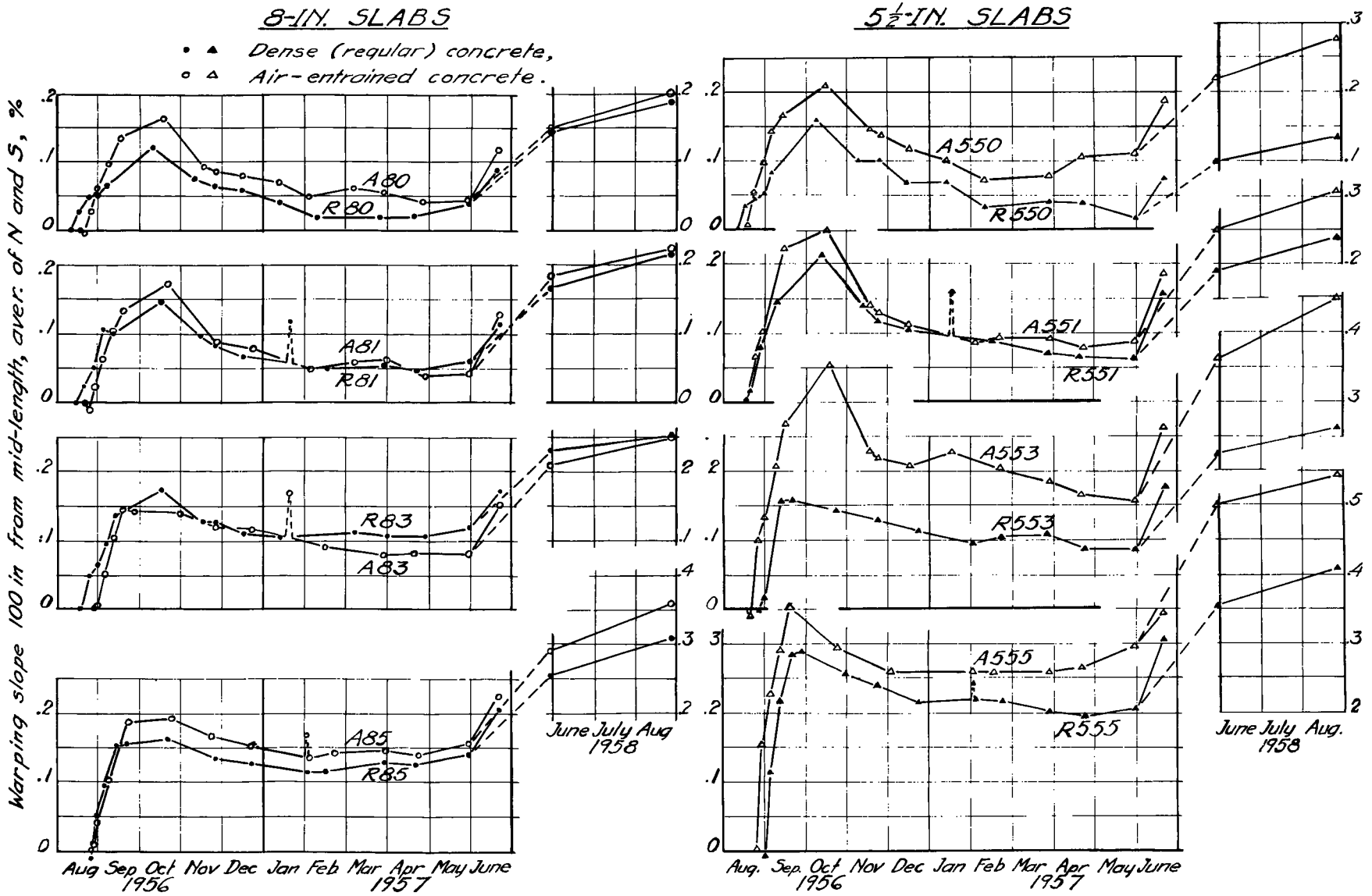


Figure 7. Progressive warping to two years; warping slopes average of north and south slopes, 100 in. from midlength.

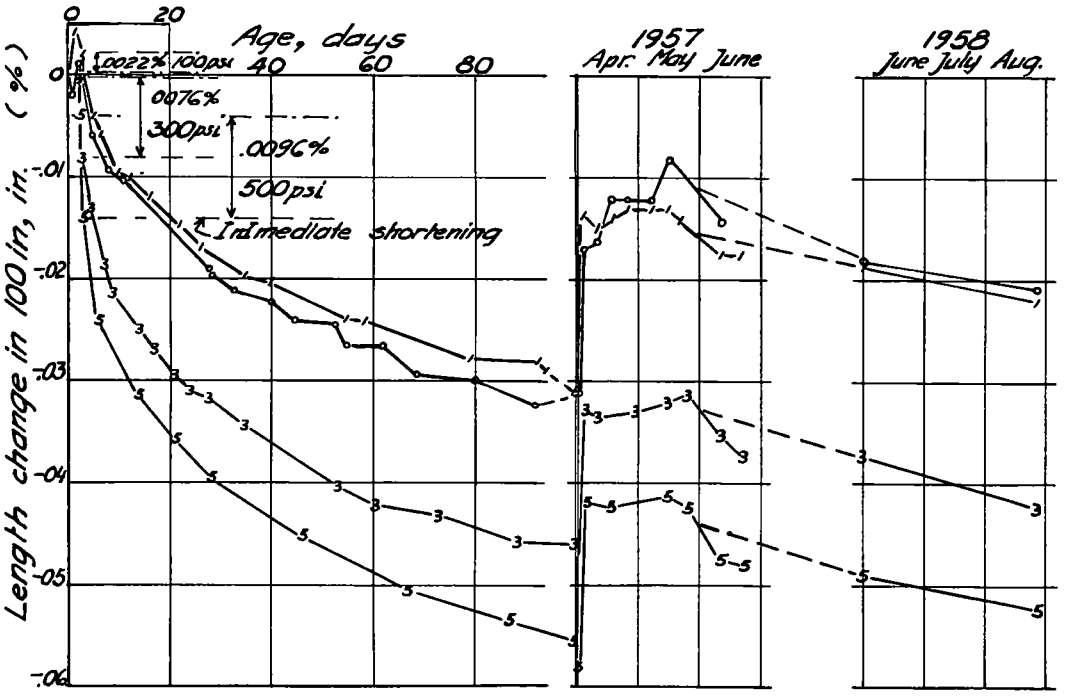


Figure 8. Length changes of correlation slabs during indoor exposure and on grade after April 1, 1957.

gradients in the curing slabs, observed at 2-day age, were +0.5 and -0.9 F/in. depth for the 8-in. slabs, +0.5 and -1.3 F/in. for the $5\frac{1}{2}$-in. slabs, average values. At the end of the 3-day curing period no significant length change, aside from temperature contraction and expansion, had taken place. No pronounced contour change occurred in the slabs during curing.

Temperature curling was observed in the curing slabs. Without pronounced upward warping, restraints to forenoon curling approached theoretical values for change in subgrade reaction proportional to deflection. After the curing period, rapidly increasing slab warping made such theoretical computations of curling restraints inapplicable.

Curling stresses during curing could reach full flexural restraint in all experimental slabs. Computed for modulus of elasticity E of 3,000,000 psi, and 2-day temperature gradients +0.5 F/in. night gradient in both 8- and $5\frac{1}{2}$-in. slabs, the curling restraint stresses were 30- and 20-psi top tension. The maximum observed noon gradients -1.6 and -1.7 F/in. in the 8- and $5\frac{1}{2}$-in. slabs would correspond to 96- and 70-psi bottom tension, respectively. Concrete modulus of rupture strengths exceeding 200 psi and possibly 300 psi could be expected at 48 hr at normal curing temperature (Part B). The wet burlap curing accordingly was effective in keeping noon curling stresses below 50 percent of the concrete strength. At least 10 to 15 F average night temperature decrease could be sustained in tension restraint without cracking, based on 15-psi per degree F temperature restraint tension stress in addition to the small night-curling top tension, under wet burlap curing. It is indicated that prestressing should be applied before, or when, covered mat curing is discontinued.

## Prestressing Effects

Length changes during application of prestressing were observed on only a few slabs. Through interpolation of length change data between 3 and 7 days, as shown in Figure 6, an approximation of immediate average shortening at prestressing has been obtained:

For 100-psi average prestress, 0.004 in. in 200 in., E = 5,000,000 psi;
For 280-psi average prestress, 0.012 in. in 200 in., E = 4,700,000 psi;
For 490-psi average prestress, 0.021 in. in 200 in., E = 4,600,000 psi.

There were fairly wide variations from slab to slab, but no significant variation in shortening could be deduced for the different ages at prestressing. Elastic shortening at prestress application at 3 days could be observed readily on the short indoor correlation slabs:

For 100 psi, 0.001 in. in 50 in., E = 5,000,000 psi;
For 280 psi, 0.0038 in. in 50 in., E = 3,700,000 psi;
For 520 psi, 0.0049 in. in 50 in., E = 5,300,000 psi.

It is apparent from Figures 6 and 7 that creep, and shrinkage of the slabs following curing, were especially noticeable up to 4 weeks age. For the same prestress, length changes for dense and air-entrained concrete and for the two thicknesses were not significantly different.

Pronounced warping, with end slopes from $\frac{1}{64}$ to $\frac{1}{32}$ in. in 10 in. and slab ends up to 0.15 in. higher than midlength, developed rapidly during the month of drying following curing, as also shown in Figure 7. The $5\frac{1}{2}$-in. slabs warped more than the 8-in. slabs, the air-entrained slightly more than the dense concrete slabs, and, most significant, the warping was greater, the greater the prestress.

## Long-Time Changes in Prestressed Slabs on Subgrade

After the initial drying period, the slabs in field exposure behaved quite differently from indoor exposed concrete. All slabs underwent a yearly cycle of length change, aside from temperature contraction and in opposite direction. Minimum yearly length occurred in September or October, followed by a rapid increase in length, opposed to the temperature contraction, to winter conditions. When adjustment for continuing creep is made, the yearly cycle of seasonal length change indicated by first year observations, was about 0.010 percent for all slabs, equivalent to some 20 F seasonal temperature compensation.

The warping increased, with seasonal fluctuations up to two years. As shown in Figure 7, warping appears to be at maximum seasonal amount during the fall. Warping contours June 1, 1958 are shown in Figure 9 for all slabs, corrected for tilt between the end points. Substantial subgrade displacements must have accompanied the warping, the subgrade accommodating itself to the warped shape, and ground support would be lacking for a short distance in from the ends under the warped slabs.

It is apparent from Figure 7 that seasonal influences were effective in decreasing warping during the late fall 1956. Lower warp persisted through the winter until late spring or early summer, when rapid increase in warp occurred in the course of a few weeks.

## Temperature Curling

All slabs at all ages underwent substantial daily contour changes in response to changing temperature gradients. Curling curvatures observed near slab ends were in general agreement with those computed from change in temperature gradient and about 0.000005 coefficient of thermal expansion.

Sufficient readings are available for clear indications of trends and approximate limits in temperature gradients during the period of observation. Maximum temperature gradients in the $5\frac{1}{2}$-in. slabs were consistently higher than in the 8-in. slabs. Recurrent observed maxima are listed subsequently.

Curling restraints during the first month and later were compared to obtain some idea of possible change in elastic modulus applicable to curling restraint. In Figure 10 the relationship between change in temperature gradient and the observed average change in slope 100 in. from midlength is shown for 8- and $5\frac{1}{2}$-in. slabs, at different ages to 21 months. The close agreement between curling at 1- and 21-month age for both 8- and $5\frac{1}{2}$-in. slabs, with fairly equal contours, is evident. The data do not

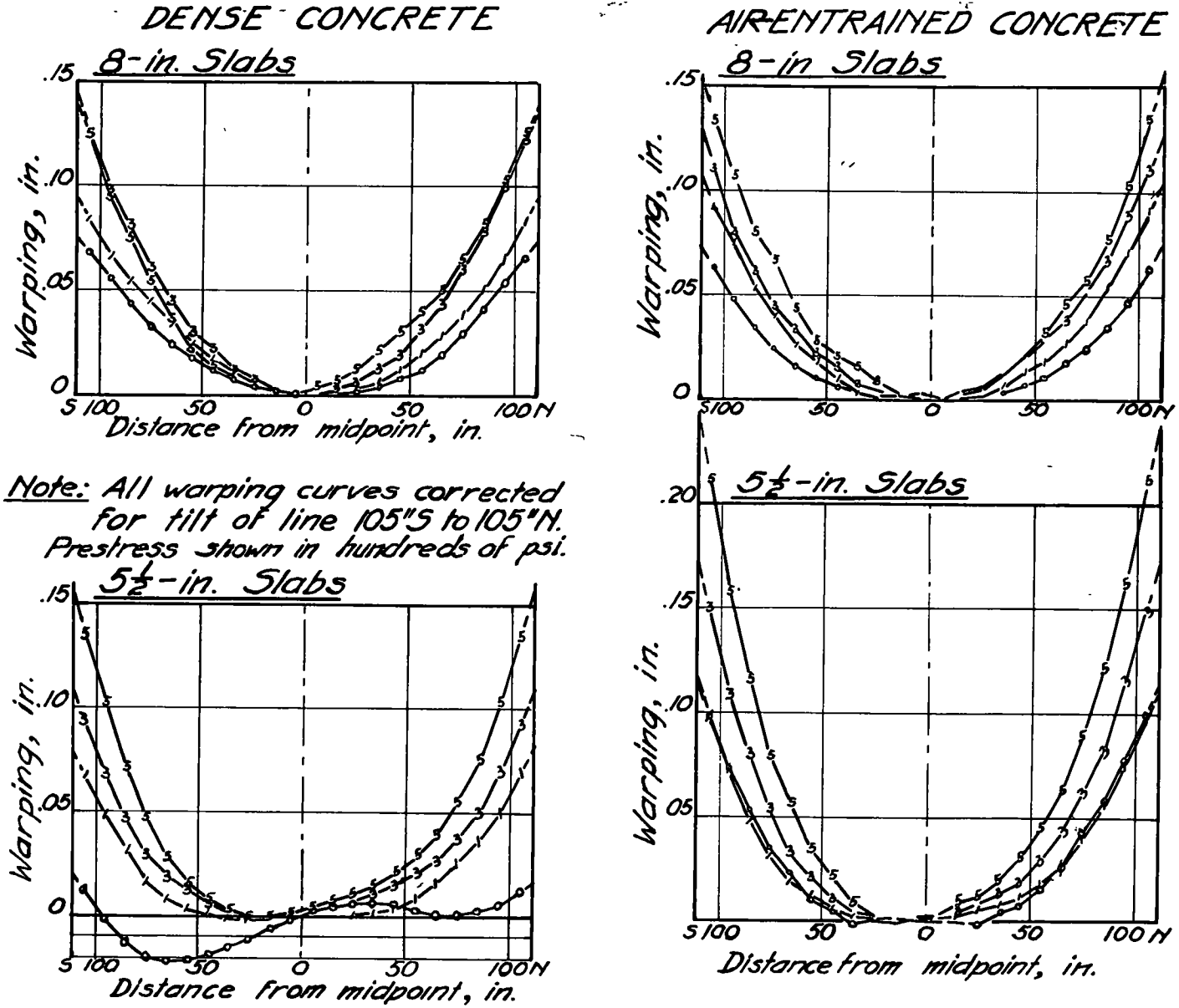


Figure 9. Warped contours at 21-month age, adjusted for slab tilt.

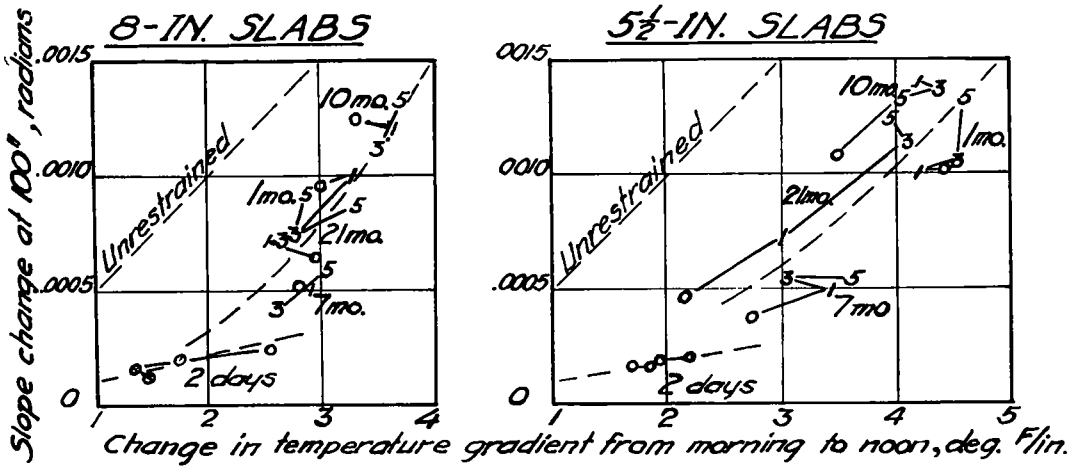


Figure 10. Curling slope change related to change in temperature gradient, at different ages up to 21 months.

indicate any great change in modulus of elasticity applicable to the daily curling restraint stresses from 1- to 21-month age.

Curling in slabs substantially longer than the test slabs must always be fully restrained except near the ends. The daily curling restraint stresses are dependent only on temperature gradients and applicable modulus of elasticity; 4,000,000 psi are assumed. Full curling restraint stresses indicated in 8- and $5\frac{1}{2}$-in. fully restrained long slabs for night and noon conditions, and for summer and winter conditions, based on 0.000005 coefficient of thermal expansion, and for maximum temperature gradients observed on several occasions are given in Table 4.

TABLE 4

FULL CURLING RESTRAINT STRESSES

| Time | Season | Tension | 8-In. Slabs | | $5\frac{1}{2}$-In. Slabs | |
|---|---|---|---|---|---|---|
| | | | Temp. Grad. (°F/in.) | Flex. Stress (psi) | Temp. Grad. (°F/in.) | Flex. Stress (psi) |
| Night | Any | Top | +1.4 | 110 | +1.8 | 100 |
| Noon | Summer | Bottom | -3.2 | 260 | -4.0 | 220 |
| | Winter | Bottom | -2.2 | 180 | -3.2 | 180 |

## Warping Restraint and Warping Restraint Stresses

The project provided the first known quantitative estimation of warping restraint stresses, due to the careful observations of length and contour changes from the earliest age for different known levels of stress. Unit deformations for the known stresses near the ends of the slabs could be determined at various ages both at top and bottom. Assuming that the same stress-deformations relations hold away from the ends, the stresses at top and bottom in the restrained midportions, and in long slabs, could be deduced.

Near the ends, the only variations to the evenly distributed and constant prestress are the small flexural stresses caused by the unsupported steel plates and spring assemblies. The ends lift incident to warping, subgrade support is shifted away from

the ends, and the static moments due to dead load increase steeply away from the ends, with stresses and strains at top and bottom in opposite direction to the warping unit deformations. Beyond the distance from the end at which full warping restraint is reached, deformations must be the same at top and bottom in those flat slab portions, and equal to the observed mid-depth length changes both at top and bottom. Frictional restraints would become noticeable only at much greater distance from the end.

Table 5 gives the top and bottom stresses 16 in. in from the ends. The table also gives the warping curvatures at these same points 2 and 21 (between the two 10-in. gage lengths nearest the ends), average for the dense and air-entrained duplicate test slabs, as determined from many sheets of slope observations at four different ages to 2 years, by the tangent to the warping slope curve as shown in Figure 5 D for one slab at one age. From the unit length changes at mid-depth, and the curvatures, top and bottom unit deformations have been computed as given in Table 5, corresponding to the known top and bottom stresses. In Figure 11, the unit deformations in relation to stresses have been plotted for the four ages, separately for top and bottom and for 8- and 5½-in. slabs. The plots indicate the relationships between the top and bottom deformations and stresses. These relations are assumed representative for each pair of slabs, irrespective of distance from the ends.

TABLE 5

TOP AND BOTTOM STRESSES AND TOP AND BOTTOM DEFORMATIONS NEAR THE ENDS, FROM 4 WEEKS TO 2 YEARS AGE

| Item | 8-In. Slabs | | | | 5½-In. Slabs | | | |
|---|---|---|---|---|---|---|---|---|
| Dense and Air-Entrained Avg. | 80 | 81 | 83 | 85 | 550 | 551 | 553 | 555 |
| Stresses near ends (psi): | | | | | | | | |
| Average prestress | 0 | -100 | -265 | -485 | 0 | -100 | -300 | -485 |
| Stresses 90 to 100 in. from mid: | | | | | | | | |
| Top | + 10 | - 80 | -240 | -450 | + 15 | - 75 | -265 | -450 |
| Bottom | - 10 | -120 | -290 | -520 | - 15 | -125 | -335 | -520 |
| Deformations[1] at 90 to 100 in.: | | | | | | | | |
| September, 4-week age: | | | | | | | | |
| Warping curvature | 16 | 19 | 27 | 31 | 24 | 30 | 42 | 55 |
| Length change at mid-depth | - 70 | - 90 | -130 | -190 | - 70 | - 80 | -150 | -230 |
| Deformations: | | | | | | | | |
| Top | -135 | -165 | -250 | -305 | -130 | -160 | -265 | -380 |
| Bottom | - 5 | - 15 | - 30 | - 60 | 0 | 0 | - 35 | - 80 |
| Spring, at about 7 months: | | | | | | | | |
| Warping curvature | 10 | 14 | 17 | 24 | 14 | 17 | 32 | 43 |
| Length change at mid-depth | + 15 | + 8 | - 85 | -140 | + 25 | + 12 | -105 | -210 |
| Deformations: | | | | | | | | |
| Top | - 25 | - 50 | -155 | -235 | - 13 | - 35 | -195 | -330 |
| Bottom | + 55 | + 65 | - 15 | - 45 | + 63 | + 60 | - 15 | - 90 |
| Spring, at 21 months: | | | | | | | | |
| Warping curvature | 19 | 28 | 30 | 40 | 32 | 35 | 55 | 70 |
| Length change at mid-depth | - 28 | - 53 | -158 | -230 | - 28 | - 58 | -180 | -290 |
| Deformations: | | | | | | | | |
| Top | -105 | -165 | -280 | -390 | -115 | -155 | -330 | -480 |
| Bottom | + 50 | + 60 | - 40 | - 70 | + 60 | + 40 | - 30 | -100 |
| At 2 years age: | | | | | | | | |
| Warping curvature | 23 | 30 | 35 | 45 | 37 | 45 | 60 | 75 |
| Length change at mid-depth | - 48 | - 98 | -188 | -278 | - 48 | - 95 | -218 | -350 |
| Deformations: | | | | | | | | |
| Top | -140 | -220 | -330 | -460 | -150 | -220 | -385 | -555 |
| Bottom | + 45 | + 20 | - 50 | -100 | + 55 | + 30 | - 55 | -145 |

[a] From midlength ($10^{-6}$) rad per in.).

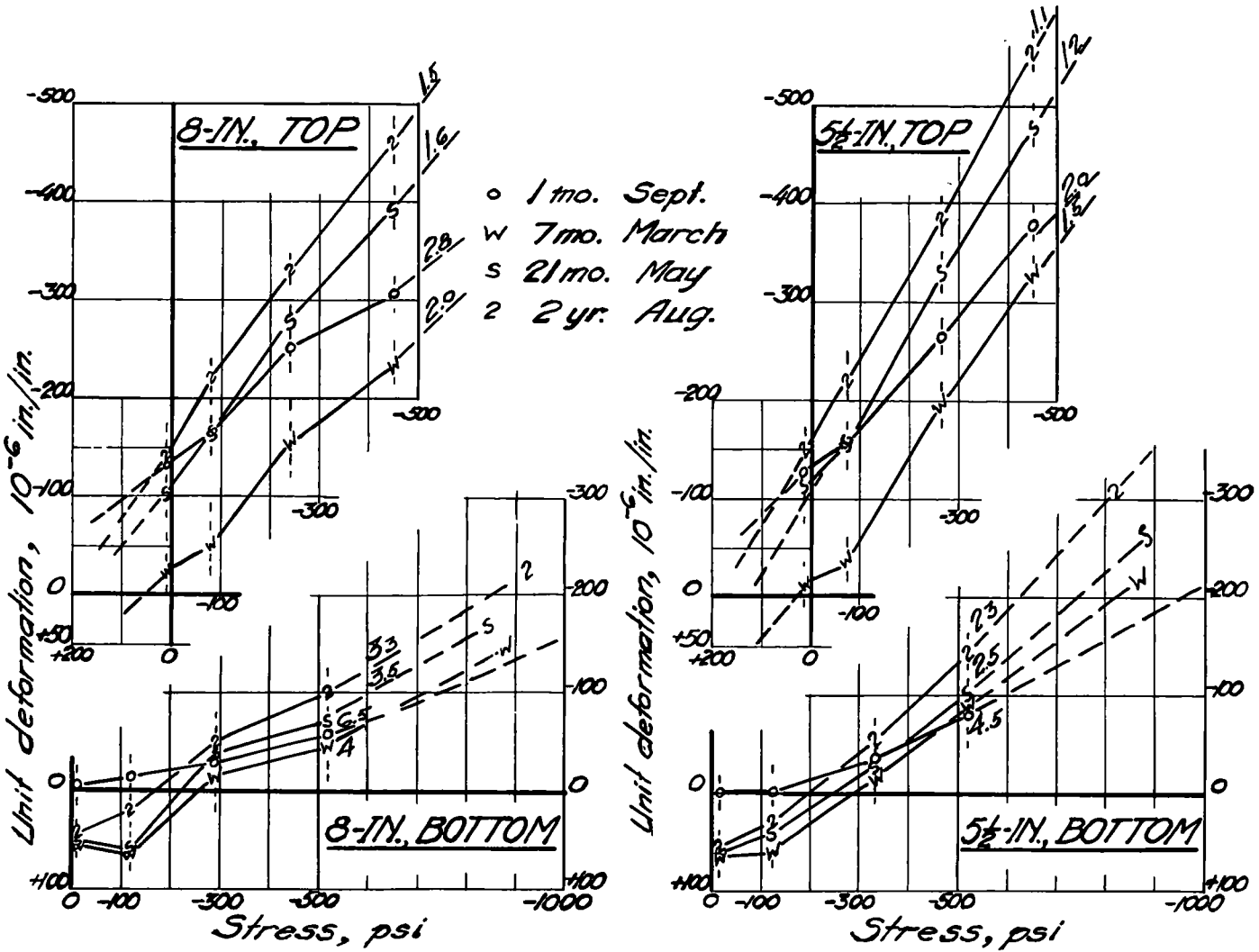


Figure 11. Observed unit deformations related to known stresses at top and bottom near ends, at different ages to 2 years. Inclinations of curves show modulus-of-deformation values in millions psi.

It is evident from the warping observations, as shown in Figure 11, that different relations between unit deformations and stresses exist at top and bottom of the slabs. The experimental use of three levels of prestress made it possible to indicate these relations with fair accuracy. The points in Figure 11 for zero stress indicate shrinkage or swell at each age at top and bottom, predominantly shrinkage at top and swell at bottom. The modulus of resistances (immediate and progressive stress deformation), as indicated by the slopes of the fairly linear stress-deformations in Figure 11, for different ages, approximate those in Table 6. The modulus of resistance as seen is over twice as high at bottom as at top of the slabs. Data on modulus of resistance in soil-supported slabs have not been known or indicated heretofore. The great differences between top and bottom values are startling, most significant, and deserve more investigation.

TABLE 6

MODULUS OF RESISTANCE

| Date | Age and Duration of Stress (mo) | Modulus of Resistance ($\times 10^6$ psi) | | | |
|---|---|---|---|---|---|
| | | 8-In. Slabs | | $5\frac{1}{2}$-In. Slabs | |
| | | Top | Bottom | Top | Bottom |
| Sept. 1956 | 1 | 2.8 | 6.5 | 1.9 | 4.5 |
| Spring 1957 | 7 | 2.0 | 4.0 | 1.5 | 2.7 |
| June 1, 1958 | 21 | 1.6 | 3.5 | 1.2 | 2.5 |
| Sept. 1, 1958 | 24 | 1.5 | 3.3 | 1.1 | 2.3 |

## Warping Restraint Stresses

Actual stresses existing on the midlength cross-section could be estimated from the top and bottom length changes at midlength, if it is assumed that the concrete there creeps under stress, as well as shrinks and swells, in the same way as the concrete near the ends (Fig. 11). Top and bottom unit deformations at midlength were computed from the observed length changes and midlength curvatures (see Fig. 5D).

Table 7 gives the computed midlength deformations at top and bottom, also the corresponding stresses for 8- and $5\frac{1}{2}$-in. slabs, average of dense and air-entrained duplicate slabs at different ages to 2 years, obtained by interpolation and extrapolation from Figure 11. Extrapolation of top deformations into the range of tension stresses as seen in Figure 11 is rather uncertain. Extrapolation of bottom deformations to indicated compression stresses up to twice the experimental prestress limit is more reliable and in line with linear relations observed in creep tests generally. High compression stresses existed in the bottom of the slabs at midlength. Full restraint to warping was reached at, or before, midlength in the slabs with 100 psi and no prestress during the winter and spring, but only in the $5\frac{1}{2}$-in. unprestressed slabs at 2 years.

The principal difference between warping of the test slabs and longer slabs is that warping curvatures must be zero in fully restrained portions of longer slabs. Deformations at top and bottom must both be equal to the length change at mid-depth. Full warping restraint stresses, as indicated by the observed unit length changes and Figure 11 stress-deformation relationships in the test slabs, are shown in Figure 12 for different prestress values in 8- and $5\frac{1}{2}$-in. slabs. The average stress on the section must equal the prestress; nonlinear distribution of stress, as shown, is accordingly indicated between the computed top and bottom chord stresses.

Figure 12 shows strikingly high compression stresses at the bottom of pavement slabs fully restrained away from slab ends. The stresses were highest after the first

TABLE 7

TOP AND BOTTOM DEFORMATIONS AND CORRESPONDING STRESSES AT MIDLENGTH, BASED ON STRESS-DEFORMATION RELATIONS OBSERVED NEAR ENDS, FROM 4 WEEKS TO 2 YEARS AGE

| Item | 8-In. Slabs | | | | $5\frac{1}{2}$-In. Slabs | | | |
|---|---|---|---|---|---|---|---|---|
| Avg. prestress (psi) | 0 | -100 | -265 | -485 | 0 | -100 | -300 | -485 |
| Deformations at Midlength[a] ($10^{-6}$ rad/in.): | | | | | | | | |
| September, 4 weeks: | | | | | | | | |
| Warping curvature | 2 | 4 | 6 | 9 | 1 | 2 | 4 | 8 |
| Deformations: | | | | | | | | |
| Top | - 80 | -110 | -165 | -225 | - 70 | - 85 | -160 | -250 |
| Bottom | - 60 | - 70 | -115 | -155 | - 60 | - 75 | -140 | -210 |
| Spring, at about 7 month: | | | | | | | | |
| Warping curvature | 0 | 0 | 3 | 6 | - 2 | - 1 | 0 | 3 |
| Deformations: | | | | | | | | |
| Top | + 15 | + 8 | -100 | -165 | + 31 | + 15 | -105 | -220 |
| Bottom | + 15 | + 8 | - 70 | -115 | + 20 | + 10 | -105 | -200 |
| Spring, at 21 month: | | | | | | | | |
| Warping curvature | 6 | 8 | 14 | 17 | - 4 | 1 | 5 | 12 |
| Deformations: | | | | | | | | |
| Top | - 52 | - 85 | -215 | -300 | - 15 | - 60 | -195 | -325 |
| Bottom | - 4 | - 20 | -100 | -160 | - 40 | - 55 | -165 | -255 |
| At 2 years: | | | | | | | | |
| Warping curvature | 8 | 11 | 16 | 22 | - 3 | 4 | 11 | 17 |
| Deformations: | | | | | | | | |
| Top | - 80 | -140 | -250 | -365 | - 40 | -105 | -250 | -395 |
| Bottom | - 15 | - 55 | -125 | -190 | - 55 | - 85 | -190 | -305 |
| Top and Bottom Stresses at Midlength[b] (psi): | | | | | | | | |
| September, 4 weeks: | | | | | | | | |
| Top | +150 | + 50 | - 80 | -200 | +150 | +100 | - 70 | -250 |
| Bottom | -520 | -600 | -800 | -1,000 | -480 | -550 | -750 | -1,000 |
| Spring, 7 months: | | | | | | | | |
| Top | +100 | + 50 | -160 | -270 | +100 | + 50 | -170 | -310 |
| Bottom | -230 | -250 | -600 | -750 | -230 | -270 | -560 | -800 |
| June 1, 21 months: | | | | | | | | |
| Top | +100 | + 30 | -150 | -290 | +100 | + 50 | -120 | -260 |
| Bottom | -230 | -260 | -600 | -800 | -370 | -400 | -650 | -850 |
| August, 2 years: | | | | | | | | |
| Top | +100 | + 10 | -130 | -310 | +150 | + 50 | -110 | -270 |
| Bottom | -220 | -330 | -600 | -800 | -350 | -410 | -600 | -800 |

[a] Values of unit length change at mid-depth same as near ends.
[b] Extrapolated stresses estimated from Fig. 11.

month's drying period, slightly lower during the first cold season, and as relieved by creep at greater age. Warping restraint stresses indicated in unprestressed slabs on the order of 300-psi compression at bottom and 100-psi tension at top are of interest for conventional pavement performance. High compression stresses near the bottom are most beneficial, to counteract load tension and daytime curling restraint tension away from ends in any concrete pavement.

## Effective Prestressing

This exploratory investigation indicated that prestressing could be applied to concrete pavements with exceptional structural advantages. Pavement behavior serves

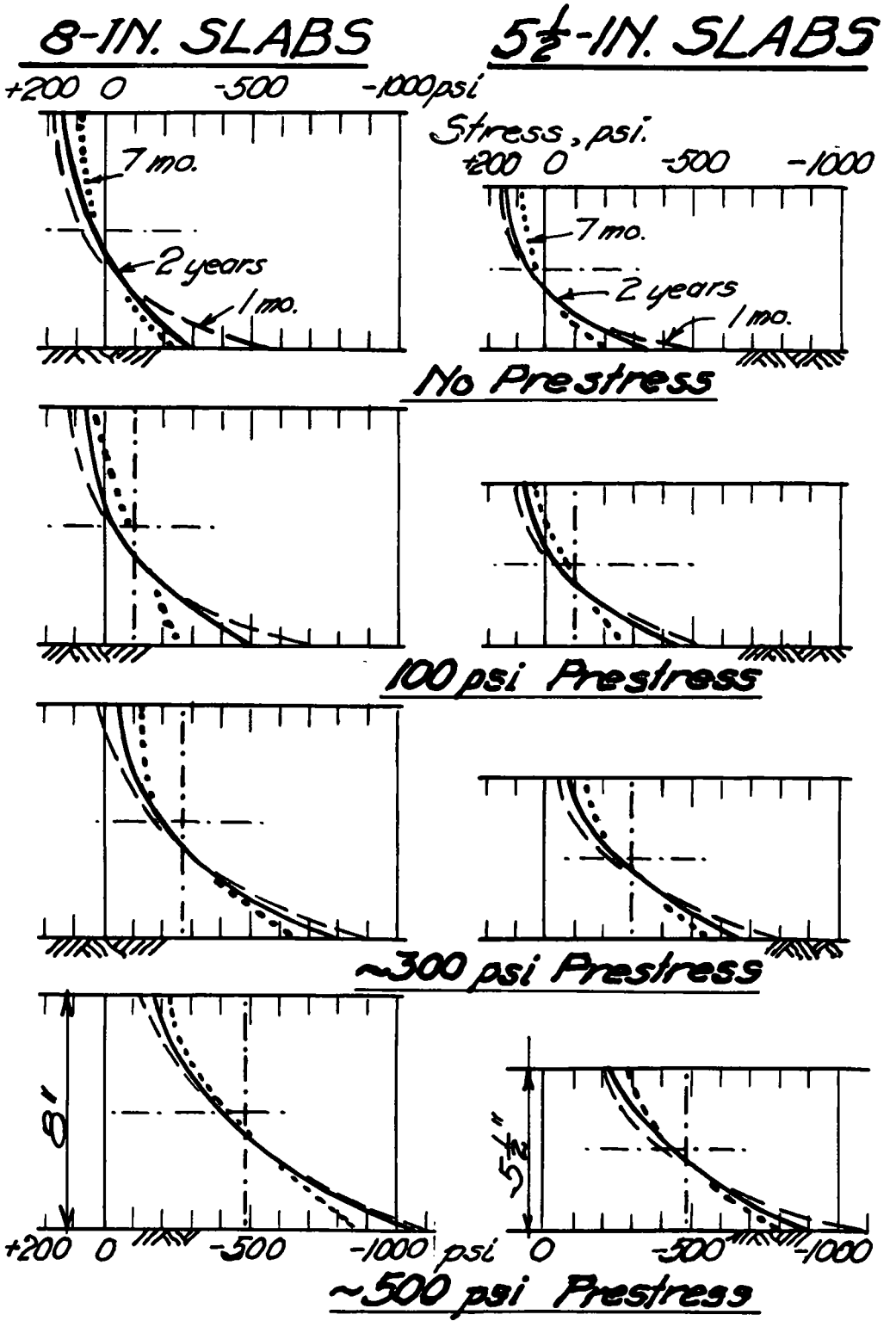


Figure 12. Stress distribution from top to bottom for full restraint of warping, based on unit deformations observed in the field slabs.

to concentrate the prestress near the bottom of pavement, where it is most needed, with corresponding decrease in prestress near the top where load tension stresses are insignificant except near corners. If prestress is applied at center depth and evenly distributed on the cross-section, the observations indicate that high warping deformations and deflections will take place, as the natural remedy by which the prestress is redistributed in accord with concrete properties.

Excessive end warping can be prevented if the prestress is centered below mid-depth, imposing the approximate distribution of stress which is otherwise naturally developed by warping. The amount of prestress can be decreased below that necessary for design based even distributed of prestress, because evenly distributed prestress would not be fully utilized in top portions of the pavement, except very near the ends.

High-tension load stresses at the surface near corners of pavement slabs are not fully counteracted by high prestress near bottom. The high top tension stresses occur only with a few feet from the corners, and can be effectively counteracted by local prestress application or other means.

## PART B — PROPERTIES OF CONCRETE AT EARLY AGE IN 100, 70, AND 40 F TEMPERATURES

The research was planned to provide information on strength increase and stress deformations in pavement concrete during early age at different construction temperatures. The exploratory investigation covered short-time tests to failure of conventional cylinder and beam laboratory specimens, which were made and stored at 100, 70, and 40 F ambient temperatures and tested at different ages from the earliest at which they could be handled, up to 28 days. Immediate stress deformations were measured in compression on both cylinders and beams and in tension on beams.

### Materials

Concrete and proportions were the same as described in Part A. Air-entrained concrete was used in one 70 F series; "Ad-Aire" agent, mixed with the water at the rate of $13\frac{1}{2}$ g per sack cement, gave air content from 3.4 to 5.3 percent, averaging 4.4 percent. The concrete was mixed in a 3-cu ft mixer not less than 2 min. Cylinders and beam forms were filled and rodded according to ASTM procedure.

The concrete materials, and the specimens up to the time of testing, were kept in a small, temperature-controlled room at substantially constant ambient temperature, selected for each series of tests. Batches were weighed in the room and brought to the mixer just outside. As soon as possible after placement in the forms, the specimens were returned to the room to remain until tested. The specimens were cured in their forms until just before testing or to 3-day age. The room temperatures and variation for the different series are given in Table 8.

TABLE 8

ROOM TEMPERATURES

| Concrete | Room Temperature (° F) | Room Humidity (%) | Concrete Placement Temperature (° F) |
|---|---|---|---|
| Dense: | | | |
| 100 F | 100 ± 2 | 73-82 | 97 |
| 70 F | 70 ± 5 | 87-94 | -- |
| 40 F | 40 ± 2 | 87-92 | 49 |
| Air-entrained | 70 ± 5 | 89-94 | -- |

Testing Schedule

As soon as the specimens could be handled and placed in the testing machine, the earliest tests were made. These ages depended on temperature. Cylinder tests could be made somewhat earlier than beam tests (see Table 9). Other tests were made at increasing ages, a few hours apart during the first day, every 12 hr to 3-day age, and at 7, 14, and 28 days. Just before testing, the individual specimen was taken to the testing machine in the laboratory at normal room temperature, instrumented, and tested immediately. A test was completed within 15 to 20 min. All tests were carried to failure. Generally, three identical specimens were tested at each age. The total number of specimens in all series included about 190 compression cylinders, 175 tensile splitting test cylinders, and 165 beam tests.

TABLE 9

EARLIEST TESTING AGE

| Specimen | Earliest Testing Age (hr) | |
|---|---|---|
| | Cylinders | Beams |
| 100 F | 3 | 6 |
| 70 F | 6 | 8 |
| 40 F | 12 | 24 |

Compression Tests. — All compression specimens were 6- by 12-in. cylinders cast in parafined paper molds with metal bottom. For tests at the earliest ages the cylinders were not capped but were tested between fiberboard sections. Plaster of paris capping was used for later tests. The cylinders were capped near the time of testing, but all 100 F cylinders for later tests were capped at 12-hr age. Deformations in all capped cylinders were measured with a Riehle compensating compressometer. An instrumented cylinder in the testing machine is shown in Figure 13. Deformations in early tests were comparatively large and probably nearly all plastic. No repeat loadings were made to show the amount of elastic deformation. To avoid confusion with conventional age concrete tests, in which a greater part of the immediate length change is elastic, the stress-deformation relation in all these tests is referred to as modulus of deformation, rather than modulus of elasticity.

Beam Tests. — All beams measured 6 by 8 by 32 in. and were tested with the 8-in. dimension vertical, loaded at the third points of a 27-in. span. The beam forms were $\frac{3}{4}$-in. plywood; the bottom was hinged 4 in. from each end, so that the beams could be placed in the testing machine while still mainly supported by the bottom form, to prevent damage at early age. Huggenberger 8- or 7-in. tensometers were attached for strain measurements 1 in. below the top and 1 in. above the bottom on one side of the beam at center span between the two loads. Figure 14 shows a beam under test. The 40 and 70 F beams were tested with half-round centering bars at both loading points; in the 100 F tests round bars were used at both load points. No pads were used at the load points.

Tensile Splitting Tests. — Cylinder splitting tests were made at the same ages as the cylinder compression tests. The cylinders were split by two diametrically opposed line loads applied through metal loading strips and $\frac{1}{2}$-in. wide 12-in. long plywood pads. Figure 15 shows a test immediately after failure.

For a concrete cylinder of diameter D loaded by opposed concentrated loads p per unit of length, the tensile splitting strength $f_d$ is taken as

$$f_d = \frac{2}{\pi} \frac{P}{D} = 0.64\ P/D \qquad (1)$$

Eq. 1 gives the true tension stress only for isotropic elastic materials and concentrated line loads.

If plastic readjustment (shear wedge failures as observed in tests Part C) occurs near the line loads, the tension on the diametric plane would be increased, because only the section between the shear wedges would be effective for tension reaction to the horizontal component of the radial distribution forces. Assuming shear wedge depth w, the average tension stress $f_t$ on the remainder of the section would be

$$f_t = \frac{2}{\pi} \frac{P}{(D - 2w)} = 0.64 \frac{P}{D - 2w} \qquad (2)$$

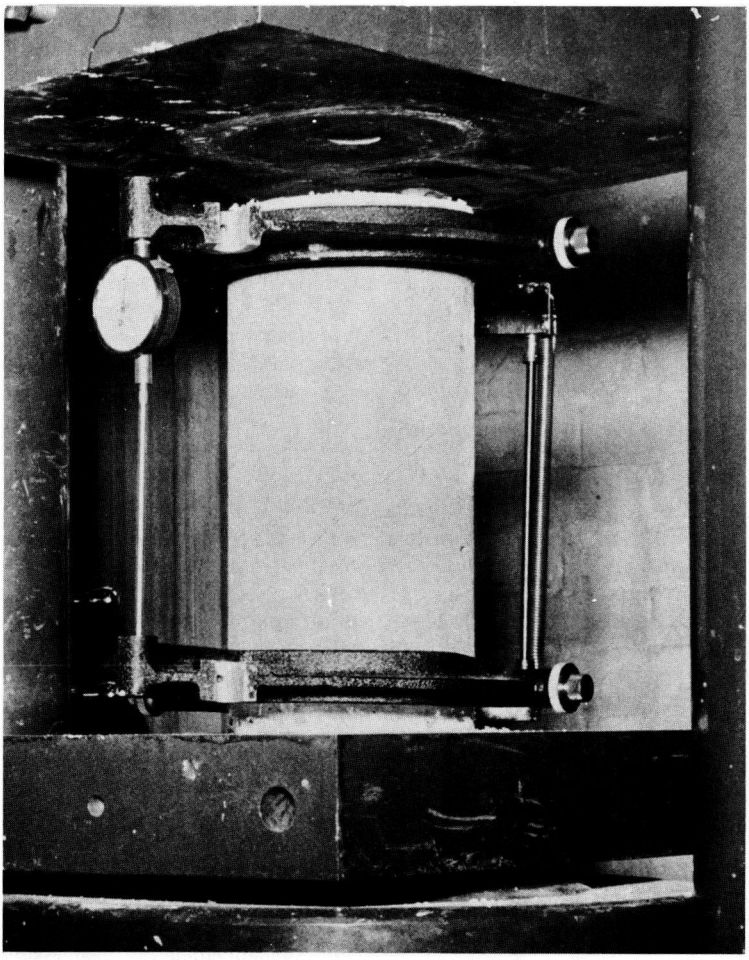

Figure 13. Compression cylinder with Riehle compensating compressometer in place in testing machine.

At early age, concrete tension strength appears to be higher in relation to compressive strength than at later age, and shear wedge failure could be expected to influence cylinder splitting stress.

## Test Data

Tables 10, 11, and 12 give basic data for cylinder compression tests, beam tests, and cylinder splitting tests, respectively, for the three ambient temperatures. In this presentation of test data, emphasis is given to early-age development of strength and to relations between strength and deformation for compressive and tensile stresses. Dense and air-entrained concrete tests at 70 F were not significantly different; average values of the two have been shown in illustrations comparing different ambient temperatures.

Compression Tests. — Typical stress-deformation diagrams for compression cylinders at different early ages are shown in Figure 16 for all three temperatures. This figure shows that 40 F concrete had very little resistance to deformation before 4-day age, but between 4 and 7 days the resistance increased to values in the range of 70 and

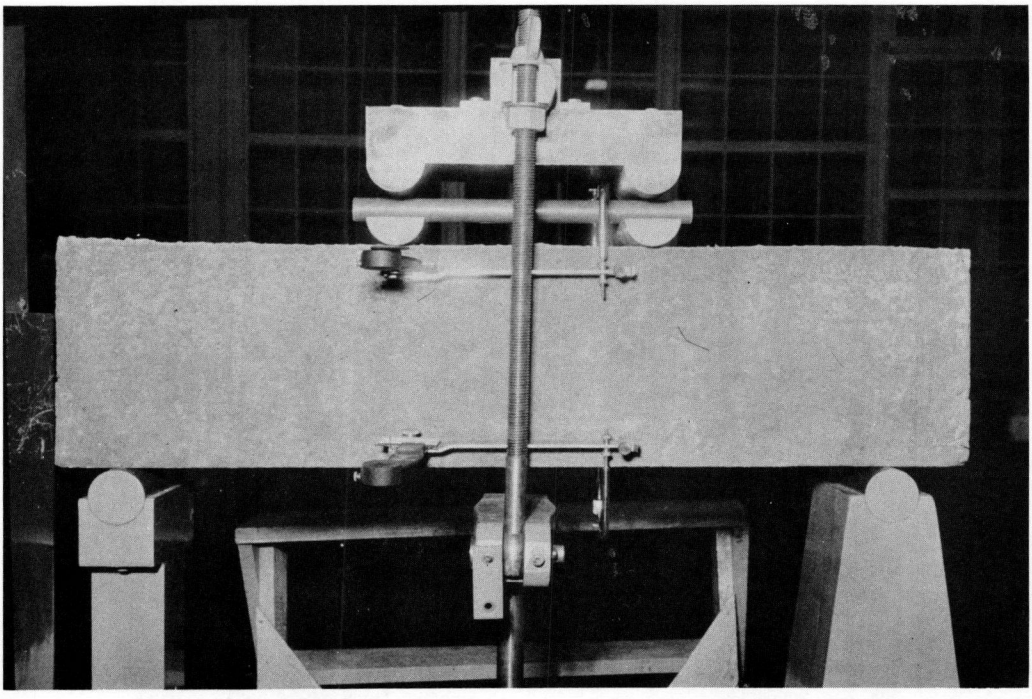

Figure 14. Beam with loading rig and Huggenberger tensometer gages attached in place in beam testing machine. Beams in 70 and 40 F tests had half-round bars at the load points; beams in 100 F tests had round bars.

TABLE 10

COMPRESSIVE STRENGTH OF 6- BY 12-IN. CYLINDERS, AND DEFORMATION AT 50 PERCENT OF COMPRESSIVE STRENGTH, FOR 100, 70, AND 40 F CONCRETE[a]

| Age at Test | 100 F | | 70 F | | | | 40 F | |
|---|---|---|---|---|---|---|---|---|
| | | | Dense | | Air-Entrained | | | |
| | Compression Str. (psi) | Deformation ($10^{-6}$ in./in.) | Compression Str. (psi) | Deformation ($10^{-6}$ in./in.) | Compression Str. (psi) | Deformation ($10^{-6}$ in./in.) | Compression Str. (psi) | Deformation ($10^{-6}$ in./in.) |
| 8 hr | | | 30 | | 25 | | | |
| 9 hr | 420 | | | | | | | |
| 12 hr | 780 | 300 | 90 | 120 | 90 | | 6 | |
| 16 hr | | | 220 | 90 | 220 | 70 | 9 | |
| 24 hr | 1,410 | 300 | 660 | 100 | 590 | 110 | 18 | |
| 36 hr | | | 1,140 | 1,170 | 1,070 | 180 | 44 | |
| 48 hr | 1,700 | 180 | 1,410 | 210 | 1,380 | 190 | 83 | |
| 60 hr | | | 1,690 | 240 | 1,660 | 220 | 250 | 5,800 |
| 3 day | 1,960 | 280 | 1,810 | 230 | 1,790 | 240 | 400 | 7,100 |
| 7 day | 2,410 | 300 | 2,510 | 260 | 2,490 | 330 | 1,270 | 200 |
| 14 day | 2,400 | 350 | 2,950 | 340 | 3,100 | 320 | 2,480 | 380 |
| 28 day | 2,410 | 390 | 3,220 | 340 | 3,340 | 360 | 2,550 | 320 |

[a]Fiber board capping was used in tests at 100 F, 9 hr; 70 F dense concrete, 8 hr; 70 F air-entrained concrete, 8 and 12 hr; and 40 F, 48 hr.

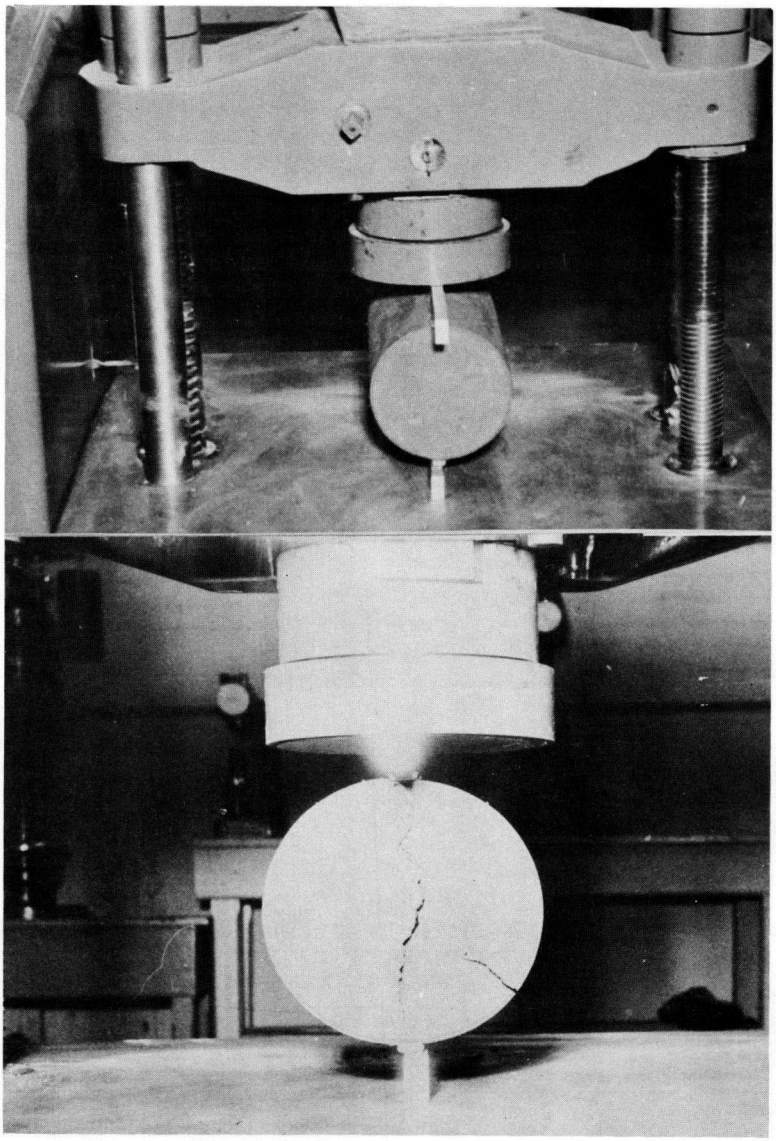

Figure 15. Tensile splitting test—cylinder in place in the testing machine (upper) and immediately after splitting failure (lower).

100 F specimens. In Figure 17 the secant moduli of deformation from 0 to different stresses, maximum 1,500 psi, at different ages, are shown for the three temperatures.

Beam Tests. – Figure 18 shows relations between applied loads (one-half at each third point) and compression edge and tension edge strains for 100 and 70 F dense concrete beams at 24-hr age, and for 40 F beams at 72-hr age, also the change in location of the neutral axis with increasing load for the three series, computed from the observed strains, assuming straight-line variation. Figure 19 shows the same data for 14-day beams.

In the 100 F beams the tension strains were generally lower than the compression strain, and nearly the same value in tests at ages of one week or more. Difference in testing arrangement between the 100 F and the other tests with possibility for some

TABLE 11

MAXIMUM MOMENTS AT FAILURE OF 6- BY 8-IN. BEAMS, LOADED AT THIRD POINTS OF 27-IN. SPAN, AND EDGE STRAINS AT FAILURE PRORATED FROM OBSERVED STRAINS[a]

| Age at Test | 100 F | | | 70 F | | | 40 F | | |
|---|---|---|---|---|---|---|---|---|---|
| | Failure Moment (kip.) | Edge Strain ($10^{-6}$ in./in.) Top | Bottom | Failure Moment (kip) | Edge Strain ($10^{-6}$ in./in.) Top | Bottom | Failure Moment (kip) | Edge Strain ($10^{-6}$ in./in.) Top | Bottom |
| 10 hr | 4.0 | -41 | +47 | | | | | | |
| 12 hr | 10.5 | -55 | +43 | 3.3 | -59 | + 74 | | | |
| 16 hr | | | | 8.2 | -72 | + 89 | | | |
| 24 hr | 22.7 | -94 | +78 | 14.4 | -59 | + 93 | 1.5 | -34 | + 52 |
| 36 hr | | | | 23.9 | -80 | +105 | 3.3 | -40 | + 68 |
| 48 hr | 23.2 | -68 | +57 | 24.7 | -68 | +111 | 6.5 | -27 | + 45 |
| 60 hr | | | | 25.8 | -66 | +102 | 11.2 | -41 | + 51 |
| 3 day | 25.7 | -74 | +78 | 27.4 | -84 | +108 | 14.6 | -35 | + 50 |
| 7 day | 26.9 | -88 | +98 | 33.2 | -85 | +122 | 25.4 | -41 | + 62 |
| 14 day | 28.3 | -82 | +80 | 33.1 | -72 | +120 | 33.8 | -38 | + 72 |
| 28 day | 32.7 | -85 | +89 | 38.6 | -90 | +140 | 37.6 | -95 | +120 |

[a]Failure moment includes moment of beam weight 1.0 lb and rigload about 8.0 lb.

TABLE 12

SPLITTING LOADS AND ULTIMATE AVERAGE TENSION STRESS EQ 1 OF 6-IN CYLINDERS

| Age at Test | 100 F | | | 70 F | | | | | | 40 F | | |
|---|---|---|---|---|---|---|---|---|---|---|---|---|
| | | | | Dense | | | Air-Entrained | | | | | |
| | Splitting Load (lb/in.) | Tension Psi | Compr. Str. (f) | Splitting Load (lb/in.) | Tension Psi | Compr. Str. (f) | Splitting Load (lb/in.) | Tension Psi | Compr. Str. (f) | Splitting Load (lb/in.) | Tension Psi | Compr. Str. (f) |
| 3 hr | 25 | 3 | 25 | | | | | | | | | |
| 5 hr | 105 | 11 | 20 | | | | | | | | | |
| 6 hr | | | | 8 | 1 | 6 | 10 | 1 | 8 | | | |
| 7 hr | 305 | 33 | 19 | | | | | | | | | |
| 8 hr | | | | 23 | 2 | 8 | 30 | 3 | 13 | | | |
| 9 hr | 725 | 75 | 18 | | | | | | | | | |
| 12 hr | 1,120 | 120 | 15 | 100 | 11 | 12 | 115 | 12 | 13 | 8 | 1 | 14 |
| 16 hr | | | | 225 | 24 | 11 | 285 | 30 | 14 | 10 | 1 | 12 |
| 24 hr | 1,730 | 185 | 13 | 640 | 70 | 10 | 695 | 75 | 13 | 18 | 2 | 11 |
| 36 hr | 2,210 | 235 | | 1,090 | 115 | 10 | 1,310 | 140 | 13 | 92 | 10 | 22 |
| 48 hr | 2,330 | 250 | 15 | 1,540 | 165 | 12 | 1,400 | 150 | 11 | 145 | 15 | 18 |
| 60 hr | | | | 1,670 | 180 | 11 | 1,800 | 190 | 12 | 300 | 32 | 13 |
| 3 day | 2,120 | 225 | 12 | 1,860 | 200 | 11 | 2,000 | 215 | 12 | 470 | 50 | 12 |
| 7 day | 3,240 | 350 | 14 | 2,480 | 265 | 11 | 2,150 | 230 | 9 | 1,530 | 165 | 13 |
| 14 day | 3,000 | 320 | 13 | 2,760 | 295 | 10 | 2,670 | 285 | 9 | 2,140 | 230 | 9 |
| 28 day | 2,950 | 315 | 13 | 3,150 | 335 | 10 | 3,040 | 325 | 10 | 2,870 | 305 | 12 |

friction at the load points, could have been a cause for the lower neutral axis in the 100 F tests; however, as shown in Figure 17, the modulus of deformation in compression at low stress at 100 F temperature also was lower than at 70 F. Tension failure stresses deduced from strain distribution are not significantly different whether or not friction was present at the load points.

Compression Deformations in Cylinders and Beams. — These exploratory tests included concrete properties observed by more than one method of testing. Concrete deformations in compression were observed both on the cylinders and in the beam tests. Tension strengths were indicated by the tensile splitting test as well as by the beam tests. Secant modulus of deformation for the cylinder tests to varying stresses

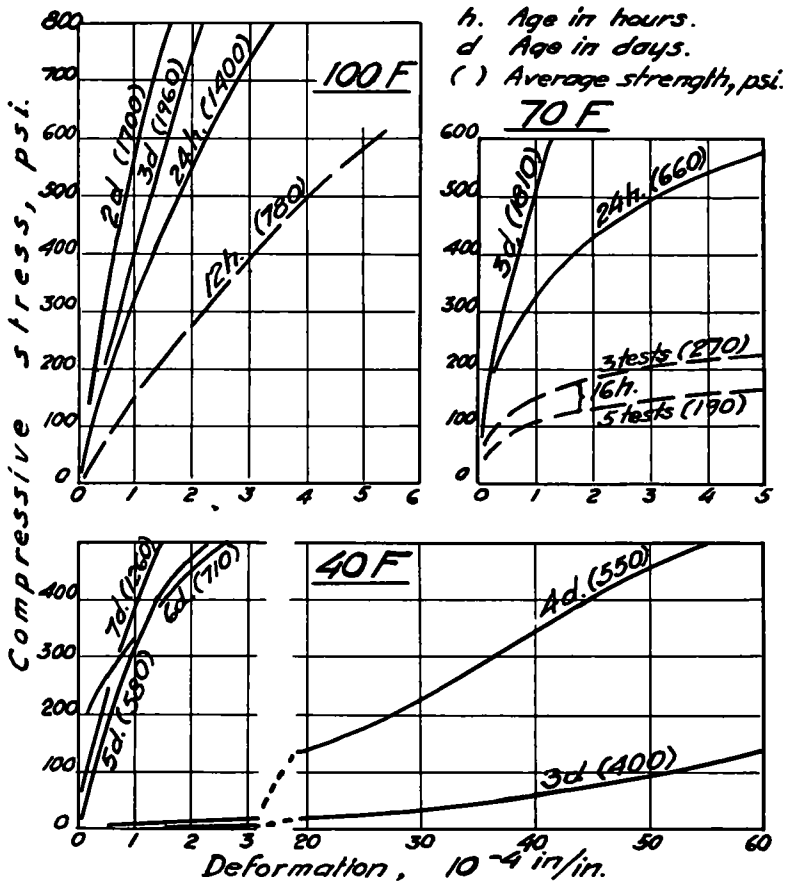


Figure 16. Average deformation-stress diagrams at early age; one cylinder only in 4-, 5-, and 6-day tests at 40 F.

are shown in Figure 17. The modulus values obtained on beams and cylinders are not radically different for the 100 F tests. The average modulus of deformation values in million psi for 24-hr and older concrete at the flexural stress range were for 100 F concrete, in compression on cylinders and beams, 5.0, in tension on beams 5.4; and for 70 F concrete, in compression on cylinders and beams, 7.0, in tension on beams 3.2. The lower compression modulus and the higher modulus of deformation in tension of the 100 F compared to 70 F concrete cannot be explained. Considering the relatively few 100 F tests, and variations in test arrangements, additional tests would be necessary for a clearer comparison.

Tensile Splitting Tests. — The tests did not indicate close or uniform relation between the tension stresses computed from the cylinder splitting tests (TSR) and the beam tension strengths. Figure 20 shows cylinder splitting resistance in relation to cylinder compression strength, and Figure 21 in relation to beam tension strength based on beam strain distribution. With exception for the isolated 40 F values in Figure 20, reasonable estimates of tensile splitting resistance in percent of compressive strength could be made from less than 1-day age for each temperature.

Beam tests are believed to indicate tension strengths closer than cylinder splitting tests at early age. In the tensile splitting test critical tension stresses occur in the interior of the cylinder, and at failure are distributed more or less evenly over a central section, the dimension of which is influenced by the depth to which plastic read-

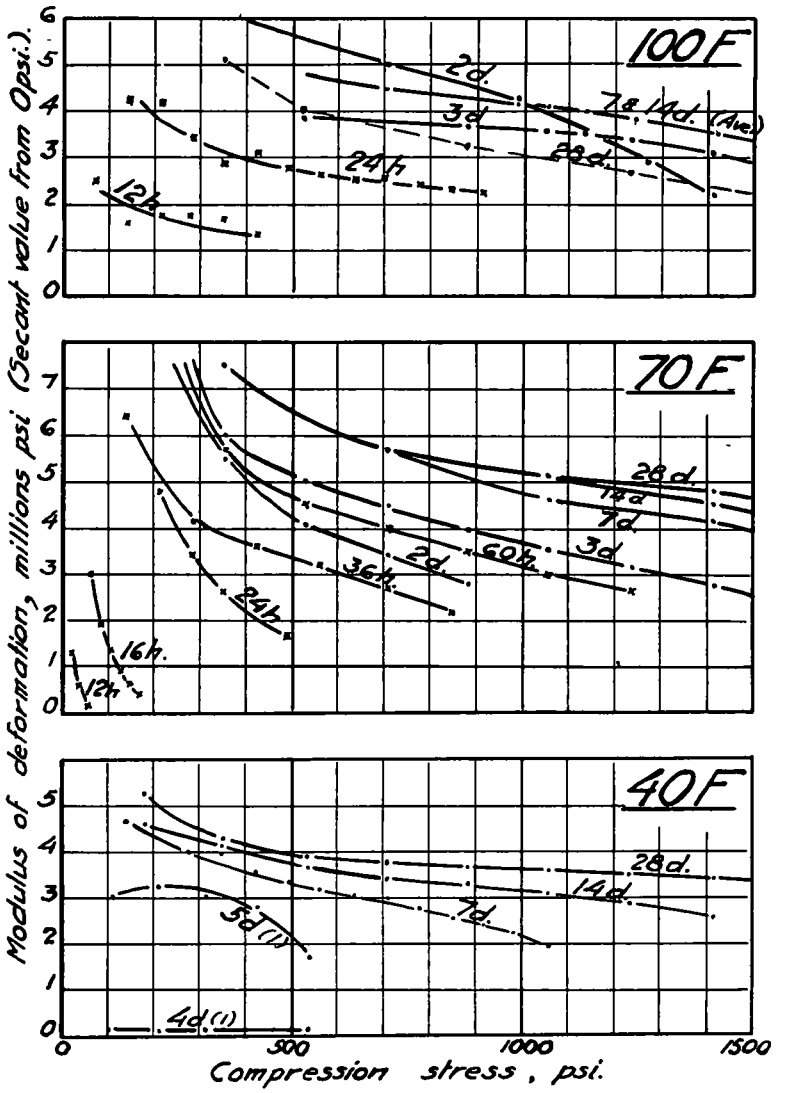


Figure 17. Secant modulus of deformation at different ages, observed on compression cylinders from 0 stress to stress indicated by abscissa.

justments (shear wedges) occur under the narrow "line" loading. The tension stress in the splitting tests, if computed in accordance with Eq. 2, assuming a shear wedge depth w of 1 in., equalled more nearly the tension strengths indicated by the beam tests at mature age. Such plastic conditions near failure seem probable.

## Ambient Temperature and Concrete Strength

Conventional strength properties, as represented by cylinder compression strength, tensile splitting resistance, Eq. 1, and modulus of rupture, for 100, 70, and 40 F concrete to mature age are shown in Figure 22. Tension strengths indicated by flexural strain observations on the beams are shown in Figure 23. The great influence of ambient temperatures on concrete strength values is clearly evident in these illustrations. Tension strengths indicated by the beam tests at different ages, expressed as percent of cylinder compression strength at the same age, are shown in Figure 24. It shows

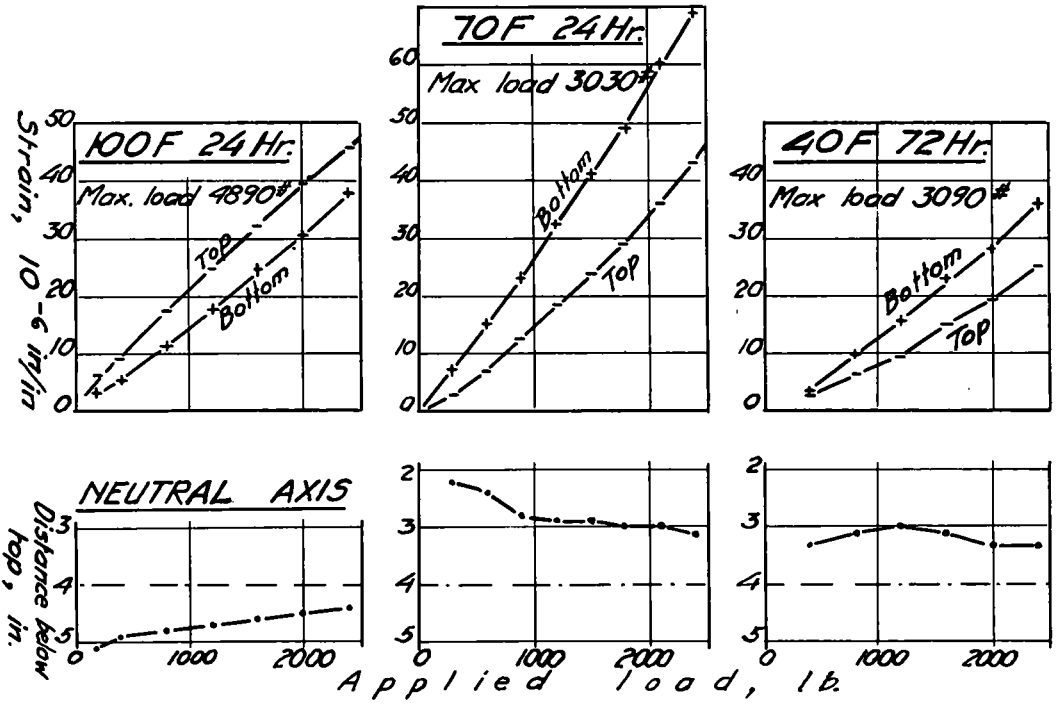


Figure 18. Top and bottom edge strains, and location of neutral axis, in beams for increasing applied load, prorated from observed strains, at early age.

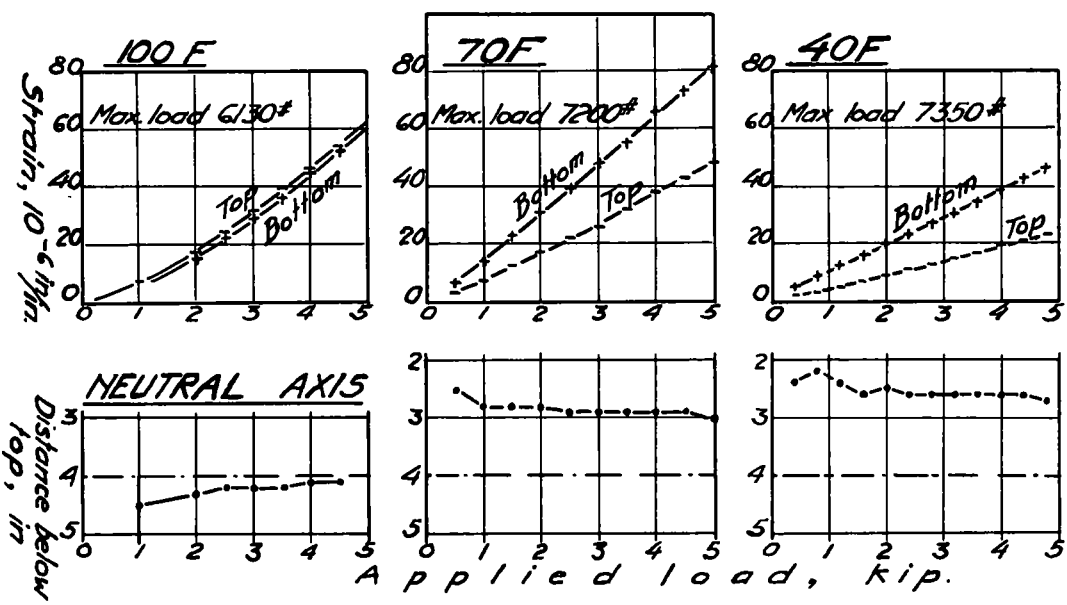


Figure 19. Top and bottom edge strains and location of neutral axis for increasing applied load on 14-day beams.

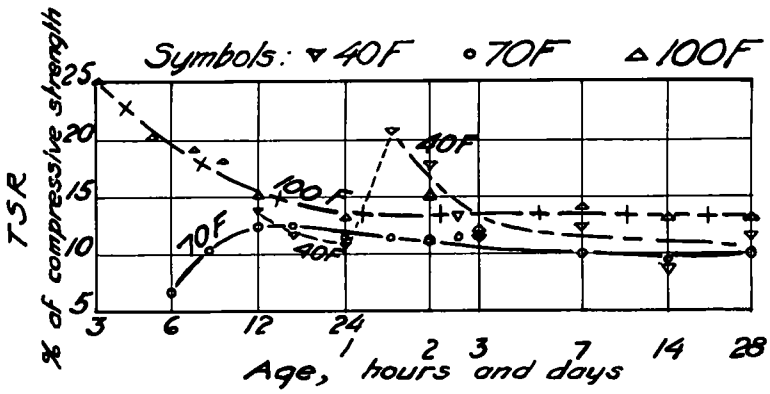


Figure 20. Cylinder splitting resistance (TSR) at early age to 28 days in relation to compression strength at same age.

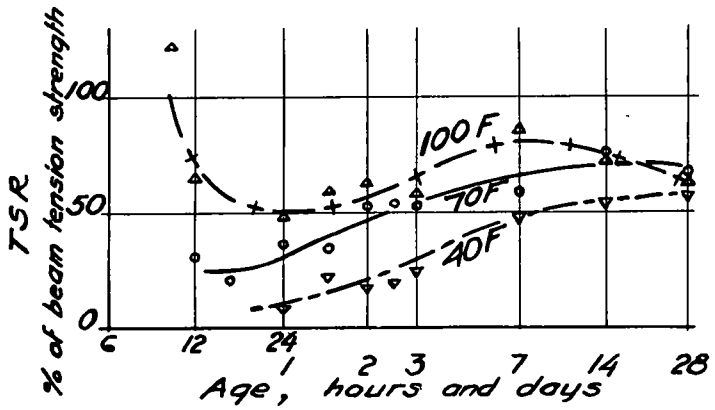


Figure 21. Cylinder splitting resistance (TSR) in relation to beam tension strength based on beam strains to 28 days.

that tension strength developed much more rapidly than compression strength. Figure 25 shows the ages at which various values of strengths in compression, and in tension as determined from beam tests, may be expected to be reached at different ambient temperatures for the particular concrete.

## Deformation Properties at Varying Ambient Temperatures

Figure 26 shows moduli of deformation in compression and in tension for increasing age, in compression based on compressometer measurements at low stress, and in tension based on beam strains at failure, for 100 and 70 F concrete. Data for 40 F concrete have not been included in the graph because of insufficient correlation. Concrete's resistance to deformation determines the restraint stresses to length changes at early age. A low modulus of deformation means a low maximum restraint stress for a given temperature drop; a high modulus means greater risk of critical stresses.

Because of the difference between tensile and compressive moduli of deformation the 2-day and older beams of 70 F concrete carried greater load than corresponding 100 F beams, in spite of the fact that the tension strengths in the 100 F concrete were equal or higher. Neither modulus of rupture as shown in Figure 22, nor modulus of

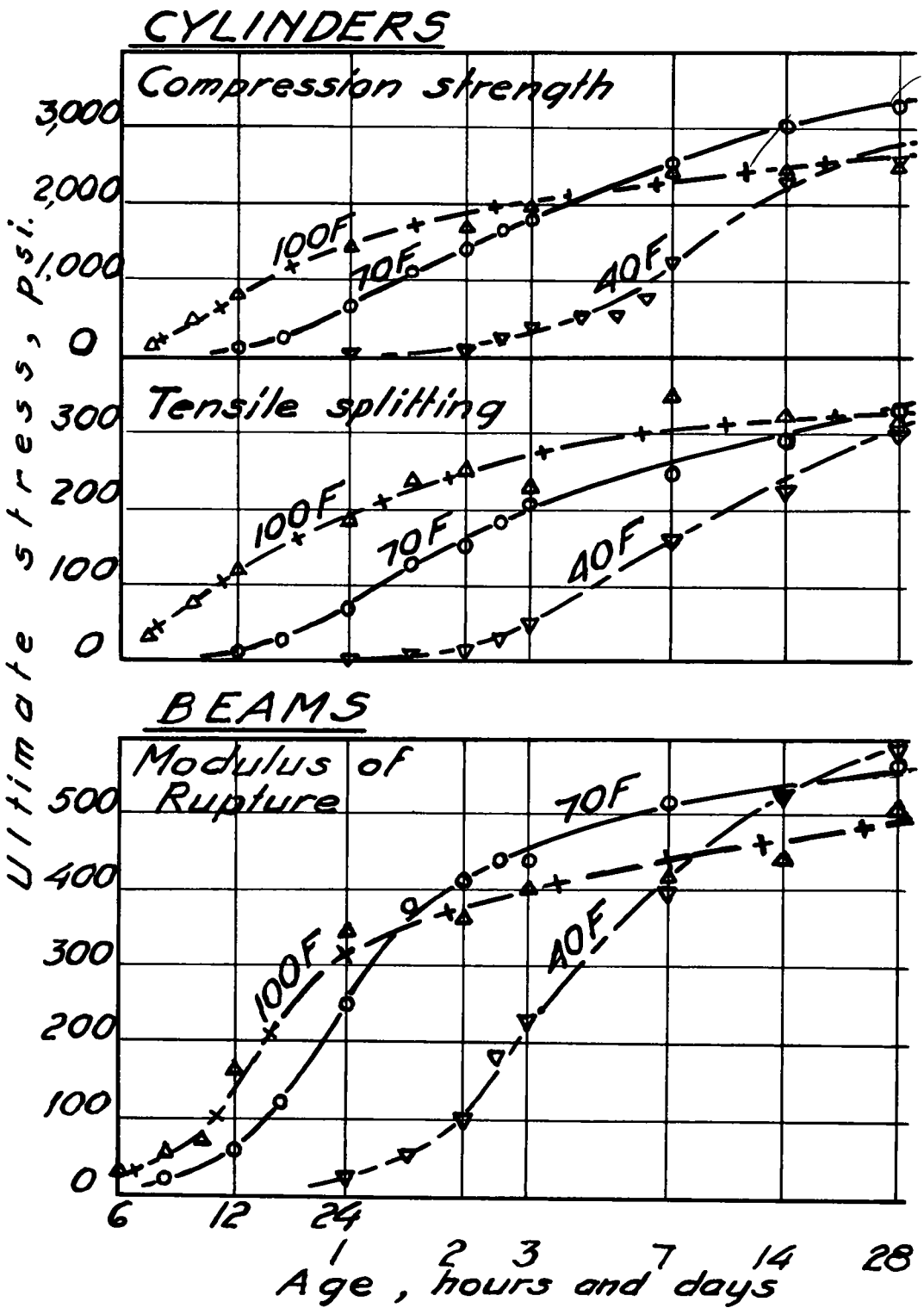


Figure 22. Compression and tensile splitting resistance on cylinders and modulus of rupture of beams at early age to 28 days.

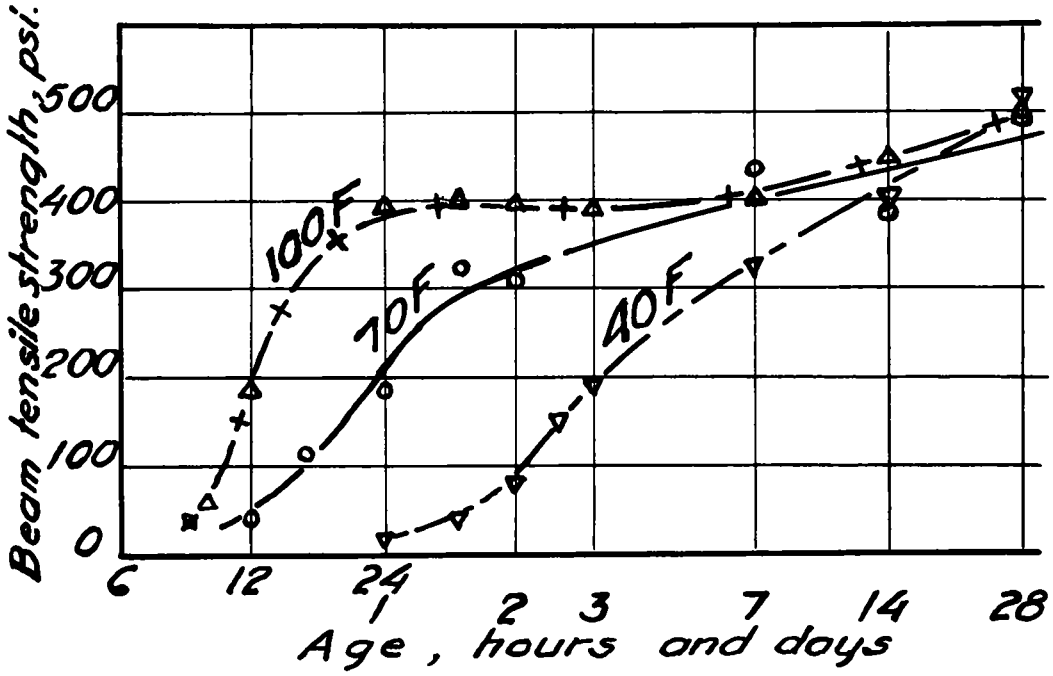


Figure 23. Beam tension strength at early age to 28 days based on stress distribution indicated by beam strains.

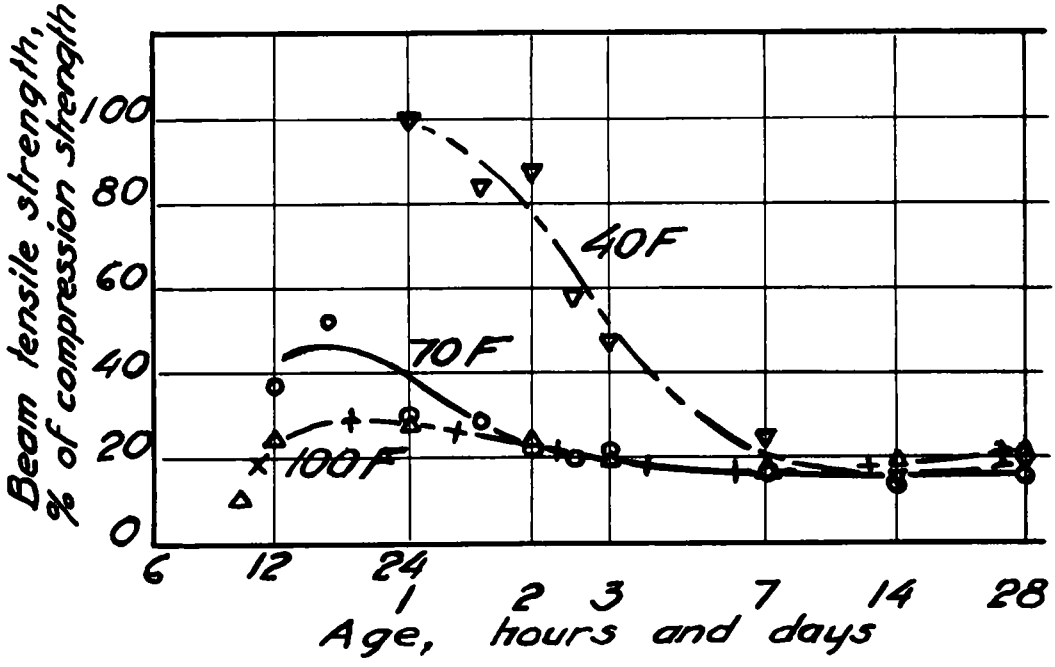


Figure 24. Beam tension strength in percent of compression strength at early age to 28 days.

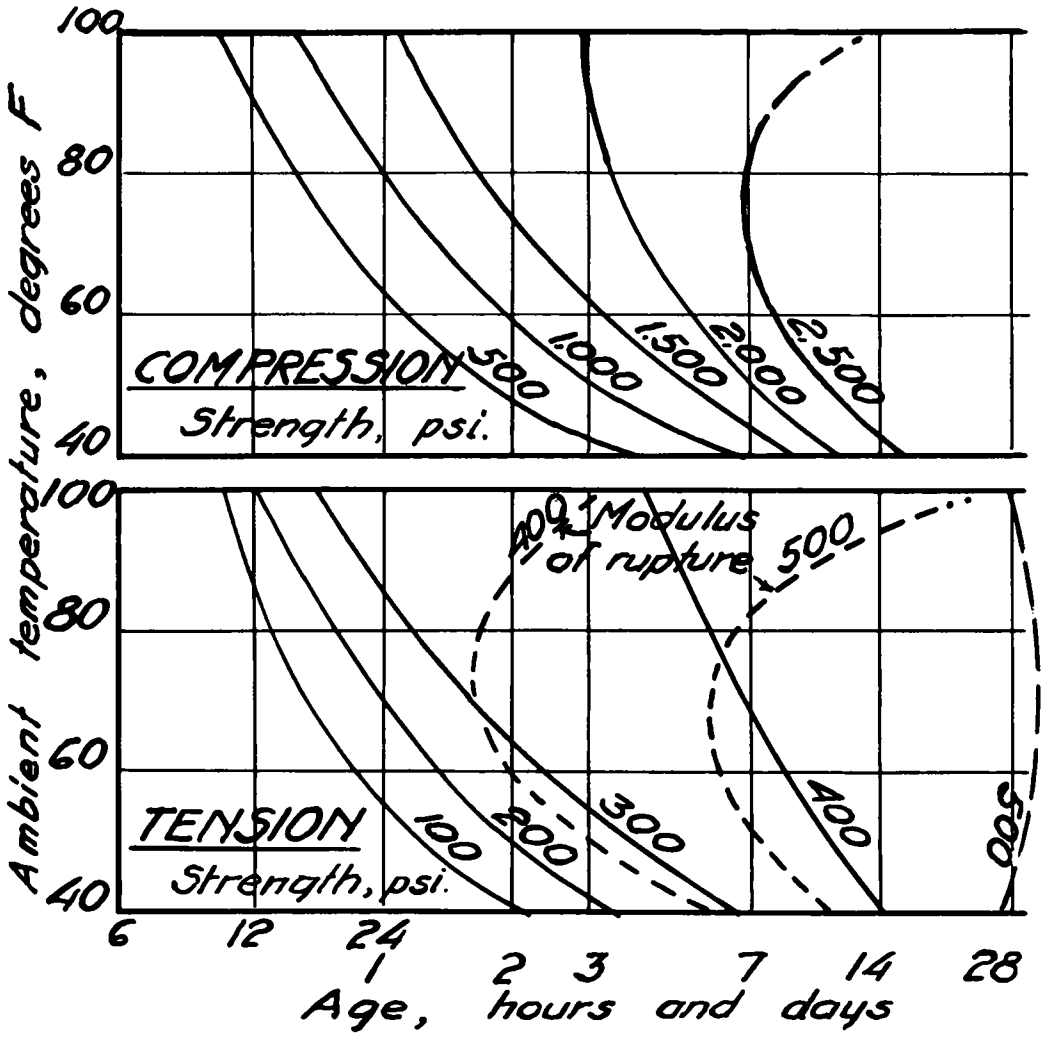


Figure 25. Relation between age and ambient temperature, for concrete to reach indicated strength values in compression and in flexural tension.

elasticity in flexure, nor observed beam deflections could indicate these conditions adequately.

Ultimate Strains

Before the concrete begins to gain strength, it has very little resistance to deformation. The least ultimate strains in compression according to these tests might be expected at 48 hr in 100 F, 16 hr in 70 F, and near 7-day age in 40 F concrete, from 200 to 400 μ in./in. extrapolated values.

Ultimate strains in tension are of more critical interest. The early-age ultimate tension strains indicated by the tests are for 100 F, from 50 μ in./in. before 1 day, to 100 μ in./in. after 1 week; for 70 F, from 80 μ in./in. before 1 day, to 140 μ in./in. after 2 days; and for 40 F, from 50 μ in./in. at 2 or 3 days, to 120 μ in./in. after 4 weeks. The ultimate tension edge strains in flexure at mature age, which might be predicted from these tests, may approximate 100 μ in./in. for 100 F concrete, and 150 μ in./in. for 70 and 40 F concrete for short-time loading.

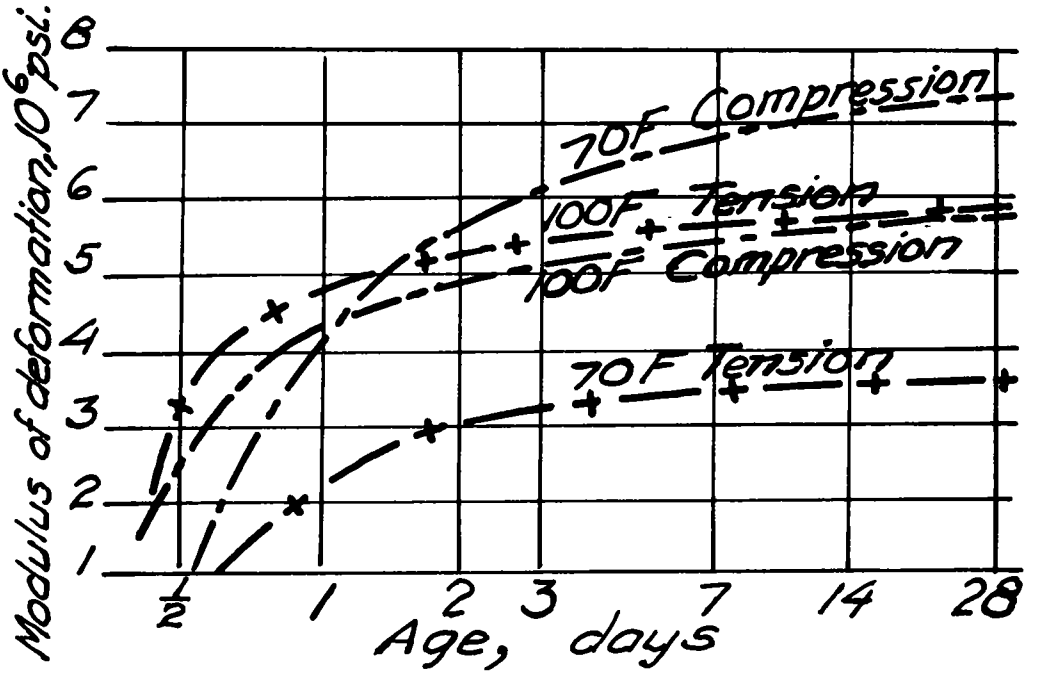


Figure 26. Modulus of deformation (elasticity) at early age to 28 days, in compression and in tension, for stress values within the flexural strengths, at 70 and 100 F ambient temperature.

## Application of Test Indications to Pavements

Minimum Age at Prestressing. — The tests gave clear indications concerning the earliest age at which prestress could be applied without crushing. The prestress imposed in pavements may range from 200 to 500 psi, applied when concrete strength is 500 and 1,000 psi minimum, respectively. The earliest age at which such strengths are reached is given in Table 13.

TABLE 13

MINIMUM AGE AT PRESTRESSING

| Prestress (psi) | Minimum Age for | | |
|---|---|---|---|
| | 100 F[a] (hr) | 70 F[a] (hr) | 40 F[a] (days) |
| 200 | 10 | 24 | 4 |
| 500 | 15 | 36 | 7 |

[a]Ambient temperature.

Prestressing Deformation. — It is necessary to protect the pavement against excessive shortening at the time of prestressing. The modulus of deformation indicates the immediate stress deformation. For anticipated modulus values at different ages and ambient temperatures, shortening at prestressing would approximate those values given in Table 14. Deformations, rather than strength, appear to indicate the earliest age at which prestress could be applied, particularly at low temperature and for prestress much over 200 psi in very long slabs. Some continuing deformations due to creep must be anticipated as well.

TABLE 14

MODULUS OF DEFORMATION

| Temperature (° F) | 200-Psi Prestress | | 500-Psi Prestress | |
|---|---|---|---|---|
| | Modulus ($\times 10^6$ psi) | Shortening (in./100 ft) | Modulus ($\times 10^6$ psi) | Shortening (in./100 ft) |
| 100: | | | | |
| At 1 hr | 1.5 | 0./6 | -- | -- |
| At 24 hr | 4.0 | 0.06 | 3.0 | 0.20 |
| 70: | | | | |
| At 24 hr | 5.0 | 0.05 | -- | -- |
| At 48 hr | 6.0 | 0.04 | 4.0 | 0.15 |
| 40: | | | | |
| At 4 days | 0.1 | 2.4 | -- | -- |
| At 5 days | 3.0 | 0.08 | 2.0 | 0.30 |
| At 7 days | 4.0 | 0.06 | 3.5 | 0.17 |

## PART C— STRESS DISTRIBUTION AND FAILURES UNDER LOADS APPLIED AGAINST AN EDGE

Prestressing of concrete pavements could involve the application of spaced concentrated forces against ends and edges of relatively thin pavement slabs, which can be assumed of unlimited length in the direction of the forces. Three critical stress conditions could be visualized near spaced concentrated edge forces against concrete slabs:

1. "Crushing" of the concrete in bearing at the force application points.
2. Tension stresses some distance away from the loaded edge, directly below and perpendicular to the direction of force application, resulting in "splitting" of the concrete along the lines of force application.
3. Tension stresses along the edge, between the force application points, evinced as cracks perpendicular to the edge.

The investigation was intended to explore the existence and severity of these stresses, including those near forces at or near slab corners. Information was obtained on the critical tension stresses between two loads. A series of long-time load tests were included to give indications of changes in concrete strains near lasting edge forces as result of creep in the concrete.

### Test Specimens and Testing Arrangement

All tests were made on 48- by 36- by 4-in. thick concrete slabs. The loads were imposed vertically against the 48-in. long edge through 1-in. steel blocks extending across the 4-in. edge and 2 in. along the edge. Pads of plywood were placed between the steel and the concrete. Loads were centered on the 4- by 2-in. bearing areas.

For short-time tests, the slabs were placed on edge in the testing machine, on a 48-in. long piece of plywood. Loads were applied in 5,000- and 10,000-lb increments to failure, with strain readings at each load increment. A test specimen in place in the testing machine is shown in Figure 27.

Long-time tests were made on specimens of the same size with identical load blocks. In these tests both 48-in. edges were loaded with directly opposed loads, maintained constant by coil springs behind one of the two opposed load blocks. Figure 28 shows the testing arrangement for center loads. Concentrated loads of 20,000 lb were applied at each load point, on 3 slabs center loads and on 3 slabs symmetrical loads 6 in. from each corner. Strains near the load were observed for a period of 50 days.

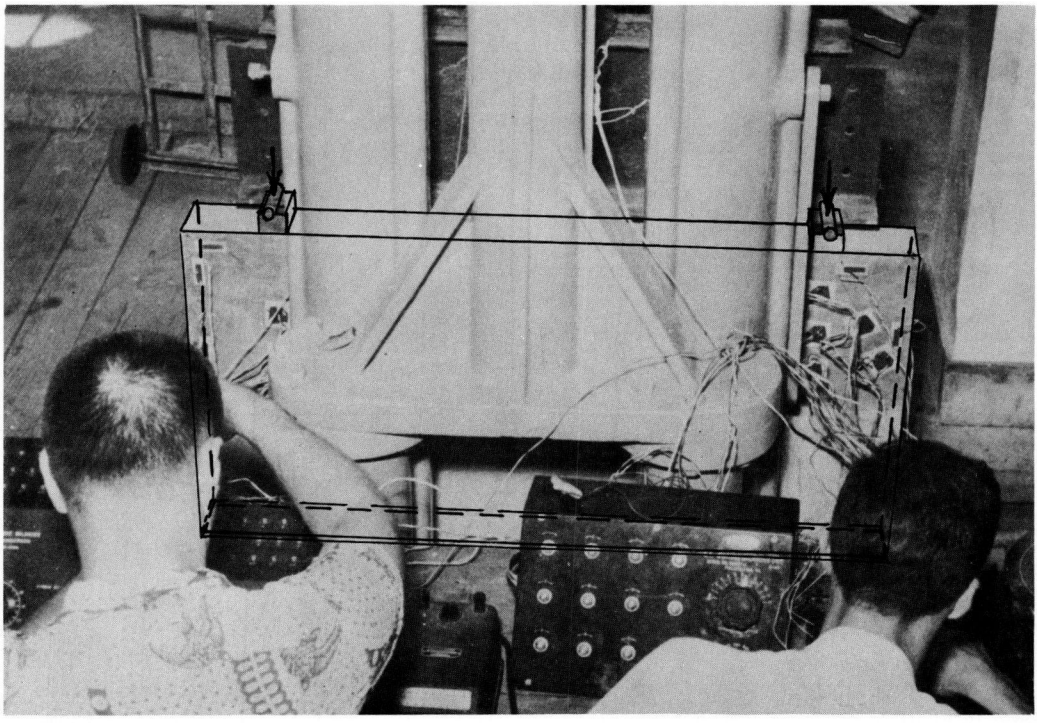

Figure 27. Short-time test specimen in place in testing machine for symmetrical loading with loads 6 in. from each corner.

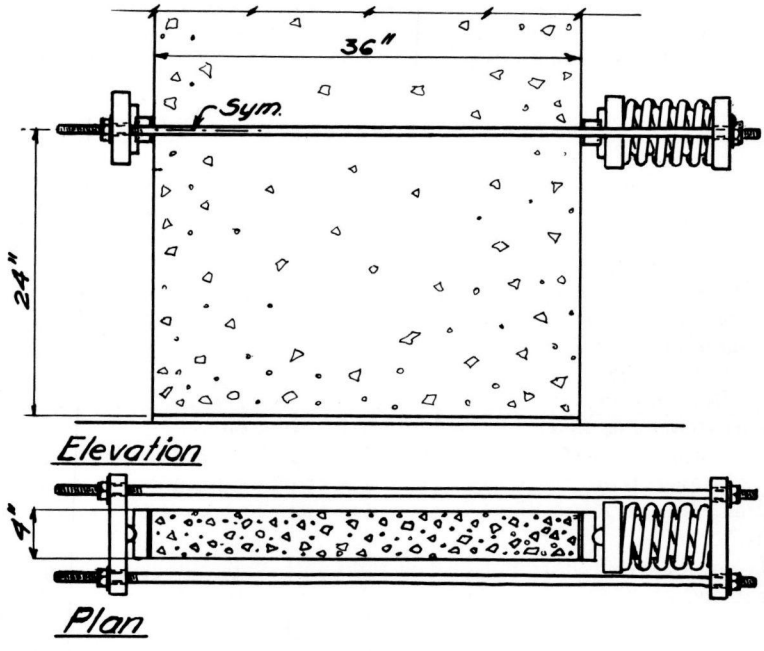


Figure 28. Loading arrangement for long-time tests, center load.

Concrete for all slabs was non-air-entrained mix, designed to conform to Missouri highway pavement construction. Maximum size coarse aggregate was limited to $\frac{3}{4}$ in. The slabs were cast in flat position and left in the forms for 7 days, curing under wet burlap. They were then stored on edge in the laboratory to the time of testing. Cylinder compressive strengths are given in Table 15. This table also gives tension strengths

TABLE 15

COMPRESSIVE AND TENSION STRENGTHS

| Time (days) | Cylinder Compress. Strength (psi) | Modulus of Rupture (psi) | Cylinder Splitting (psi) | Secant Moduli of Elasticity (x $10^6$ psi)[a] | | |
|---|---|---|---|---|---|---|
| | | | | Max. | Min. | Avg. |
| 14 | 3,000 | 520 | 290 | 4.6 | 2.5 | 3.8 |
| 28 | 3,300 | 570 | 330 | 5.6 | 2.9 | 4.5 |
| 42 | 3,500[b] | | | 5.6 | 3.8 | 4.9 |
| 84 | 3,600[b] | | | 6.0 | 4.3 | 5.2 |

[a]To 50 percent of compression strength.
[b]Estimated.

for concrete beams 6 by 8 by 36 in., tested with the 8-in. dimension vertical on 30-in. span and third-point loading and cylinder splitting tests, as well as the secant moduli of elasticity to 50 percent of compression strength.

All slabs were provided with bonded wire resistance strain gages, applied in principal directions near the loads and parallel to the loaded edges. SR-4 gages with $\frac{13}{16}$-in. active lengths were used, Type A-1 linear gages parallel to the edges 1 in. away, and strain rosette gages, Type AR-1 away from the loaded edge. Figure 29 shows orientation and identification of the gages. The relatively short $\frac{13}{16}$-in. gages were intended to give accurate orientation as to amount and directions of strains near the load. Large variations due to coarse aggregate near some gages were to be expected; however, the substantial number of slabs and duplicate gages were used so as to produce representative averages.

## Theoretical Studies

Theories for two-dimensional plane stress distributions of concentrated loads have been compiled and developed by Timoshenko (1). Stresses in wall-like girders of different depths and support conditions have been studied by Dischinger (2), covered in a publication of the Portland Cement Association (3). Similar stress problems, with reference to stresses in end blocks of prestressed structural members have been studied by Guyon (4), and with reference to bridge pier stresses by Bleich (5). Bleich's computations have been applied to end block stresses in prestressed members by Ban, Muguruma, and Ogaki (6).

Stresses on Sections in Line With and Between Loads Against an Edge. — A slab with spaced concentrated loads against an edge can be considered as an infinitely deep beam, with the concentrated loads as reactions to evenly distributed pressure q on the slab section some distance from the edge. On the section at distance from the edge equal to the load spacing, the variation in stress is less than 2 percent up or down from the uniform stress q.

Figure 30 shows stress distributions on the center-span section, and on the load centerline sections at midsupport, here called "midsection," according to Dischinger (2), with dimensions from the edge given in decimals of span length L. At center-span, tension at the edge is found to equal about 1.0 q, with nearly linear decrease to zero stress at a distance about 0.20 L from the edge for beams of large depth. The

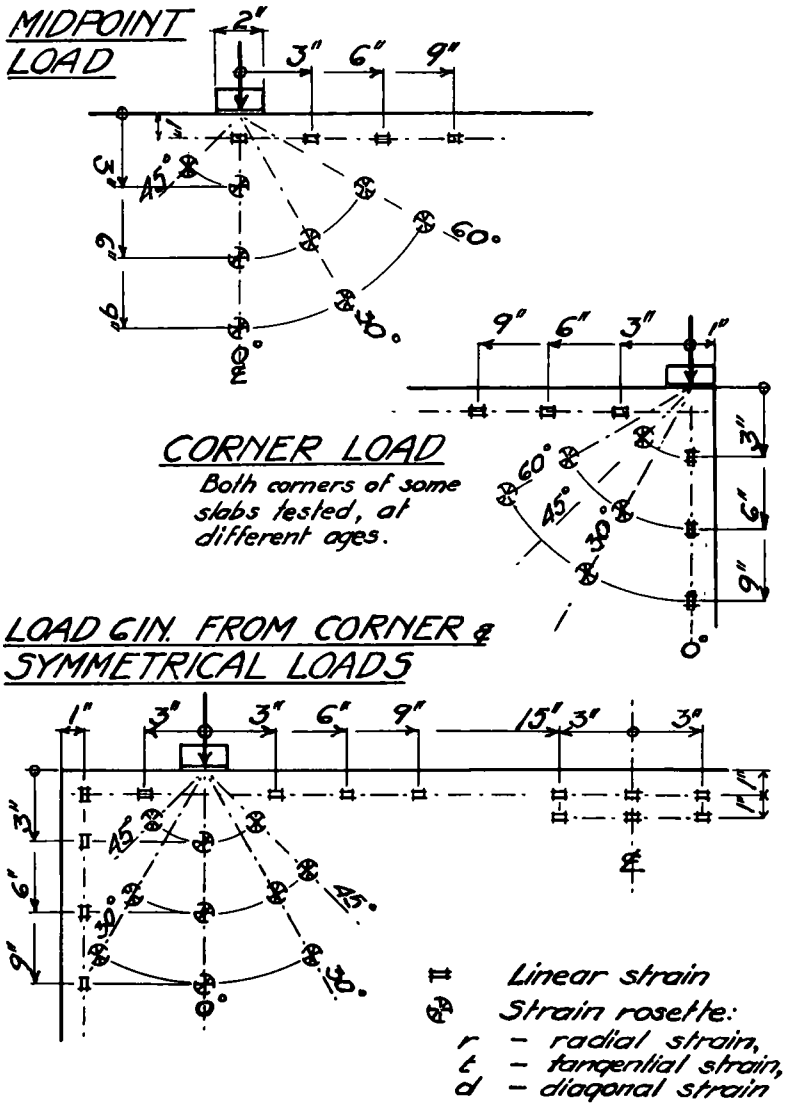


Figure 29. Dimensional orientation and identification of linear and rosette strain gages.

total force in the tensile stress portion of the center-span section is 0.10 q L. The stresses on midsections (3) are given in Table 16. The total force on the tensile stress portion of the midsections over the supports is between 0.21 q L and 0.24 q L for the three support dimensions.

Stresses at center-span have been developed (3) for single, as well as continuous spans (Table 17). Although, for single-span deep beams, bottom edge tension stress is about the same as in continuous spans (Fig. 30), zero stress is further from the edge, with corresponding increase in total tension on the section.

Stress Studies for End Blocks of Prestressed Structural Members. — Guyon (4) found the transverse splitting tension stresses (in end blocks called "bursting stresses") to be distributed substantially as shown in Figure 31 for different ratios of bearing length c to load spacing a. The mathematical expressions for stresses in deep piers by Bleich (5) have been solved by Ban, Muguruma, and Ogaki (6), for stresses on the

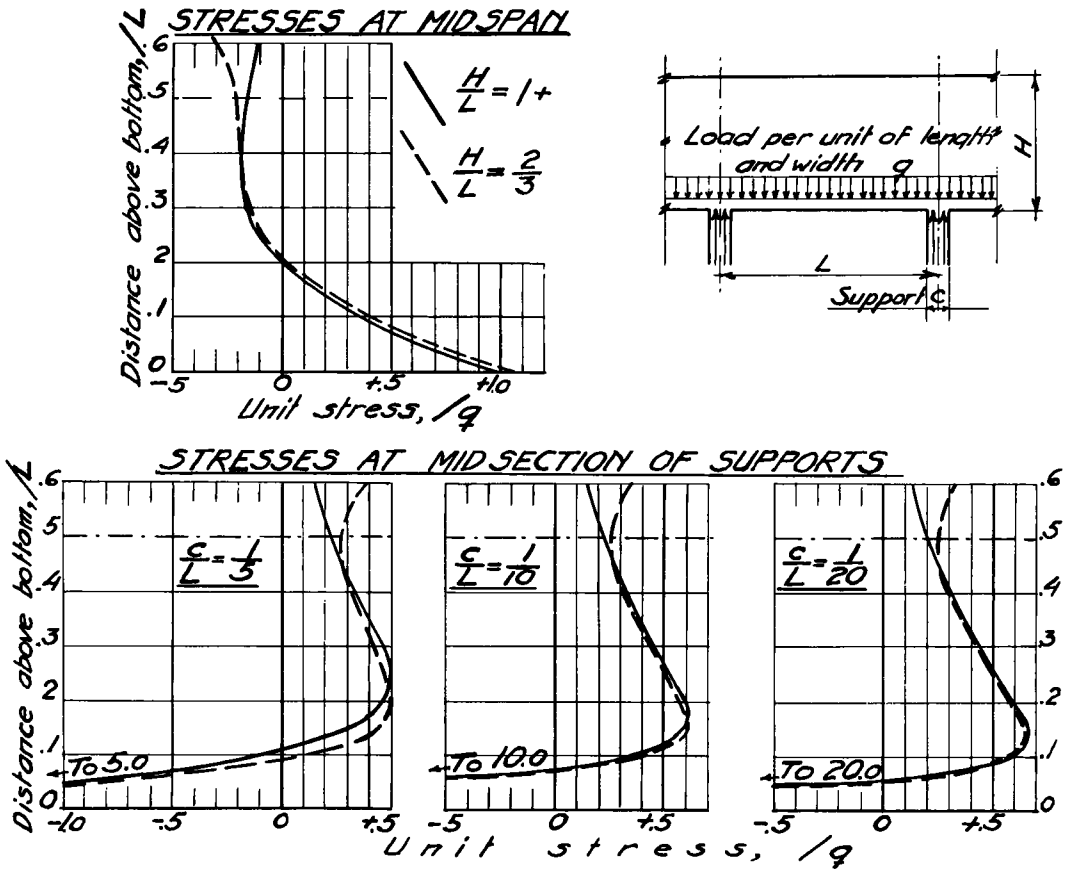


Figure 30. Stress distribution on sections of deep continuous beams with evenly distributed loading, at center span and midsections of the supports, for different support concentrations, Dischinger solutions.

TABLE 16

MIDSECTION STRESSES

| Support Width | Compressive Edge Stress at Support | Max. Tension Stress over Support | Location Above Support |
|---|---|---|---|
| L/5 | 5q | 0.5q | 0.25L |
| L/10 | 10q | 0.6q | 0.18L |
| L/20 | 20q | 0.65q | 0.15L |

midsections, shown in Figure 31 for different widths of loading c/a. At a depth equal to the effective width of load distribution a, the tension stresses on the midsection are insignificant according to this Figure.

Simple Radial Stress Distribution. — For simple radial stress distribution (1) in a plate of unit thickness (Fig. 32) at radius r and angle $\theta$ with the perpendicular edge force p the principal stress $f_r$ is directed toward the force application point:

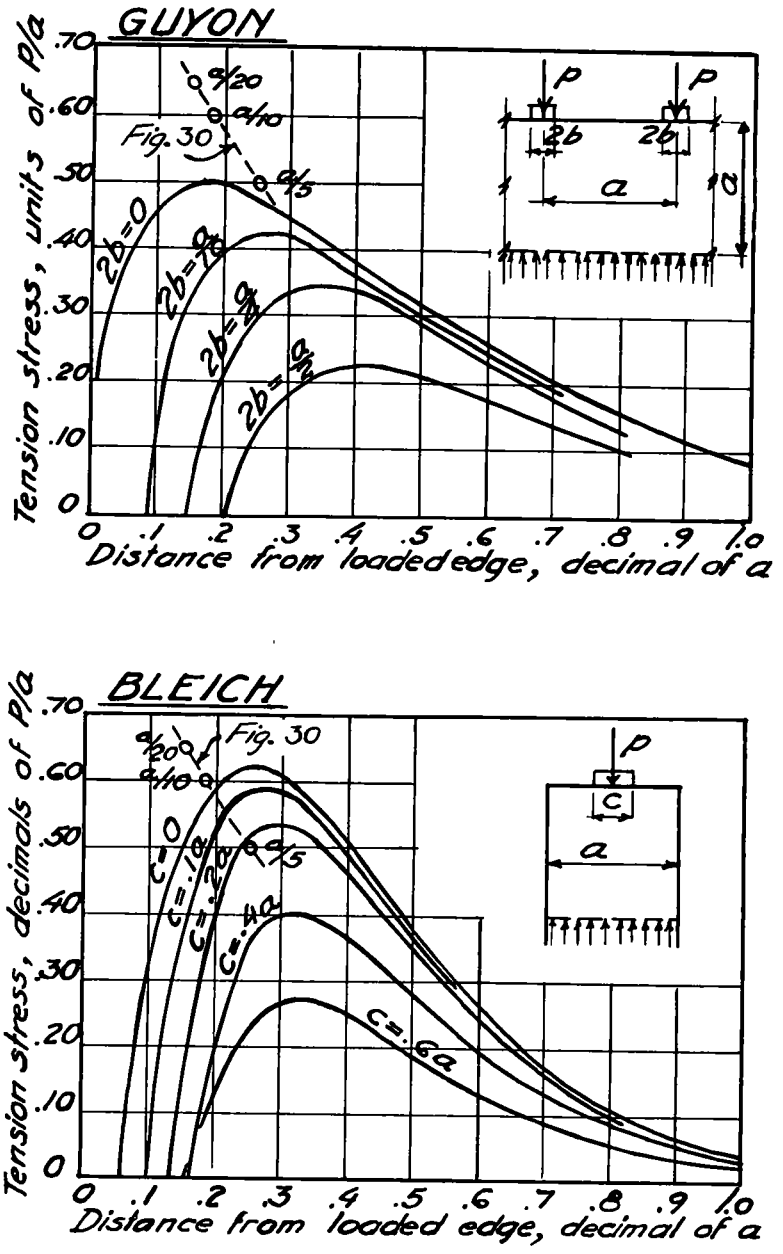


Figure 31. "Bursting" stresses under concentrated loading. End block stresses in prestressed members studied by Guyon; Bleich solutions computed by Ban, Muguruma, and Ogaki.

$$f_r = -\frac{2p}{\pi}\,\frac{\cos\theta}{r} \qquad (3)$$

The tangential stress $f_t$ is zero. On the midsection through the load there is no normal stress and no shear stress. As there are no stresses on the midsection, the resultant component forces on any section through the 90° quadrant on each side of the midsection are a vertical force p/2 and a horizontal force $p/\pi$. The resultant makes an angle of $32\frac{1}{2}°$ with the midsection, and is 0.59 p.

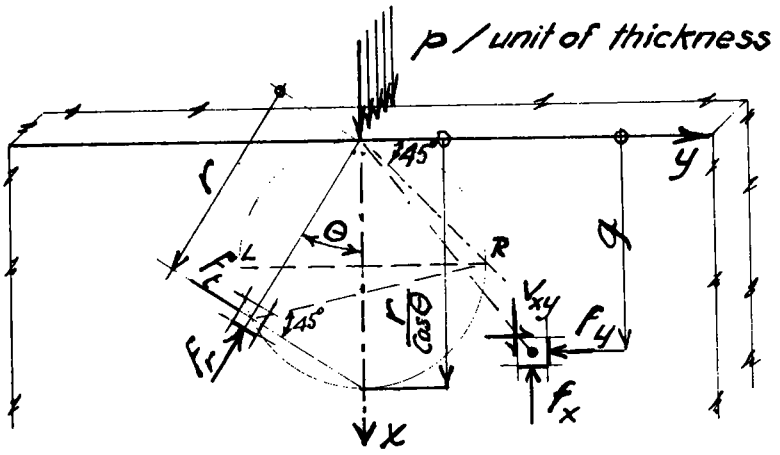


Figure 32. Orientation of stresses in simple radial distribution. Circle of equal radial stress, and direction of critical shear stresses shown.

TABLE 17

CENTER-SPAN STRESSES

| Support Width | Tension Edge Stress | Zero Stress[a] |
|---|---|---|
| 1.0 | 1.2q | 0.35L |
| 1 1⅓ | 1.05q | 0.36L |
| 2 2 | 0.95q | 0.36L |

[a] From edge.

The normal stresses on horizontal planes $f_x$ and on vertical planes $f_y$ and shear stress on the horizontal and vertical planes $v_{xy}$ at a distance g below the loaded edge (1) are

$$f_x = -\frac{2p}{\pi g}\cos^4\theta \qquad (4)$$

$$f_y = -\frac{2p}{\pi g}\sin^2\theta\cos^2\theta \qquad (5)$$

$$v_{xy} = -\frac{2p}{\pi g}\sin\theta\cos^3\theta \qquad (6)$$

The coordinate stress values $f_x$, $f_y$, and $v_{xy}$ can be used as influence values for a distributed load. The vertical and horizontal compressive stresses directly below the center of the load p, distributed over a total length 2 b, are given in Table 18, as well as the vertical stress in percent of stress for equal point force. For depth over 2 b, there is no great difference between stresses for distributed load and point force. The resultant of the horizontal stresses on the midsection is $p/\pi$, and is centered 0.8 b below the edge.

TABLE 18

VERTICAL AND HORIZONTAL COMPRESSIVE STRESSES

| Depth | Vertical Stress | Horizont. Stress | Vertical Stress/ Conc. Force Stress (%) |
|---|---|---|---|
| 0 | 0.5 p/b | 0.5 p/b | -- |
| bb | 0.41 p/b | 0.09 p/b | 64 |
| 2b | 0.28 p/b | 0.02 p/b | 86 |
| 3b | 0.20 p/b | 0.01 p/b | 93 |

Under conditions of simple radial stress distribution, only compression and shear stresses exist in the semi-infinite isotropic material. Failure would be the result of critical shear stresses, and bearing pressure would not be equal to the compression strength $f'_c$ obtained from unconfined cylinder test, which is also a shear failure on 45° planes. It is assumed that initial failure is the result of ultimate shear, extending over a plane surface between the edge on each side of the load and the midsection, the so-called "shear wedge." The resultant force 0.59 p at $32\frac{1}{2}°$ angle with the midsection is the only force on any sloping plane, at an angle u with the midsection. The average shear stress v on a plane, intersecting the edge at a distance s from the force, is

$$v = 0.59 \frac{p}{s} \cos (32\tfrac{1}{2} + u) \sin u$$

The angle u, for which the shear v is a maximum, is found by derivation procedure. For maximum average shear, the angle u is $\frac{90 - 32\frac{1}{2}}{2}$, or 28 ¾°. The average shear $v_{max}$ on this weakest plane would be

$$v_{max} = \frac{0.59\, p}{s} \sin^2 28\tfrac{3}{4} = 0.14 \frac{p}{s}. \qquad (7)$$

If the average ultimate shear v is taken as $f'_c/2$ the ultimate load per inch of thickness $p_{ult}$ in terms of $f'_c$ is obtained directly from Eq. 7, $f'_c\, s/2 \times 0.14$, or $3.6\, f'_c\, s$. Actually, critical shear stresses occur along curved planes, especially so under distributed loads, for which the reasoning that maximum average shear on two plane surfaces governs failure is a much simplified approximation. Failure loads, so determined, probably would be conservative. The equations used to determine the angle of planes for maximum average shear are therefore applied to distributed as well as concentrated load. The dimension 2 s would equal the length 2 b over which the load is uniformly distributed, probably with some addition for tangential stress effect, and load spread through hard and strong coarse concrete aggregate near the bearing, resulting in lower shear stress than indicated by Eq. 7 for the longer actual shear planes. Accordingly, for distributed loads over a short length 2 b = the bearing length c, the estimate for ultimate load is

$$p_{ult} = 4\, b\, f'_c = 2\, c\, f'_c \qquad (8)$$

Stress Distribution for Corner Load. — Figure 33 shows stresses according to Timoshenko (1) for a force in line with the bisector of a wedge of unit thickness with 2 $\alpha$ contained angle. For this "axial" force $p_s$, the principal radial stress $f_{sr}$, at angle $\theta_s$ with the bisector is

$$f_{sr} = - \frac{p_s \cos \theta_s}{r\,(\alpha + \frac{1}{2} \sin 2\alpha)} \qquad (9)$$

A "transverse" force $p_t$, according to Figure 33, can be considered the equivalent of a "moment" force on the circular sections. The radial stress $f_{tr}$ is

$$f_{tr} = \frac{p_t \sin \theta_s}{r\,(\alpha - \frac{1}{2} \sin 2\alpha)} \qquad (10)$$

For pavements, it is especially desired to determine stresses for force along one of the sides of a 90° corner. Force p per unit of thickness along one edge equals two components $p/\sqrt{2}$ in axial and transverse direction. The combined radial stress $f_r$ for $\alpha = \frac{\pi}{4}$ obtained by summation of Eqs. 9 and 10 would be

$$f_r = \frac{p}{r} (2.47 \sin \theta_s - 0.55 \cos \theta_s) \qquad (11)$$

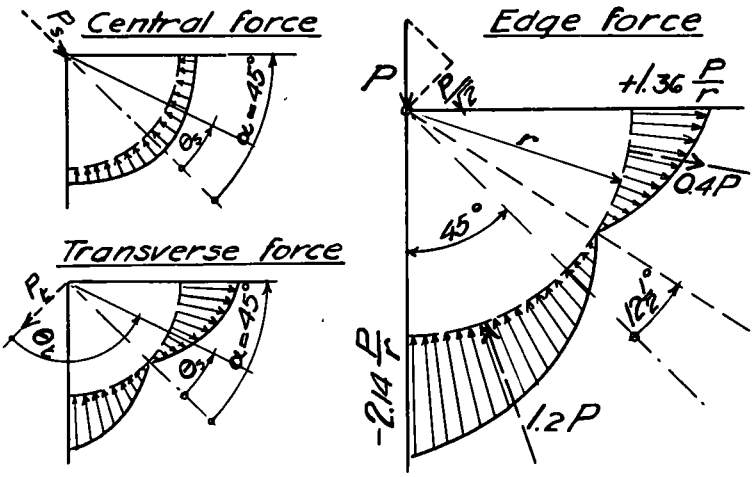


Figure 33. Concentrated forces against 90° corner. Stress distribution for central and transverse force and for force along one edge at the corner.

The radial stress distribution for the corner point force is shown in Figure 33. Zero radial stress is at an angle of $32\frac{1}{2}^\circ$ below the "tension" edge. The variation in the radial stresses is nearly linear along the circular sections.

Distributed Load at 90° Corner. — Directly under the distributed load, the radial stress $f_r$, the tangential stress $f_t$ and the radial-tangential shear stress $v_{rt}$, according to Timoshenko (1), are independent of r (<c); both the tangential (or vertical) stress at the loaded edge and the radial stress at the side edge equal -P/c. The horizontal stress at the loaded edge is zero. The maximum diagonal and tangential shear stress is at the 45° bisector, 0.5 p/c.

Radial stresses on circular sections at greater distances r from the corner than the loaded length c can be appraised from the stresses for corner load, by the following reasoning. A resultant load p perpendicular against one side of a 90° corner, and a distance t in from the corner, can be considered applied at the bisector at a distance $t\sqrt{2}$ from the corner, with axial and transverse components each $P/\sqrt{2}$. The stresses of the axial component are represented by Eq. 9. The transverse component load can be considered to cause a "moment on the circular sections"; the radial stresses due to the transverse component would be proportionate to the stresses for corner load (Eq. 10) decreased in proportion to the lesser moment arm $(r - t\sqrt{2})$ along the bisector. The stresses due to the transverse load $p/\sqrt{2}$, would then be given by Eq. 10 multiplied by the approximate ratio $(r - 1.5\,t) / r$. The resultant radial stress on circular cross-sections, combining Eqs. 9 and 10 for loads $p/\sqrt{2}$, is

$$f_r = \frac{p}{r}\left(\frac{r - 1.5\,t}{r}\,\frac{\sin\theta_s}{0.40} - \frac{\cos\theta_s}{1.82}\right) \qquad (12)$$

Radial stresses on circular sections in accordance with Eq. 12 are shown in Figure 34, which also shows the stresses along the two edges. At near 2 t distance from the corner the top edge stress would be zero, and a maximum of 0.17 P/t tension at about 4 t distance from the corner. The neutral axis for radial stresses is above the $32\frac{1}{2}^\circ$ line as an asymptote. Eq. 12 can be used for stresses due to a load distributed over a length c from the corner, assumed concentrated at t = c/2, or Figure 34 can be used as an influence diagram for such loads.

Critical Stresses Near Distributed Corner Loads. — The shear on the 45° corner sections directly below the load is 0.5 p/c. Failure would occur when the shear reached $f'_c/2$ stress. Critical load $p_{ult}$ per unit of thickness for a "shear wedge" failure at the corner would accordingly be

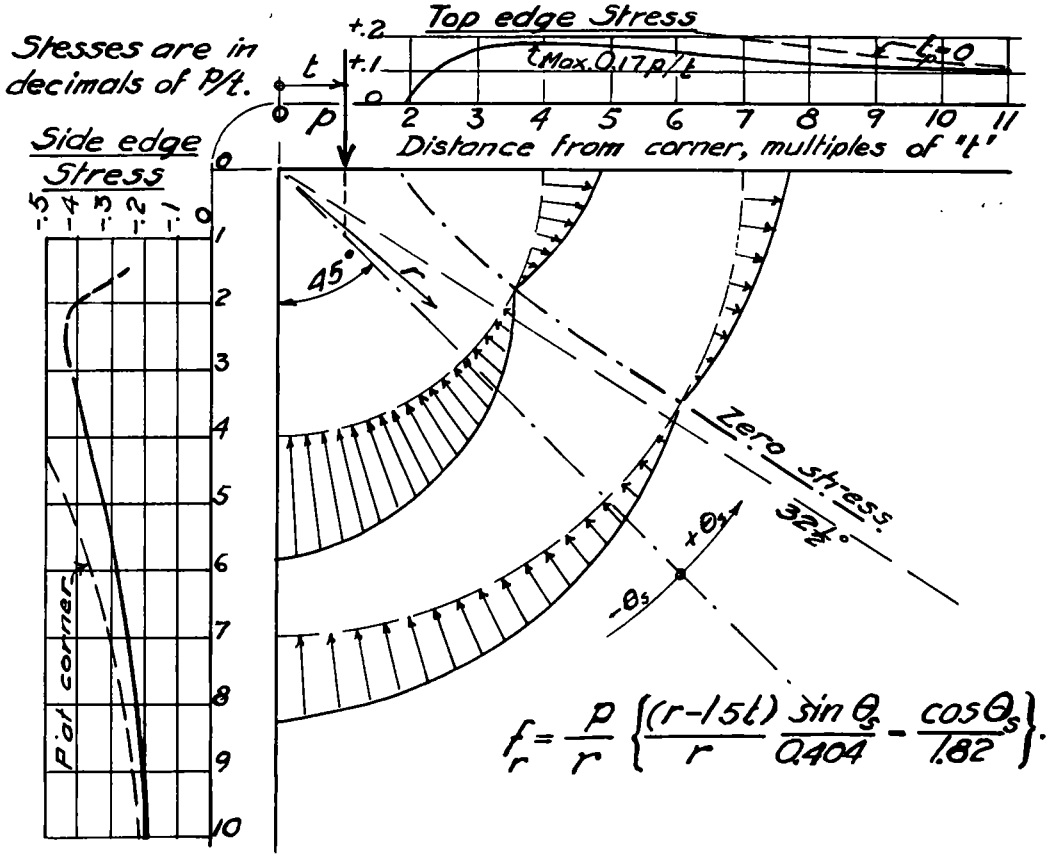


Figure 34. Approximate radial stress distribution on circular slab sections at varying radii from the corner, for load some distance in from and parallel with one edge of a 90° corner.

$$p_{ult} = c \times f'_c \qquad (13)$$

Top Tension. — The tension along the loaded edge for c = 2 t would be 0.34 p/c maximum, up to a distance of 2 c from the corner, as derived from Figure 34. If influence conditions govern, the maximum stress along the tension edge 0.34 p/c would be constant between c and 2 c from the corner. For crushing load (Eq. 13), the tension along the top edge would reach 0.34 $f'_c$, much above normal ultimate tension strength. Tension cracks would accordingly occur before crushing loads; however, cracks perpendicular to the tension edge could relieve the tension stresses without necessarily decreasing the load capacity as long as the distributed load could be supported by the strip of concrete along the edge in compression.

Stresses Between Two Corner Loads. — Stresses between two loads near the corners of an edge of length L can be computed in accordance with Eq. 13. This is the load condition that applied for two loads each 6 in. from the corner on the 48-in. edge of the experimental slabs. For two concentrated loads p per inch of thickness L/8 from the corners, the top edge would deform in response to both loads, the tension stress (Eq. 7) for each 0.17 p/0.125 L would be a maximum at the center between the loads. The total edge stress midway between the loads would be 2.72 p/L, or 1.36 q, higher than indicated in Ref. (3) for single spans. Zero stress on the center section in accordance with Eq. 12 would be about 0.25 L below the top edge. The total tension on

TABLE 19

FAILURE LOADS AND APPROXIMATE CRITICAL STRESSES AT FAILURE OF EDGE LOADED SLABS

| Load No. | Load Location | Load Means of Failure | Slab No. | Age (days) | Ultimate Load At Each Point (lb) | Ultimate Load At Each Point (lb/in.) | Ultimate Load Avg. (lb/in.) | Theoretical Stress at Failure Avg. Shear on Wedge | Theoretical Stress at Failure Maximum Tension Below Load | Theoretical Stress at Failure Maximum Tension Along Edge |
|---|---|---|---|---|---|---|---|---|---|---|
| 1 | Center of edge | Shear wedge and splitting | 1 | 14 | 40,000 | 10,000 | | | | |
| | | | 5 | 14 | 66,890 | 16,720 | | | | |
| | | | 9 | 14 | 60,000 | 15,000 | 13,900 | 1,950[a] | 190[b] | -- |
| | | | 19 | 42 | 77,000 | 19,250 | | | | |
| | | | 27 | 42 | 46,800 | 11,700 | | | | |
| | | | 30 | 42 | 65,000 | 16,250 | 15,700 | 2,200[a] | 210[b] | -- |
| | | | 10 | 84 | 37,000 | 9,250 | | | | |
| | | | 14 | 84 | 78,000 | 19,500 | | | | |
| | | | 18 | 84 | 72,000 | 18,000 | 15,600 | 2,180[a] | 210[b] | -- |
| | 6 in. from corner | Shear wedge and splitting | 1 | 84 | 76,700 | 19,200 | | | | |
| | | | 6 | 84 | 59,000 | 14,750 | | | | |
| | | | 16 | 84 | 54,900 | 13,720 | 15,900 | 2,230[a] | -- | -- |
| | At corner | Top tension and shear wedge | 3 | 14 | 23,550 | 5,890 | | | | |
| | | | 7 | 14 | 29,940 | 7,480 | | | | |
| | | | 15 | 14 | 26,650 | 6,660 | 6,640 | 1,660[c] | -- | < 1,130[d] |
| | | | 12 | 42 | 35,420 | 8,870 | | | | |
| | | | 15 | 42 | 28,800 | 7,200 | | | | |
| | | | 31 | 42 | 17,600 | 4,400 | 6,820 | 1,700[c] | -- | < 1,160[d] |
| | | | 3 | 84 | 28,000 | 7,000 | | | | |
| | | | 7 | 84 | 26,800 | 6,700 | | | | |
| | | | 12 | 84 | 24,000 | 6,000 | 6,570 | 1,640[c] | -- | < 1,120[d] |
| 2 | 6 in. from corner | Tension at center of slab | 11 | 14 | 32,970 | 8,240 | | | | |
| | | | 13 | 14 | 34,980 | 8,740 | | | | |
| | | | 17 | 14 | 24,060 | 6,020 | 7,660 | -- | -- | 430[e] |
| | | | 21 | 42 | 26,500 | 6,620 | | | | |
| | | | 24 | 42 | 29,100 | 7,280 | | | | |
| | | | 25 | 42 | 21,500 | 5,380 | 6,430 | -- | -- | 370[e] |

[a] For edge load, based on Eq. 7, s = b = 1.0 in.
[b] For edge load, based on Bleich, 0.65 p/L, (L = 48 in.)
[c] For corner load, based on Eq. 13, c = 2 in., also average shear on 45° plane from inner edge.
[d] For corner load, based on 0.17 p/t, t = 1.0 in. Absence of reactive forces prevents high-tension stresses away from load.
[e] For two corner loads, based on 2 x 0.17 p/t, t = 6 in., (r = 24 in.)

TABLE 20

LOADS AT FAILURE ON 2-IN. LONG BEARING

| Load No. | Load Weight (lb) | Location | Failure (lb/in.) |
|---|---|---|---|
| 1 | 60,400 | At center | 15,100 |
| 9 | 63,500 | 6 in. from corner | 15,900 |
| 4 | 26,800 | At corner | 6,680 |
| 2 | 28,200[a] | 6 in. from corner[a] | 7,050[b] |

[a] Each.
[b] Failure between loads.

the center section near the top edge between the two loads, would be 0.34 p, in substantial agreement with (3), for single spans.

## Failure Loads

Only the short-time tests were carried to failure. Ultimate loads and modes of failure for all the specimens are given in Table 19. No significant increase in ultimate loads was noticeable from 14- to 84-day age. Averaging the results for all three ages, the loads at failure on the 2-in. long bearing are given in Table 20. Figure 35 shows slabs after failures for single load at center, 6 in. from the corner, and at the corner.

The views show a "shear wedge" below the load block, with indications of local failures a short distance out from the edge of the block as well. For all single loads the shear wedge was accompanied by a vertical crack splitting the slab.

For corner load the shear wedge extended to the edge. The vertical crack at the inner edge of the load block appeared before development of the shear wedge. The failure at the center of the slab between two loads 6 in. from the corners (Fig. 35) was an apparent tension failure in flexure.

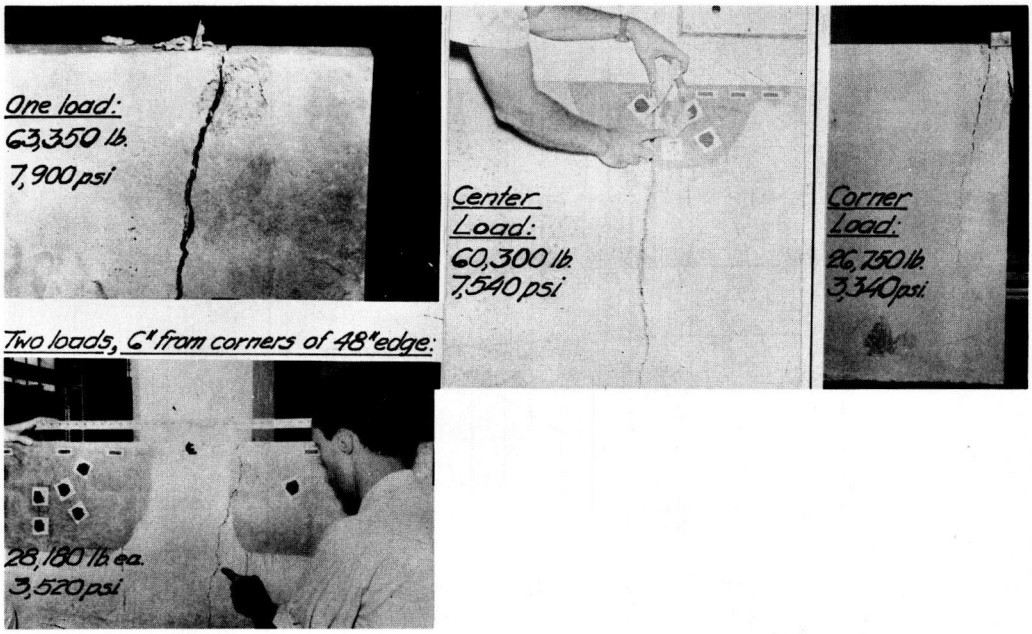


Figure 35. Typical test slab conditions after failure, for single load at center of edge, at one corner, and 6 in. from one corner, Bottom view shows crack near center between two symmetrical loads.

## Critical Stresses at Failure

In Table 19 the critical stresses for average failure loads at each age have been computed in accordance with applicable equations as indicated.

The maximum average shear stress for shear wedge failure under single loading, including one load 6 in. from the corner, was 2,140 psi according to Eq. 7, compared to an average cylinder strength $f'_c$ of 3,400 psi, or 0.62 $f'_c$. The average ultimate load was 12 percent higher than indicated by Eq. 8. For the corner load the average shear stress, 0.5 p/c, was 1,670 psi or 0.48 $f'_c$.

The theoretically derived maximum tension stress on the midsection below a single load, 0.65 p/L would not have exceeded 210 psi in the tests (Table 19). This stress is not sufficient to explain the typical splitting crack. Splitting failure is believed to have been secondary to the shear wedge formation and caused by high horizontal pressure incident to confined vertical displacement of the shear wedge during failure.

The maximum corner tension stress (Table 19), according to Eq. 12 is higher than either the modulus of rupture or tension strength of the concrete; however, in these tests equalizing moments beyond the normal critical sections were lacking in the 4-ft long test slabs under a single corner load. High radial tension stresses, therefore, could occur only extremely near the corner load.

The computed tension stresses, Eq. (12) at the midsection between two loads each 6 in. from the corner, average 400 psi (Table 19) agrees well with the tension strength indicated by the beam and cylinder splitting tests. The cracking between the two loads gave ample evidence of high tension stress along the edge, provided that radial stress distribution could take place from loads near corners.

## Critical Strains

Strains were examined for possible information on the modes of failure. Figure 36 shows average rosette strains 3, 6, and 9 in. below the load center, and 3 in. away on

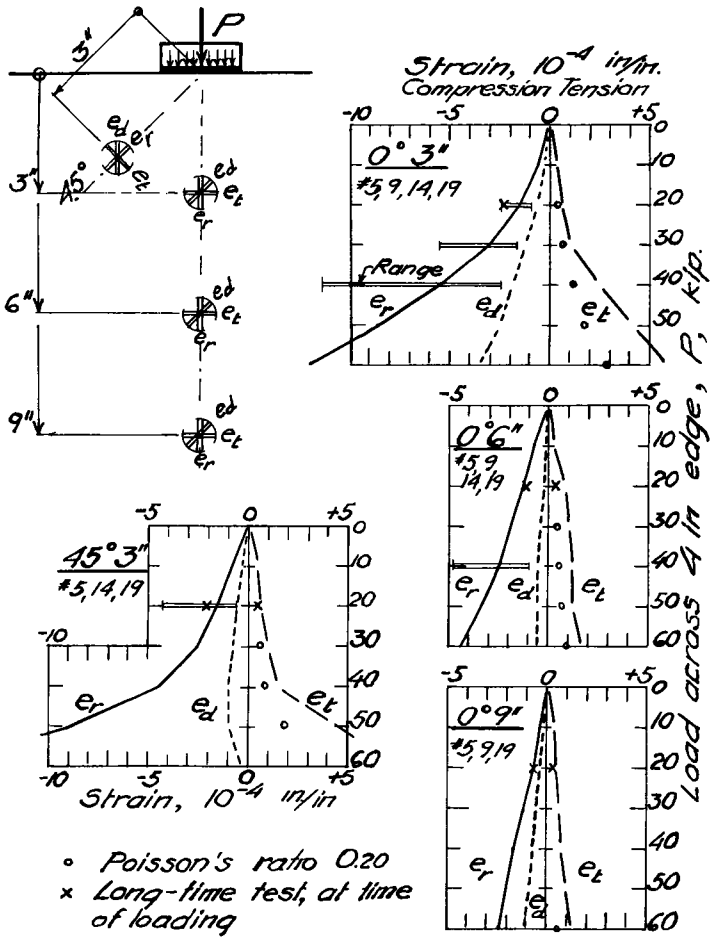


Figure 36. Average rosette strains and range of observed strains for increasing load; for 3, 6, and 9 in. under load; and at 45° angle 3 in. from load at center of edge.

the 45° plane. The graphs in the figure show disproportionate increase in tangential strains 3 in. away from the load above 30 kip, but not 6 and 9 in. below the edge. Maximum strains to failure in tension indicated by flexural tests do not exceed 150 to 200 μ in./in. Higher horizontal strains, Poisson's ratio of 0.2 deducted, were observed at 3 in. depth for 50 kip and higher load. According to the straingraphs, net tension strains 6 and 9 in. below the load for 60 kip load were 50 to 60 μ in./in. Tension strains, and stresses, at 6 and 9 in. depth accordingly, would have to increase abnormally near ultimate load to explain splitting of the test slabs.

The location of the strain gages, and graphs of the strains in relation to load are shown in Figure 37. The tension strains along the top edge 7 and 10 in. from the corner, prorated from strains 1 in. below, were in the critical range at failure.

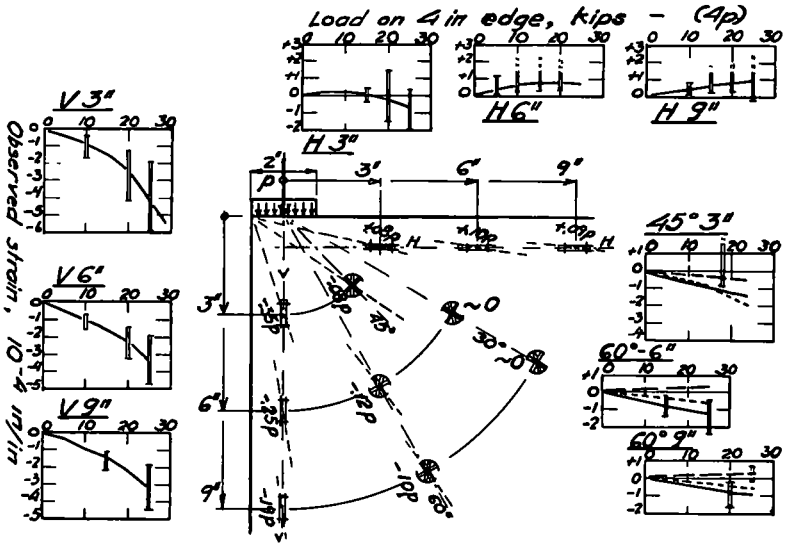


Figure 37. Observed strains in relation to load for linear and rosette strain gages near corner load; radial computed stresses at gage point locations for distributed load indicated.

Figure 38 shows directions and values of the principal stresses computed from all rosette strains, and the stress corresponding to linear strains 1 in. below the top edge, near a 20,000-lb edge load. For determination of principal stresses from observed rosette strains, Poisson's ratio of 0.20 was assumed. The theoretical compressive stresses, assuming simple radial distribution, are shown within parentheses. The magnitude of principal compression with increasing depth, as well as principal stress direction, shows good agreement with stresses based on simple radial distribution. Tangential tension stresses are indicated consistently below the load, maximum at 6-in. depth. These limited exploratory tests indicate closer agreement with the higher Bleich and Dischinger stress values than with the lower values suggested by Guyon.

Figure 38 also shows directions and values of the principal stresses computed from the rosette strains, and from the linear strains 1 in. from the top and side edges for a 16,000-lb corner load. Based on 4,000,000-psi modulus, the principal stresses and linear-strain stresses are not in close agreement near the load. Some deformation of the test slab toward the loaded corner probably could occur, and there was undoubtedly some friction at the load point to direct the load inwardly and, at the same time, decrease the tension stresses along the top edge, below values in a large slab.

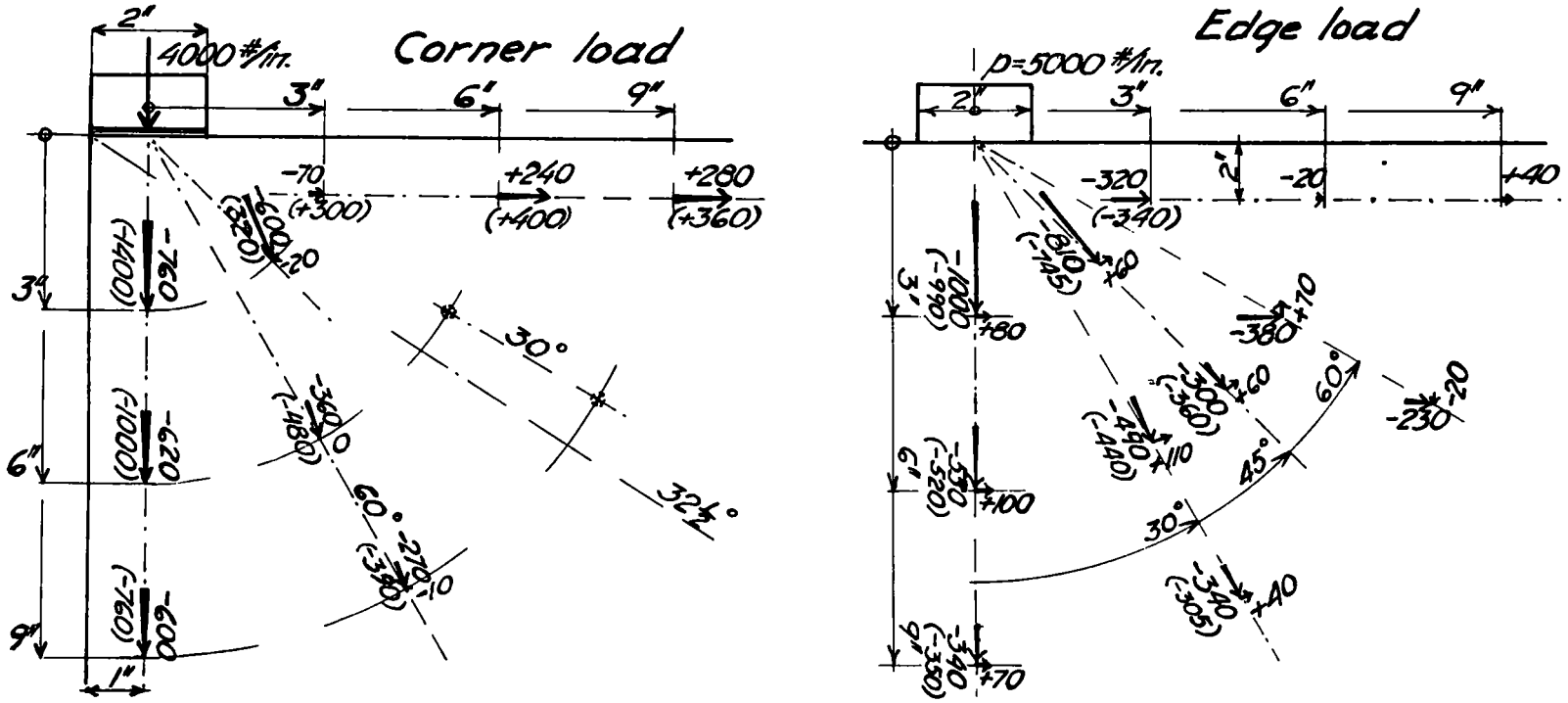


Figure 38. Principal observed stresses near an edge load and a corner load. Theoretical radial stresses shown in parentheses; loads on 4-in. thickness were 20,000 lb for edge load, and 16,000 lb for corner load; assumed modulus of elasticity 4,700,000 psi for edge load, 4,000,000 psi for corner load; Poisson's ratio for edge load, 0.20.

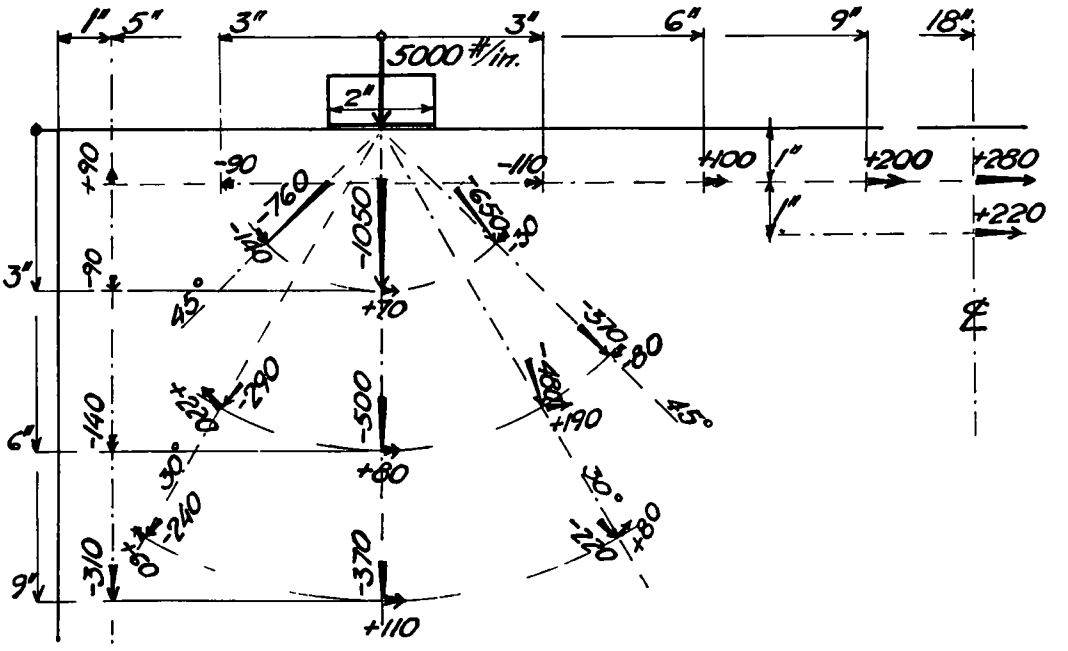


Figure 39. Direction and magnitude of experimental principal stresses for two loads applied 6 in. from each corner, each load 20 kips. Stresses computed from strains, for 4,500,000 psi, modulus of elasticity, and 0.20 Poisson's ratio.

Figure 39 shows principal stresses computed from rosette and linear gages for two 20,000-lb loads, each 6 in. from the corner of the 48-in. top edge. The high tension stress near the top edge on the slab center section is apparent, in excess of 300 psi at the top edge prorated. For the symmetrical loads, Eq. 12 would indicate that stresses were at the top edge 290 psi; 1 in. below the edge, 270 psi; and 2 in. below the edge, 240 psi, as compared to 280 and 220 psi observed 1 and 2 in. down, respectively. Further experimental investigation of the critical stress conditions between loads is needed.

## Long-Time Tests

The long-time tests included strain observations for 20,000-lb concentrated loads opposite each other across the 36-in. slab dimension. Strain gages and rosettes were applied to one side of the slabs only. Figure 40 shows the changes in strains near the load points to 50-day ages, including center loads as well as symmetrical loads. For rosette gages, the radial r, the tangential t, and the diagonal strains d have all been shown in the same graphs. Under the loads 6 in. from the corners, tangential elongation increased sharply during the first week or two, visible 3 in. below the loads, and more particularly at strain rosettes 45° on each side. Such tension strains could precipitate radial cracking and decrease the resistance to local failure near concentrated loads.

## Design Applications

These tests have given exploratory indications of critical tension stresses which must be considered near and between force concentrations imposed by end anchorages of prestressing cables at the edges of pavement slabs.

The ultimate capacity in bearing $p_{ult}$/in. thickness along the edge away from a corner for concrete cylinder strength $f'_c$ could be estimated in accordance with Eq. 8. For the 2-in. bearing used in the tests, local shear wedge failure evidently preceded splitting. Bearing capacity could be increased in direct proportion to bearing length; tension

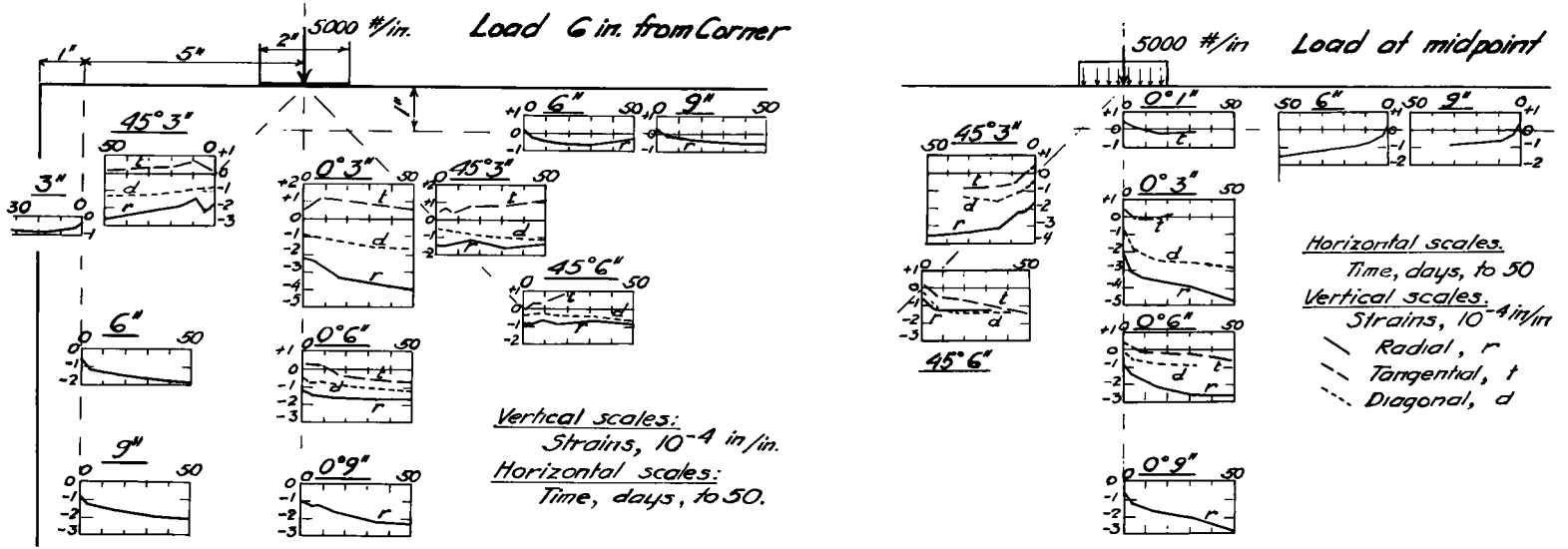


Figure 40. Variation in observed strains near 20-kip loads, for 50 days duration of loading. Loads at center of edge and 6 in. from each corner.

splitting stresses, on the other hand, increase in nearly linear proportion to bearing force, and would decrease only slightly with increase in bearing length.

Maximum tension stress on the sections in line with prestressing cables spaced distances a apart, according to this investigation should be anticipated to at least equal the values found by Bleich and Dischinger: 0.65 p/a for 0.05 a bearing length c, and 0.60 p/a for 0.10 a bearing length c. For ultimate bearing loads (Eq. 8), the corresponding tension stresses would be $0.065 f'_c$, and $0.12 f'_c$, for 0.05 a and 0.10 a bearing, respectively. For larger bearing dimensions, splitting stress might be more critical than bearing stress. Tests with larger specimens and bearing dimensions would be necessary to determine whether splitting tensions could become critical without prior shear wedge formation.

The tests have shown that loads applied immediately adjacent to a corner are limited by compression failure at bearing stress equal to the concrete cylinder strength $f'_c$, also that a 2-in. bearing centered 6 in. from a corner has the higher bearing capacity governed by edge loading.

The critical edge tension stresses between two concentrated forces was demonstrated experimentally. The maximum tension at the edge would be at least numerically equal to the distributed prestress. The stress between several spaced forces was not investigated experimentally. The total tension to be provided for would approximate 0.10 p. Reinforcement should be centered 0.07 a from the edge. Considering combinations of relatively high edge stresses at and between achorages with flexural wheel load stresses near an edge, transverse prestressing near and parallel to the pavement edge would seem necessary if spaced prestressing cables bear against the edge.

For bearings near a corner, critical tension edge stresses for some distance inward from the bearing must be anticipated. The edge tension is about three times that indicated between spaced edge anchors. For a single concentrated load at the corner, the resultant tension force is 0.4 p (Fig. 33). Reinforcement must be anchored at the corner to be fully effective a short distance away. The edge tension decreases in reversed ratio to increase in distance from the corner to the bearing; prestressing cables near edges might be placed sufficiently far away to keep edge tension stresses within safe limits.

## Summary

Considering the exploratory nature of the investigation, the indications obtained from the tests were unusually wide. Stresses near edge loads were in good agreement with predictions based on simple radial distribution. Observed maximum tension strains were in substantial agreement with stresses computed in deep beams on sections of spaced force concentrations; but tension stresses increased disproportionately, above computed values, at shear wedge failure. Tension failure occurred between symmetrical loads long before critical bearing stresses were reached. Cracks at failure under corner loading were similar to so-called restraint cracks frequently observed at transverse contraction and expansion joints of conventional concrete pavements.

## ACKNOWLEDGMENTS

F. V. Reagel, Engineer of Materials for the Highway Commission, initiated and directed the program. E. W. Carlton, Head of the School's Department of Civil Engineering, supervised the research work and the nine master's theses on different parts of the projects. E. O. Axon was highway department liaison engineer for materials, construction and continuing observations. The author served as consultant on planning, instrumentation, and analytical phases of the research for combination of the theses into reports published by the Highway Commission:

Part A. — Field slab research of normal and air-entrained concrete by J. L. Best and W. D. Stites, respectively, and indoor slabs by W. F. Alch; Report "Length Changes in Prestressed Concrete Slabs on Subgrades."

Part B. — Physical properties of normal concrete at 100 F by K. H. Dunn, at 70 F by P. G. Hansen, at 40 F by C. E. Weddle, Jr., and of air-entrained concrete at 70 F

by J. A. Spilman; Report "Strength Properties of 100 F, 70 F, and 40 F Concrete at Early Age."

Part C. – Short-time edge loading tests by W. M. Baldwin, and strains under long-time loading by J. B. Roberts; Report "Stress Distribution and Failures in Concrete Slabs Under Loads Applied Against an Edge."

## REFERENCES

1. Timoshenko, S., "Theory of Elasticity." McGraw-Hill (1934).
2. Dischinger, F., "Beitrag zur Theorie der Halbscheibe und des Wandertigen Balkens." Publications Internat. Assoc. for Bridges and Structual Engineering, 1:69 (1932).
3. "Design of Deep Girders." Portland Cement Assoc., ST 66 (1951).
4. Guyon, Y., "Prestressed Concrete." Wiley (1953).
5. Bleich, F., "The Column of Rectangular Section As a Plane Problem." Der Bauingenieur, Nos. 9-10 (1923). (In German)
6. Ban, S., Muguruma, H., and Ogaki, Z., "Anchorage Zone Stress Distributions in Post-tensioned Concrete Members." Proc., World Conf. on Prestressed Concrete, San Francisco (July 1957).

THE NATIONAL ACADEMY OF SCIENCES—NATIONAL RESEARCH COUNCIL is a private, nonprofit organization of scientists, dedicated to the furtherance of science and to its use for the general welfare. The ACADEMY itself was established in 1863 under a congressional charter signed by President Lincoln. Empowered to provide for all activities appropriate to academies of science, it was also required by its charter to act as an adviser to the federal government in scientific matters. This provision accounts for the close ties that have always existed between the ACADEMY and the government, although the ACADEMY is not a governmental agency.

The NATIONAL RESEARCH COUNCIL was established by the ACADEMY in 1916, at the request of President Wilson, to enable scientists generally to associate their efforts with those of the limited membership of the ACADEMY in service to the nation, to society, and to science at home and abroad. Members of the NATIONAL RESEARCH COUNCIL receive their appointments from the president of the ACADEMY. They include representatives nominated by the major scientific and technical societies, representatives of the federal government, and a number of members at large. In addition, several thousand scientists and engineers take part in the activities of the research council through membership on its various boards and committees.

Receiving funds from both public and private sources, by contribution, grant, or contract, the ACADEMY and its RESEARCH COUNCIL thus work to stimulate research and its applications, to survey the broad possibilities of science, to promote effective utilization of the scientific and technical resources of the country, to serve the government, and to further the general interests of science.

The HIGHWAY RESEARCH BOARD was organized November 11, 1920, as an agency of the Division of Engineering and Industrial Research, one of the eight functional divisions of the NATIONAL RESEARCH COUNCIL. The BOARD is a cooperative organization of the highway technologists of America operating under the auspices of the ACADEMY–COUNCIL and with the support of the several highway departments, the Bureau of Public Roads, and many other organizations interested in the development of highway transportation. The purposes of the BOARD are to encourage research and to provide a national clearinghouse and correlation service for research activities and information on highway administration and technology.